

**INVESTIGATION OF MECHANICAL PROPERTIES OF EXPANDED  
POLYSTYRENE LOW-DENSITY FIBRE-REINFORCED CONCRETE MADE  
WITH DIFFERENT FIBRE TYPES**

by

**John Chimaobi Ibeawuchi**

B. Eng. (Civil Engineering) Federal University of Technology Owerri, Nigeria, 2014

A Thesis Submitted in Partial Fulfillment  
of the Requirements for the Degree of

**Master of Science in Engineering**

in the Graduate Academic Unit of Civil Engineering

Supervisors: Alan Lloyd, PhD, Department of Civil Engineering  
Edward Moffatt, PhD, Department of Civil Engineering

Examining Board: Michael Thomas, PhD, P. Eng., Department of Civil Engineering  
Peter H. Bischoff, PhD, P. Eng., Department of Civil Engineering  
Gobinda Saha, PhD, P. Eng., Department of Mechanical Engineering

This thesis is accepted by the Dean of Graduate Studies

THE UNIVERSITY OF NEW BRUNSWICK

December, 2018

© John Chimaobi Ibeawuchi, 2019

## **ABSTRACT**

Fibre reinforced and low-density concrete have become popular in the construction industry today. In order for a combination of both materials to be widely accepted for use in design, a good understanding of their behaviour is needed. This study presents an experimental investigation to determine the effects of polypropylene and hooked-end steel fibres on the behaviour of low-density concrete made with expanded polystyrene beads. Digital image correlation (DIC) was used to measure displacements and strains as opposed to conventional methods of using LVDT and strain gauges and was validated as a better alternative. Crack initiation and propagation were also monitored using the DIC technique. To further understand the behaviour of both fibre types, cross-sectional analysis was carried out on a cracked section and results show steel fibres provide better resistance to cracking and improved mechanical properties than polypropylene fibres. An existing model was used to further show the behaviour of the specimens in tension.

## ACKNOWLEDGEMENTS

I would like to extend my gratitude to the following people:

- My supervisors, Dr. Alan Lloyd and Dr. Ted Moffatt, for their guidance and advice throughout the completion of my program. I really appreciate their help and support.
- The administrative staff of the Civil Engineering department, MaryBeth Nicholson, Alisha Hanselbacher and Alicia Farnham and the laboratory technicians for their assistance all through my stay as a Masters student at UNB.
- My parents, my siblings and entire family for their unconditional love, motivation and assistance during my studies in Canada.
- My friends and colleagues who have contributed in one way or the other towards the successful completion of my Masters program.

# Table of Contents

ABSTRACT.....	ii
ACKNOWLEDGEMENTS.....	iii
Table of Contents.....	iv
List of Tables.....	vii
List of Figures.....	viii
Nomenclature or Abbreviations.....	x
List of Symbols.....	xi
1.0. INTRODUCTION.....	1
1.1. General.....	1
1.2. Aims and Objectives.....	2
1.3. Scope of the Research.....	3
1.4. Outline of Thesis.....	4
2.0. LITERATURE REVIEW.....	6
2.1. Lightweight Concrete (LWC).....	6
2.1.1. Overview.....	6
2.1.2. History.....	6
2.1.3. Classification of Lightweight Concrete.....	8
2.1.4. Properties of Structural Lightweight Aggregate Concrete.....	15
2.2. Fibre Reinforced Concrete (FRC).....	18
2.2.1. Overview.....	18
2.2.2. History and Origin of FRC.....	20
2.2.3. Types of Fibres.....	22
2.2.4. Fibre Terminology.....	27
2.2.5. Mechanical Properties of FRC.....	28
2.2.6. FRC Testing Methods.....	32
2.2.7. Analysis, Design and Modelling of Fibre Reinforced Concrete.....	39
2.2.8. Pull-out Behaviour of Steel Fibres.....	54
2.2.9. Fibre Distribution.....	58
2.2.10. Finite Element Modelling.....	58

3.0. EVALUATION OF FLEXURAL BEHAVIOUR OF LOW-DENSITY FIBRE-REINFORCED CONCRETE USING DIGITAL IMAGE CORRELATION. <sup>1</sup> .....	59
3.1. Introduction.....	60
3.2. Materials .....	63
3.3. Mix Proportions .....	64
3.4. Specimen Preparation .....	64
3.5. Test Setup and Procedure.....	65
3.5.1. Compression Test.....	65
3.5.2. Flexural Test .....	65
3.5.3. Digital Image Correlation .....	66
3.6. Results and Discussions.....	67
3.6.1. Fresh Concrete Properties (Slump).....	67
3.6.2. Density .....	68
3.6.3. Compressive Strength .....	68
3.6.4. Flexural Strength.....	69
3.6.5. Crack Detection .....	71
3.6.6. Neutral Axis Movement.....	73
3.7. Conclusions.....	77
3.8. References.....	78
4.0. POST-CRACKING SECTIONAL ANALYSIS OF LOW-DENSITY FIBRE REINFORCED CONCRETE USING DIGITAL IMAGE CORRELATION (DIC) .....	80
4.1. Introduction.....	80
4.2. Experimental Work.....	83
4.2.1. Materials .....	83
4.2.2. Mix Design.....	84
4.2.3. Preparation of Test Specimens.....	85
4.2.4. Digital Image Correlation .....	86
4.3. Experimental Test and Results.....	88
4.3.1. Density and Slump.....	88
4.3.2. Compression .....	89
4.3.3. Flexure .....	93
4.4. Post-Cracking Sectional Analysis.....	97
4.5. Conclusions.....	107

4.6. References.....	109
5.0. MODELLING OF POST-CRACKING BEHAVIOUR OF STEEL FIBRE REINFORCED LOW DENSITY CONCRETE.....	112
5.1. Introduction.....	112
5.2. Experimental Program.....	116
5.3. Experimental Results.....	118
5.4. Determination of Post-Cracking Stress-Crack Width Relationship.....	123
5.5. Discussion of Results.....	127
5.6. Conclusion.....	127
5.7. References.....	128
6.0. SUMMARY AND CONCLUSION.....	132
6.1. Discussion.....	132
6.2. Conclusions.....	133
6.3. Recommendations for Future Research.....	135
7.0. REFERENCES.....	137
Curriculum Vitae	

## List of Tables

Table 2.1: Low-density aggregate concrete classified according to use and physical properties.....	14
Table 2.2: Physical properties of fibres. ....	27
Table 3.1: Properties of fibres.....	63
Table 3.2: Concrete mix proportions .....	64
Table 3.3: Concrete properties.....	68
Table 3.4a: Neutral axis position for SFRLDC .....	77
Table 3.4b: Neutral axis position for PFRLDC .....	77
Table 4.1: Properties of fibres.....	84
Table 4.2: Mix design details.....	85
Table 4.3: Concrete properties.....	90
Table 4.4: Values corresponding to points A, B, C, D .....	101
Table 4.5: Neutral axis and force locations corresponding to points on the Moment vs Curvature plots.....	105
Table 5.1: Mix proportions .....	117
Table 5.2: Properties of fibres.....	118
Table 5.3: Summary of results .....	120

## List of Figures

Figure 2.1: Classification of aerated concrete .....	10
Figure 2.2: Classification of lightweight aggregates. ....	12
Figure 2.3: Density range for lightweight concrete according to classification based on use. ....	14
Figure 2.4: Behaviour of fibre reinforced concrete. ....	20
Figure 2.5: Typical steel fibre geometries. ....	23
Figure 2.6: Typical steel fibre cross-sections. ....	24
Figure 2.7: Compressive behaviour of concrete. ....	30
Figure 2.8: Test set-up for uniaxial tension test.....	34
Figure 2.9: Test set-up for three-point bending test.....	35
Figure 2.10: Test set-up for four-point bending test. ....	36
Figure 2.11: Test set-up for wedge-splitting test. ....	37
Figure 2.12: Schematic of panel test according to ASTM C1550. ....	38
Figure 2.13: Photo of test set-up for panel test. ....	39
Figure 2.14: Crack propagation in plain concrete.....	41
Figure 2.15: Fictitious crack model. ....	42
Figure 2.16: Crack propagation in FRC.....	43
Figure 2.17: Zones of fracture process in fibre reinforced concrete.....	44
Figure 2.18: Stress vs crack width relationship for SFRC.....	47
Figure 2.19: Bi-linear relationship.....	48
Figure 2.20: Multi-linear relationship.....	49
Figure 2.21: Drop-constant relationship. ....	49
Figure 2.22: Stress-strain diagram according to. ....	51
Figure 2.23: RILEM stress-strain diagram . ....	52
Figure 2.24: Crack-band theory by Bazant and Oh. ....	53
Figure 2.25: Pull-out test configurations. ....	54
Figure 2.26: Pull-out of straight fibre. ....	56
Figure 2.27: Pull-out behaviour of hooked and straight fibres . ....	57
Figure 3.1: Test Setup for flexural test. ....	66

Figure 3.2: Speckle pattern on specimen .....	67
Figure 3.3: DIC setup .....	67
Figure 3.4: Load-Displacement curve for polypropylene fibre reinforced low-density concrete.....	70
Figure 3.5: Load-Displacement curve for steel fibre reinforced low-density concrete ....	70
Figure 3.6: Load-Displacement curve for non-fibre low-density concrete.....	71
Figure 3.7: Contour diagram showing longitudinal strain distribution.....	73
Figure 3.8: Neutral axis movement of PFRLDC shown from DIC .....	75
Figure 3.9: Neutral axis movement of SFRLDC shown from DIC .....	75
Figure 3.10: Neutral axis movement of SFRLDC plotted from DIC .....	76
Figure 3.11: Neutral axis movement of PFRLDC plotted from DIC .....	76
Figure 4.1: DIC test set-up.....	88
Figure 4.2: Speckle pattern on cylinder and prism. ....	88
Figure 4.3: Virtual extensometers shown on SFRLDC0.5 specimen.....	91
Figure 4.4: Stress-strain relationship in compression.....	92
Figure 4.5: Longitudinal strain on SFRLDC0.5 specimen for various loading stages .....	92
Figure 4.6: Load vs deflection curves.....	95
Figure 4.7: Contour diagram from DIC showing longitudinal strains along the prisms at various stages of loading .....	96
Figure 4.8: Moment vs curvature relationship for the steel fibre mix .....	99
Figure 4.9: Moment vs curvature relationship for the synthetic fibre mix.....	100
Figure 4.10: Modelled compressive stress-strain behaviour.....	102
Figure 4.11: Cross-section of beam showing stresses and strain profile .....	103
Figure 4.12: Force location versus curvature.....	106
Figure 5.1: Simplified post-cracking constitutive law.....	113
Figure 5.2: Test setup for flexural test.....	117
Figure 5.3: Crack mouth opening deflection shown in four-point bending.....	120
Figure 5.4: Load – CMOD relationships .....	122
Figure 5.5: Key points on Load-CMOD curve .....	125
Figure 5.6: Tensile stress vs crack width ( $\sigma - w$ ) curves obtained from inverse analysis .....	126

## **Nomenclature or Abbreviations**

AAC	- Autoclaved aerated concrete
AR-GRFC	- Alkali Resistant glass fibre reinforced concrete
CMOD	- Crack mouth opening deflection
DIC	- Digital Image correlation
EPS	- Expanded polystyrene
FRC	- Fibre reinforced concrete
fps	- Frame per second
GFRC	- Glass fibre reinforced concrete
HRWRA	- High range water reducing admixture
LDC	- Low density concrete
LWC	- Lightweight concrete
LVDT	- Linear variable differential transducer
PFRLDC	- Polypropylene fibre reinforced low density concrete
SFRC	- Steel fibre reinforced concrete
SFRLDC	- Steel fibre reinforced low density concrete
SIFCON	- Slurry infiltrated fibre concrete
SLS	- Serviceability limit state
THFRC	- Tension hardening FRC
TSFRC	- Tension softening FRC
ULS	- Ultimate limit state
W/CM	- Water cementitious material ratio
4PBT	- Four point bending test
3PBT	- Three point bending test

## List of Symbols

- $a$  = Shear span
- $a_g$  = Maximum size of aggregate in matrix
- $b$  = Width of section
- $c_1$  = Coefficient that accounts for beneficial effects of fibres on peak strength of matrix.
- $c_2$  = Coefficient that controls the steepness of the descending branch.
- $C$  = Compression force, N
- $d_f$  = Fibre diameter, mm
- $d$  = Depth of section
- $E_{co}$  = Measured modulus of elasticity in tension, MPa
- $f_{ct}$  = Tensile strength of concrete
- $f_w$  = Tensile stress carried by fibres
- $f_c$  = Concrete stress in the extreme compression fibre in bending, MPa
- $f_{cr}$  = Cracking strength of the concrete matrix, MPa
- $f_{Fi}$  = Post-cracking tensile strength at crack width  $w_i$ , MPa
- $f_{Fp}$  = Tensile strength at peak force in bending test for TSFRC inverse analysis, MPa
- $F_j$  = Represents the values of load corresponding to CMOD of 0.5, 1.5, 2.5 and 3.5 mm, respectively
- $F_1$  = Load in the four-point bending test corresponding to  $CMOD_1$  for the inverse analysis, N
- $F_2$  = Load in the four-point bending test corresponding to  $CMOD_2$  for the inverse analysis, N
- $F_3$  = Load in the four-point bending test corresponding to  $CMOD_3$  for the inverse analysis, N
- $F_4$  = Load in the four-point bending test corresponding to  $CMOD_4$  for the inverse analysis, N
- $L_f/d_f$  = Aspect ratio
- $\ell_F$  = Fibre length, mm
- $l_\tau$  = Critical fibre length
- $L_p$  = Length of the fracture process zone
- $L$  = Span in four-point bending test for both TSFRC and THFRC inverse analyses
- $M$  = Moment, kNm

- $P$  = Load measured in four-point bending tests to determine tensile properties of TSFRC and THFRC through inverse analysis, N  
 $P_{cr}$  = Cracking load in the four-point bending test for the TSFRC inverse analysis, N  
 $P_{max}$  = Maximum load in the four-point bending test used for the THFRC inverse analysis, N  
 $P_p$  = Maximum load in the four-point bending test for the TSFRC inverse analysis, N  
 $T$  = Tension force, N  
 $V_f$  = Fibre volume fraction  
 $w$  = Crack opening displacement  
 $W_T$  = Point of maximum effectiveness of fibres usually the crack width corresponding to the maximum post-cracking load.  
 $w_i$  = Crack width associated with the post-cracking strength  $f_{Fi}$ , mm  
 $w_m$  = Maximum crack width for which fibre contribution is considered at ULS for TSFRC associated with  $f_{Fm}$ , mm  
 $Y_T$  = Distance from extreme tension fibre to tension force of a cracked FRC section at SLS, mm  
 $Y_C$  = Distance from extreme tension fibre to compression force of a cracked FRC section at SLS, mm  
 $Y_{NA}$  = Distance from extreme tension fibre to neutral axis of a cracked FRC section at SLS, mm  
 $Y$  = Height of section  
 $\zeta(w)$  = Transition function representing a transition zone between cracking point and a point corresponding to where the influence of uncracked concrete are considered insignificant  
 $\delta$  = Displacement at mid-span measured in four-point bending tests to determine tensile properties of TSFRC and THFRC through inverse analysis, mm  
 $\varepsilon_c$  = Strain at the extreme compression fibre in bending  
 $\varepsilon_{cr}$  = Strain at the cracking strength of the concrete matrix  $\varepsilon_{cr} = f_{cr} / E_c$   
 $\varepsilon_{cu}$  = Ultimate compressive concrete strain (= 0.0035)  
 $\varepsilon_t$  = Strain at the extreme tension fibre in bending  
 $\varepsilon_{ts}$  = Tensile strain at SLS; strain variation under fatigue loading  
 $\varepsilon^{pcr}$  = Post-cracking strain  
 $\varepsilon$  = Strain  
 $\sigma$  = Concrete stress

$\sigma_w$  = Stress for a given crack width

$\sigma_t$  = Concrete tensile stress

$\sigma_c(w)$  = Stress carried by the concrete for a given crack width

$\sigma_f(w)$  = Stress carried by the fibres for a given crack width

$\emptyset$  = Curvature, 1/mm

$\rho_f$  = Fibre volume fraction

## **1.0. INTRODUCTION**

### **1.1. General**

The use of concrete can be seen in everyday life in bridges, buildings and dams. This use of concrete does not come without its short falls. A few of these short falls can be seen in its high self-weight, weakness in tension and brittleness among others. An effort to make concrete a more efficient material has resulted in inventions such as self-compacting concrete, lightweight concrete and fibre-reinforced concrete among others.

The use of lightweight concrete results in improved thermal insulation and reduced dead load of structures which ultimately results in fewer sections and a reduction in the size of columns, footings and other structural members thereby reducing overall construction costs (Kim et al., 2010).

Fibre-reinforced concrete on the other hand, is mainly advantageous from a structural standpoint in its improvement of the post-cracking resistance of concrete, and improved fracture properties through the ability of fibres to bridge cracks. In areas of cost reduction the use of fibres can be used to partially, and in some cases fully replace traditional reinforcement. Depending on the type of fibre used, this replacement means savings in cost of reinforcing steel bars which can be more expensive than fibres, savings in cost of labour needed to place bars and reduction in section sizes due to the fact that when more bars are needed the section size is often increased to accommodate the bars (Jansson, 2011).

Numerous studies on fibre reinforcement have highlighted the benefits in the ultimate and serviceability states of concrete. In the service states, the use of fibres provide improved crack resistance and controlled crack propagation. Improved ductility, increased load resistance and carrying capacity after cracking are some of the benefits in the ultimate limit state of concrete (Löfgren, 2005).

Both fibre-reinforced concrete (FRC) and lightweight concrete (LWC) have high potential in the construction industry and appear to be gaining wide acceptance as construction materials. Guidelines have been developed by RILEM TC 162-TDF (2002), ACI 544 (2010), and the fib model code (2010) for the use of FRC. Research also exists in literature with the aim of contributing to the validation of the use of FRC and relating to design such as Amin et al. (2014). The same can be said of LWC. Some noteworthy practical applications of FRC exist today including the oceanographic museum in Valencia (Serna et al., 2009) and tunnel linings (Nanakorn and Horii, 1996). An example of lightweight concrete construction is the Guggenheim museum in Bilbao, Spain (*fib*, 2000).

## **1.2. Aims and Objectives**

The main aim of this research work is to improve the current knowledge and investigate the mechanical properties and structural performance of expanded polystyrene low-density concrete containing fibre reinforcement. More specific objectives are;

- To compare the behaviour of various fibre types and volume fractions on mechanical properties of expanded polystyrene (EPS) low-density, fibre-reinforced concrete.
- To investigate crack formation and propagation.
- To investigate the applicability of digital image correlation (DIC) in measuring fibre reinforced concrete response under load.
- To investigate the behaviour of a cracked section of fibre reinforced concrete.

This will make it easier for engineers and researchers to characterize the behaviour of a combination of lightweight concrete and fibre reinforced concrete for design and modelling purposes.

### **1.3. Scope of the Research**

The scope of this study includes experimental and analytical investigations of expanded polystyrene low density fibre reinforced concrete specimens comprising of the following procedures:

- Literature review on previous experimental studies on the effects of fibre type, content and geometry on the properties of concrete.
- Evaluation of techniques used to produce light-weight concrete.
- Mix development and production of expanded polystyrene, low-density fibre-reinforced concrete specimens.

- Test concrete specimens to generate compression and flexural test data on effects of fibre types and contents using traditional testing methods and digital image correlation.
- Analyze test data and compare with test results obtained by other researchers.
- Report of results obtained during the study and presentation of design recommendations.

The work has been limited to investigations on synthetic and steel fibre reinforced low density concrete. The loading conditions investigated have also been limited to compression and bending using the ASTM four-point bending test (4PBT). The study was not focused on types of lightweight aggregates and their effects on concrete. Expanded polystyrene was only used to achieve a reduction in density.

#### **1.4. Outline of Thesis**

The thesis consists of an introduction, literature review, two publications, a chapter on modelling fibre reinforced concrete and conclusions.

The present chapter (Chapter 1) is part of the introduction and provides information regarding the aims, objectives, scope and background of thesis. The following chapters are as follows:

- Chapter 2 is an extensive review of the literature/state of the art on both fibre reinforced concrete and light weight concrete. A study on the history of both

concrete types is presented here. This chapter also highlights the types, structural applications and mechanical properties of FRC. A review of testing methods and models of FRC is also presented in this chapter.

- Chapter 3 (paper 1) is centered on the evaluation of flexural behaviour of the low density fibre reinforced concrete. The paper was aimed at validating DIC for measurement and data extraction purposes related to FRC. DIC was used to show the initiation and propagation of cracks and position and movement of the neutral axis which will be used in the next paper (Chapter 4) for sectional analysis.
- Chapter 4 (paper 2) is on sectional analysis of a wide range of mixes. Location and values of the compression and tension force at the critical cracked location were determined and DIC was also used throughout the work in measuring displacements, strains and position of the neutral axis.
- In Chapter 5, an existing model used to predict the post-cracking behaviour of FRC was examined and used to model select mixes.
- Conclusions and summary are presented in Chapter 6 together with recommendations for future research.

## **2.0. LITERATURE REVIEW**

### **2.1. Lightweight Concrete (LWC)**

#### **2.1.1. Overview**

Light weight concrete (LWC) is concrete with unit weight (density) lower than  $2350 \text{ kg/m}^3$ . It is used in modern day construction as an alternative to normal weight concrete due to the benefits of low density, higher specific strength (strength to weight ratio), thermal and sound insulation and fire resistance (Al-Khaiat and Haque, 1999).

Depending on the type of lightweight aggregate, the use of light weight concrete has also been known to effectively reduce the risk of earthquake damage as the magnitude and acceleration of earthquake forces is significantly affected by the weight of a structure (Sayadi et al., 2016; Muralitharan and Ramasamy, 2017). Most lightweight aggregates are manufactured from industrial by-products such as fly ash, expanded slag and are non-biodegradable which if left unused can result in pollution of the environment. The use of light weight aggregates in producing lightweight concrete has proven to be of benefit to the environment and can also be considered as an advantage (Al-Khaiat and Haque, 1998).

#### **2.1.2. History**

Lightweight concrete has been used in construction over 20 centuries ago in the Mediterranean region. Some noteworthy structures of the region are the port of Cosa built

in 273 B.C using volcanic material in making lightweight concrete, the pantheon dome completed in 27 B.C. with diameter of 43.3 m still in use today and the gigantic amphitheater 50,000 capacity Coliseum built in 75 to 80 A.D. with foundations cast using crushed volcanic lava lightweight concrete (ACI 213R-03). At the dawn of the 20<sup>th</sup> century, the modern lightweight concrete industry was started. In 1917, Stephen J. Hayde developed the rotary kiln process using heat to expand clays, slates and shale in the production of bricks (ACI 213R-03). The rejected bricks from the process were reduced to aggregate size and used as lightweight aggregate for concrete. In 1918 lightweight concrete with maximum density of 1760 kg/m<sup>3</sup> and compressive strength of approximately 27 MPa was used in the construction of ships and barges by the U.S. Emergency Fleet Building Corporation (ACI 213R-03). Post World War 2, extensive research was carried out by the Housing and Home Finance Agency, National Bureau of Standards and U.S. Bureau of Reclamation to determine the suitability of most lightweight aggregates for structural use in building frames, bridge decks and precast products. The Bank of America Corporate Center in Charlotte, the watergate apartments in D.C., the 42-story Prudential Life Building in Chicago and Hilton hotel in Dallas are among notable structures post World War 2 that were designed and built using lightweight concrete. (ACI 213R-03; Mindess et al., 2003).

### **2.1.3. Classification of Lightweight Concrete**

#### **2.1.3.1. Based On Method of Production**

Lightweight concrete can be produced by various means which forms one of the bases of its classification. These production methods can be by introduction of air into the mix, using lightweight aggregate or removing fine aggregates (Neville and Brooks, 2010; Malik, 2016; Muralitharan and Ramasamy, 2017). These methods are explained in detail in the following sections.

##### **2.1.3.1.1. No-Fines Concrete**

No-fines concrete is a type of lightweight concrete produced by removing fine aggregates from a normal concrete mix. It is a mixture of water, single-sized coarse aggregate, binder and admixtures when needed (Patil et al, 2017). This removal of fine aggregates creates interstitial voids and a reduced density (Muralitharan and Ramasamy, 2017). It is most times referred to as porous, pervious, or open textured concrete. This type of concrete was developed as a sustainable and eco-friendly means of construction mainly because of the need to eliminate the mining and extraction of river sand in some parts of the world. The demand and increase in cost of sand was also a factor that prompted researchers to develop this type of concrete thus solving the need for sand and also reducing the dead load of concrete. An advantage of using no-fines concrete is that it requires less cement in

production than normal concrete due to less surface area needed to be coated with cement paste, making it less expensive to make (Malik, 2016). When used as a pavement, it creates a permeable surface for storm water to filter through to the underlying soil and can be used to eliminate the need for storm water sewers (Patil et al, 2017).

#### **2.1.3.1.2. Aerated Concrete**

Aerated concrete is also referred to as foamed, gas or cellular concrete (Neville and Brooks, 2010). It is mainly produced by adding aluminum powder of about 0.2-0.5% mass of cement to a plastic mix. The aluminum powder reacts with the alkalis in the binder to produce hydrogen gas bubbles that create voids in the hardened matrix (Van Rooyen, 2013; Mohammed and Hamad, 2014). It can also be produced by using a foam generator or by adding a synthetic based foam-producing admixture to the mix resulting in foamed concrete (Mohammed and Hamad, 2014; Muralitharan and Ramasamy, 2017). This concrete type is known to be resistant to molds, rot and fire (Mohammed and Hamad, 2014). Figure 2.1 shows a classification of aerated concrete culled from Mohammed and Hamad (2014).

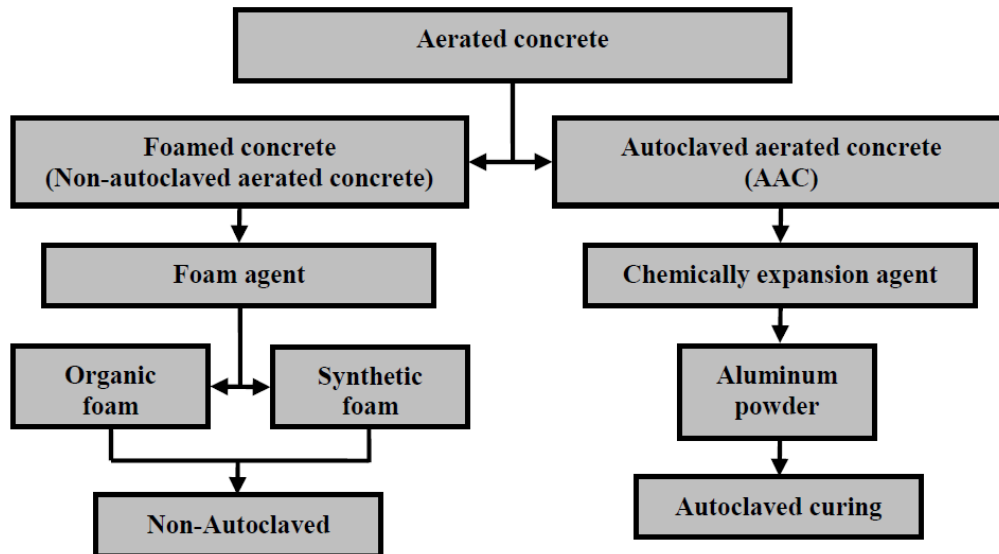


**Figure 2.1: Classification of aerated concrete (Mohammed and Hamad, 2014).**

#### **2.1.3.1.3. Lightweight Aggregate Concrete**

As the name implies, lightweight aggregate concrete is concrete produced using lightweight aggregates (LWA) typically as coarse aggregate. The use of lightweight aggregates is more expensive per cubic meter of concrete but can be cheaper in construction due to reduced dead load and smaller sections when compared to normal weight concrete (Mehta and Monteiro, 2006). According to ASTM C330-2014, the maximum bulk density of lightweight aggregates are  $1120 \text{ kg/m}^3$  and  $880 \text{ kg/m}^3$  for fine and coarse aggregate respectively. Lightweight aggregates can be grouped into natural lightweight aggregate and

artificial lightweight aggregate (Mohammed and Hamad, 2014; Eser, 2014). See Figure 2.2 for this classification.

Natural lightweight aggregates are those obtained from their natural deposits without any alteration to their nature. They are mostly of volcanic origin and obtained from volcanic rocks. Examples are pumice, tuff, scoria, and perlite (Mohammed and Hamad, 2014; Eser, 2014; Asik, 2006). Synthetic or artificial lightweight aggregates are expanded forms of materials. They are usually by-products of industrial process and are mostly produced by heat treatment from industrial processes such as rotary kiln processes, sintering processes and machine processes involving the agitation of molten slag. Examples are expanded clay, shale, slag, vermiculite, and expanded polystyrene (Zareh, 1971; Klieger and Lamond, 1994). Lightweight aggregates usually have a specific gravity less than 2.4 (Asik, 2006). The expanded polystyrene used in this study is a type of artificial lightweight aggregate with a density range of 11 to 32 kg/m<sup>3</sup>.

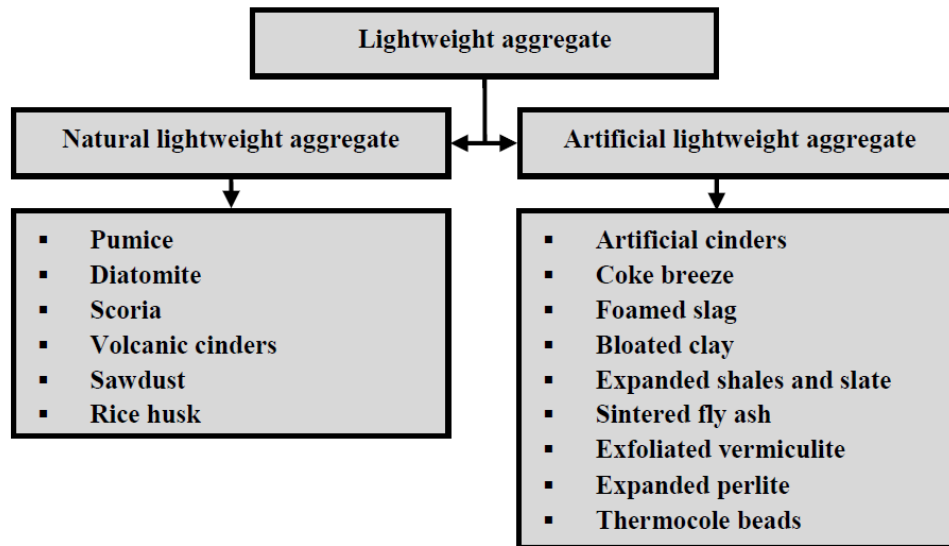


**Figure 2.2: Classification of lightweight aggregates (Mohammed and Hamad, 2014).**

### **2.1.3.2. Based On Purpose of Use**

ACI 213R-2003 classifies concrete under this category into three as structural lightweight concrete, moderate-strength lightweight concrete and non-structural low-strength concrete.

#### **2.1.3.2.1. Non-Structural Low-Strength Concrete**

Non-structural low-strength concretes are used mainly for high thermal resistance and insulation purposes not intended for exposed use (Klieger and Lamond, 1994). This concrete type is characterized by a compressive strength ranging from 1.0 MPa to 7.0 MPa and density of about 800 kg/m<sup>3</sup> (ACI Committee 213, 1987; Holm and Bremner, 2000). This concrete is covered by ASTM C332 (2009).

#### **2.1.3.2.2. Moderate Strength Lightweight Concrete**

Moderate strength lightweight concrete falls between the structural and non-structural lightweight categories and is used mainly for masonry works such as infills. Compressive strengths range from 7 MPa to 17 MPa. It has intermediate insulation properties (ACI 213R-87).

#### **2.1.3.2.3. Structural Lightweight Concrete**

Structural lightweight concrete has an air-dried density ranging from 1440 kg/m<sup>3</sup> to 1850 kg/m<sup>3</sup> and compressive strength greater than 17.2 MPa (ACI 213R-87). Insulation properties are very low for this concrete type (ACI 213R-87). Minimum compressive strength and specifications for this concrete class are given by ASTM C330 and ACI 318. Figure 2.3 shows ranges of density of each class of concrete.

The U.S. Army Corps of Engineers State-of-the-Art-Report (Holm and Bremner, 2000) gave another definition for high strength lightweight concrete with compressive strength higher than 35 MPa and density less than 2000 kg/m<sup>3</sup>. Table 2.1 shows a summary of classification of low-density concrete by ASTM.

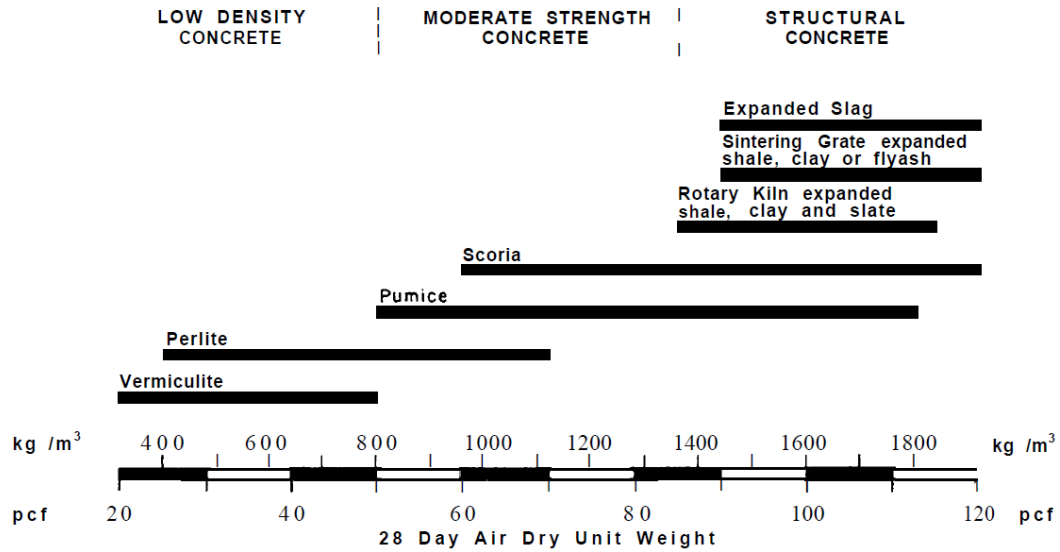


**Figure 2.3: Density range for lightweight concrete according to classification based on use (ACI 213R-87).**

**Table 2.1: Low-density aggregate concrete classified according to use and physical properties (Holm and Bremner, 2000).**

Class of Low-Density Aggregate Concrete	Type of Low-Density Aggregate Used in Concrete	Typical Range of Mass of Low-Density Concrete kg/m <sup>3</sup> (lb/ft <sup>3</sup> )	Typical Range of Compressive Strength MPa (psi)	Typical Range of Thermal Conductivities W/m · °K (Btu · in./h · ft <sup>2</sup> · °F)
Structural	Structural-grade LDA C 330	1,440 - 1,840 (90 - 115) at equilibrium	>17 (>2,500)	Not specified in C 330
Structural/Insulating	Either structural C 330 or insulating C 332 or a combination of C 330 and C 332	800 - 1,440 (50 - 90) at equilibrium	3.4 - 17 (500 - 2,500)	C 332 from 0.22 (1.50) to 0.43 (3.00) oven dry
Insulating	Insulating-grade LDA C 332	240 - 800 (15 - 50) oven dry	0.7 - 3.4 (100 - 500)	C 332 from 0.065 (0.45) to 0.22 (1.50) oven dry

## **2.1.4. Properties of Structural Lightweight Aggregate Concrete**

### **2.1.4.1. Compressive Strength**

Typical compressive strength values of 20-35 MPa are common for cast-in-place lightweight concrete (ACI Committee 213, 2003).

### **2.1.4.2. Splitting Tensile Strength**

Structural grade lightweight concrete is required to have a minimum splitting tensile strength of 2.0 MPa (ASTM C330). The splitting strength of lightweight concrete is about 75 – 100% of normal weight concrete of equal compressive strength. The use of normal weight fine aggregates are known to improve tensile strength of lightweight concrete (Klieger and Lamond, 1994). When lightweight specimens are moist cured, it is observed that the tensile strength is similar to the normal weight counterpart of equal compressive strength but when air-dried there is a reduction in tensile strength (ACI Committee 213, 2003).

### **2.1.4.3. Modulus of Elasticity**

Similar to normal density concrete, the elasticity of lightweight concrete is affected by the quantity of paste and aggregate and the individual modulus of their constituent materials. Differences in aggregate gradation have little or no effect on modulus of elasticity (ACI 213R-03; Aşık, 2006).

#### **2.1.4.4. Poisson's Ratio**

Poisson's ratio value varies with age of concrete, strength and aggregate used. A conservative value of 0.20 is assumed for design purposes when experimental data are not readily available (ACI Committee 213, 2003). Similar value was reported by Hoff et al. (1995) for normal weight concrete.

#### **2.1.4.5. Creep**

Creep in lightweight concrete can be reduced by 20-40% by using high-strength concrete. The method of curing also has an effect on creep as it can also be reduced by steam curing and low-pressure curing by 25-40% and 60-80% respectively (ACI Committee 213, 2003). Reichard (1964) and Shideler (1957) reported higher creep strains for low-density concrete when compared to their reference normal weight concrete.

#### **2.1.4.6. Drying Shrinkage**

Low strength lightweight concrete when compared to its normal weight counterpart has greater drying shrinkage and at higher strengths the shrinkage value is reduced. Holm and Bremner (2000) noted that shrinkage strains in lightweight concrete develop more slowly than normal weight concrete. The use of normal weight fines also reduces the problem of shrinkage. Steam curing can also be used to reduce drying shrinkage (ACI Committee 213, 2003).

#### **2.1.4.7. Modulus of Rupture**

Modulus of rupture is also a measure of the tensile strength of concrete. When moist-cured, the modulus of rupture is slightly different from the normal weight concrete counterpart (ACI Committee 213, 2003). Flexural strength of lightweight aggregate concrete was reported to be less than 4% of the compressive strength for air-dried specimens and 9 to 11% of continuously moist cured specimens (Hoff, 1992). Hoff (1992) also reported the modulus of rupture to be approximately 2/3 and 3/2 of the splitting strength for dry cured and moist cured specimens respectively.

#### **2.1.4.8. Thermal Properties**

The coefficient of thermal expansion (CTE) varies from  $7 \times 10^{-6}$  to  $11 \times 10^{-6}$  mm/mm/ $^{\circ}$ C for lightweight aggregate concretes and  $6 \times 10^{-6}$  to  $9 \times 10^{-6}$  mm/mm/ $^{\circ}$ C for normal weight concrete containing limestone aggregates and  $9 \times 10^{-6}$  to  $13 \times 10^{-6}$  mm/mm/ $^{\circ}$ C for those containing siliceous aggregates (ACI Committee 213, 1987). The CTE is governed by the expansion properties of aggregates, volume proportions of constituents and moisture content of the concrete (Holm and Bremner, 2000). When compared to normal weight concrete, this coefficient is lower for lightweight concrete (Neville, 2003).

#### **2.1.4.9. Shear**

Lightweight concrete has lower shear strengths and capacity in relation to normal weight concrete of the same compressive strength (Zareh, 1971; ACI Committee 213, 2003).

## **2.2. Fibre Reinforced Concrete (FRC)**

### **2.2.1. Overview**

Fibre reinforced concrete is defined by the American Concrete Institute as a composite material (concrete or mortar) made up of hydraulic cement, aggregates, and discrete discontinuous reinforcing fibres of various types, shapes and geometry (ACI Committee 544, 2010). As noted in the previous chapter, fibre reinforcement can be used for non-structural purposes in place of conventional reinforcement replacing traditional wire mesh fully for slabs on grade or in combination with rebars for structural elements such as columns and beams. Some characteristic advantages of fibre reinforcement in serviceability when compared with traditional reinforcement are fibres are dispersed within the cross-section while reinforcement bars are placed only where needed, fibres are also closely spaced while rebars are continuous (Löfgren, 2005). This however, can be a disadvantage in strength. Some of the advantages of FRC are seen in its crack control ability, improved flexural strength and toughness, improved ductility, increase in shear and torsional strength, increase in impact and shatter resistance and control of shrinkage cracking (ACI Committee 544, 2010).

In order to choose the most suitable fibre type, the desirable effects from the fibres should be considered. These effects can be structural in the case of crack control and improved strength or non-structural in the case of preventing shrinkage (Jansson, 2008). For fibres to

be effective in a concrete matrix, they must have the following properties; a tensile strength two or three times higher than the concrete, a bond strength higher or similar to the tensile strength of the matrix and elastic modulus higher than the concrete matrix (Naaman, 2003).

FRC can be classified based on its mechanical behaviour and response to loads as deflection or, tension hardening and deflection or tension softening. When hardening occurs, the post cracking tensile strength is usually higher than the first cracking strength and is accompanied by multiple cracks rather than a single crack. Strain softening on the other hand shows a decrease in strength with no further increase after first cracking. Hardening usually occurs when a higher volume fraction of fibres are used and it still depends on the properties of the fibres used. Concrete showing hardening behaviour is called high performance fibre reinforced concrete. Engineered cementitious composites developed at Michigan University is an example of strain hardening concrete (Li et al., 1995; Fischer and Li, 2006). Figure 2.4 shows these classes of fibre reinforced concrete behaviour.

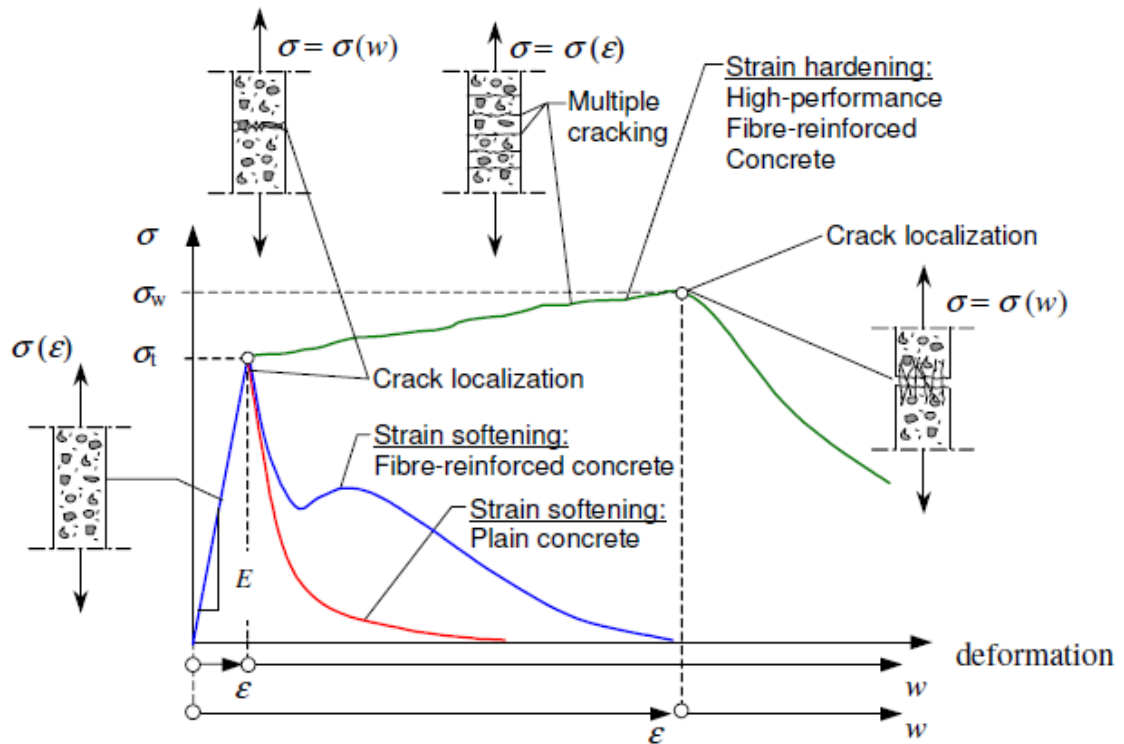


Figure 2.4: Behaviour of fibre reinforced concrete (Löfgren, 2005).

### 2.2.2. History and Origin of FRC

The use of fibres in construction is not an entirely new concept. It has been in existence since ancient times and can be traced back to mortar and sunbaked bricks used in construction of mud and clay huts which were reinforced with horse hair, straw, grass or natural fibrous materials (ACI Committee 544.1R, 2002). The 1540 built pueblo house which is considered the oldest house in the U.S. was built with sunbaked adobe reinforced with straw (ACI Committee 544.1R, 2002). In the late 1800s and early 1900s, it was

common practice to incorporate asbestos fibres and metallic waste in concrete (Oikonomou-Mpegetis, 2013; Tameemi and Lequesne, 2015). This use of asbestos began with the invention of the Hatschek process in 1898 and grew to become largely used but was later discovered to pose health risks. Due to the health risks researchers shifted the focus to alternative forms of fibre reinforcement (ACI Committee 544.1R, 2002). FRC development was given a boost with the invention of high range water reducing admixtures in the 1980s which proved to be the perfect cure for the workability problems posed by use of fibres and this subsequently gave rise to the increase in use of metallic fibres of different shapes and geometry (Dupont, 2003).

Early patents on FRC date back to the early 1900s. In 1914 W. Ficklen got a patent on inclusion of small metal segments in concrete mix (Oikonomou-Mpegetis, 2013). Other patents followed including A. Berard, USA, 1874; G. Martin, USA, 1927; G. Constantinesco, England 1943 (Löfgren, 2005).

In the 1960s, a major investigation was made in the United States to evaluate the potential use of fibres in concrete reinforcement with steel fibres as a case study. Other fibre types have also been used and investigated at the turn of the 20<sup>th</sup> century. In the 1950s, the USSR attempted the use of glass fibres in concrete. This led to the development of alkali-resistant glass fibres as it was observed that ordinary glass fibres were attacked by the alkali in cement. Further research has led to the development of synthetic fibres and more increased use of fibres in concrete mixes. In modern times, fibres are used not only in construction

but also in a wide range of engineering materials such as ceramics to improve composite properties (ACI Committee 544.1R, 2002).

### **2.2.3. Types of Fibres**

Various fibre types exist today for both experimental and industrial use. These fibre types are grouped into the following categories; steel fibres, synthetic fibres, glass fibres and natural fibres.

#### **2.2.3.1. Steel Fibres**

Steel fibres are small individual lengths of steel of various cross sections with an aspect ratio ranging from 20 to 100, diameter from 0.2 to 1 mm and length from 6.4 to 76 mm and made of either carbon steel or stainless steel. Steel fibres are known for their high strength and modulus of elasticity (ACI Committee 544.1R, 2002). Steel fibres are classified based on the product used in manufacture (ASTM A820, 2016) and the shape of the cross-section (JSCE standard III-1, 1983). Based on their method of production five types exist; cold-drawn wire, cut sheet, melt extracted, mill cut and modified cold-drawn fibres. Based on the shape of the cross-section we have; square section, circular section and crescent section (ACI Committee 544.1R, 2002).

The performance of steel fibres depends on their aspect ratio, the shape and geometry and surface treatment (if any). The change in geometry can be achieved by roughening the fibre or by mechanical deformations in order to improve the bond characteristics. This results in

crimped, coiled, twisted, hooked-end and indented fibres. Cross-sections of steel fibres can be circular, rectangular, square, triangular, polygonal or other shapes. The surface treatment of steel fibres is mostly for improved corrosion resistance (coated with brass) or improved bond characteristics (coated with zinc) (Löfgren, 2005). Figure 2.5 and 2.6 shows examples of some typical fibre geometries and cross sections respectively.

Fibre reinforced concrete containing steel fibres are referred to as steel fibre reinforced concrete (SFRC). SFRC can be produced by direct addition into the mix or can be pre-placed into a mould with the cementitious material subsequently infiltrated (slurry infiltrated fibre concrete, SIFCON).

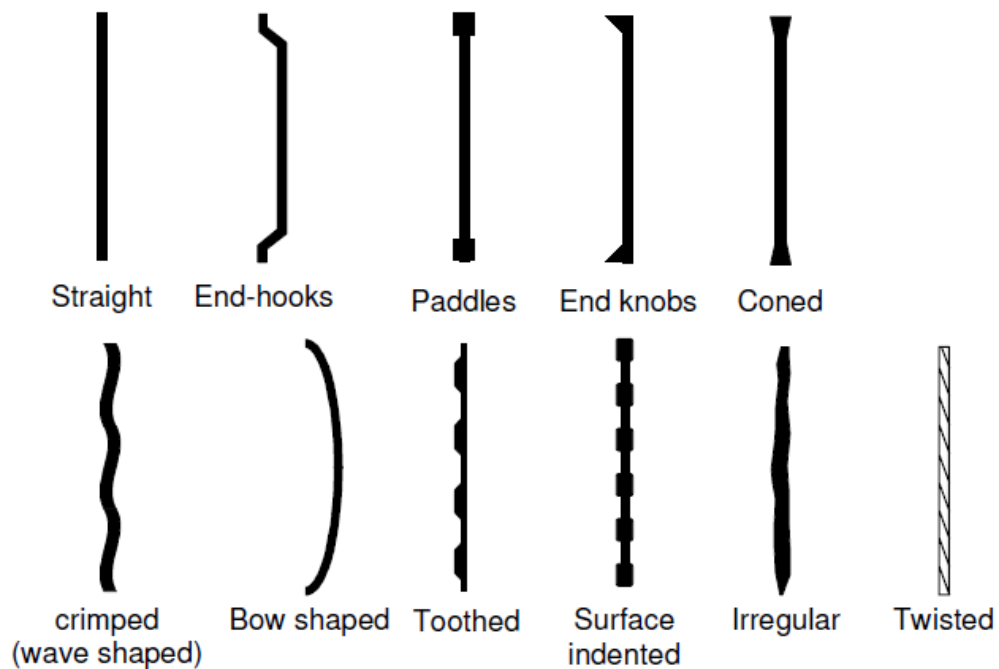


**Figure 2.5: Typical steel fibre geometries (Löfgren, 2005).**

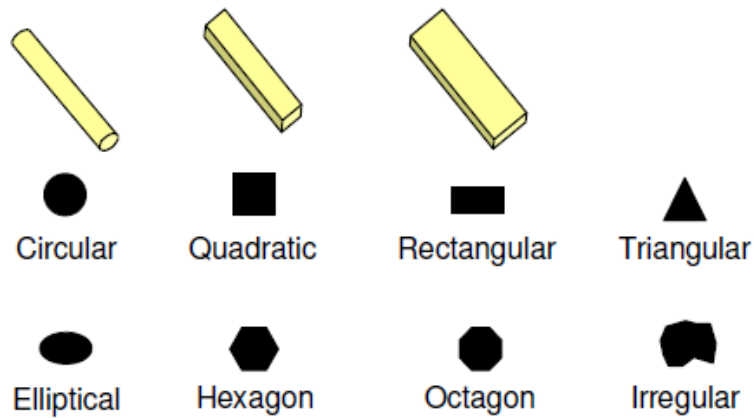


**Figure 2.6: Typical steel fibre cross-sections (Löfgren, 2005).**

### **2.2.3.2. Glass Fibres**

Glass fibres can be grouped into alkali-resistant and non-alkali-resistant. The non-alkali resistant fibres are borosilicate (E-glass) and soda-lime-silica (A-glass) fibres. The non-alkali resistant fibres are known to lose strength rapidly due to the high alkalinity of cement and are not usually used for construction works. Fibre reinforced concrete containing glass fibres are referred to as glass fibre reinforced concrete (GFRC) and are produced by either a spray up process involving mixing and depositing of the mix using a spray gun or by a premix method using traditional methods of mixing and placement. It is recommended that GFRC products be moist cured for a minimum of 7 days or produced with a 5% volume and no moist curing. Alkali Resistant GFRC (AR-GRFC) is a non-combustible material and has good freeze-thaw resistance when compared with unreinforced matrix. It can be used for concrete works because of its resistance to alkaline from cement. Some

applications of GRFC is in architectural works for the manufacture of building façade panels, surface bonding for sealing walls, and electrical utility products. It has also been used in marine applications for hollow buoys, floating pontoons, workboats, dinghies etc. (ACI Committee 544.1R, 2002).

#### **2.2.3.3. Synthetic Fibres**

Synthetic fibres are micro or macro man-made fibres from organic polymers in the textile and petrochemical industries. (ACI Committee 544.1R, 2002). Types of synthetic fibres that exist today include carbon, aramid, acrylic, nylon, polyester, and polyethylene and polypropylene fibres. These fibres have been observed to increase ductility, impact resistance, and provide improved toughness, shrinkage and crack control of concrete. Synthetic fibres typically have a diameter of 0.8 to 1 mm. The properties of synthetic fibres vary based on their modulus of elasticity (Löfgren, 2005).

#### **2.2.3.4. Natural Fibres**

Natural fibres as their name implies occur naturally and can be organic or inorganic, unprocessed or processed to enhance their abilities. Examples of natural occurring organic fibres are sisal, coconut, sugarcane, bamboo, cotton, and jute. Inorganic fibres include asbestos, wollastonite and basalt (ACI Committee 544.1R, 2002; Löfgren, 2005). Research has shown that the minimum effective fibre content for natural fibres is 3% by volume (Racines and Pama, 1978). Impact resistance has been observed to improve with use of

natural fibres. Natural fibre reinforced concrete has been used in the production of pipes, roof tiles, silos, panel linings, eaves, soffits and for fire insulation amongst others. Unprocessed fibre reinforced concrete is not durable as the alkaline in the mix deteriorates the fibres (ACI Committee 544.1R, 2002).

#### **2.2.3.5. Summary**

In general, the effectiveness of fibres in a mix depends on aspect ratio, tensile strength, and bond strength between fibres and matrix. For an equal volume of fibre, fibres with large aspect ratio will have a greater number of individual fibres (Tameemi and Lequesne, 2015). Some general properties of different fibres are given in Table 2.2.

**Table 2.2: Physical properties of fibres (Löfgren, 2005)**

Type of Fibre	Diameter [ $\mu\text{m}$ ]	Specific gravity [ $\text{g}/\text{cm}^3$ ]	Tensile strength [MPa]	Elastic modulus [GPa]	Ultimate elongation [%]
<b>Metallic</b>					
Steel	5-1 000	7.85	200-2 600	195-210	0.5-5
<b>Glass</b>					
E glass	8-15	2.54	2 000-4 000	72	3.0-4.8
AR glass	8-20	2.70	1 500-3 700	80	2.5-3.6
<b>Synthetic</b>					
Acrylic (PAN)	5-17	1.18	200-1 000	14.6-19.6	7.5-50.0
Aramid (e.g. Kevlar)	10-12	1.4-1.5	2 000-3 500	62-130	2.0-4.6
Carbon (low modulus)	7-18	1.6-1.7	800-1 100	38-43	2.1-2-5
Carbon (high modulus)	7-18	1.7-1.9	1 500-4 000	200-800	1.3-1.8
Nylon (polyamide)	20-25	1.16	965	5.17	20.0
Polyester (e.g. PET)	10-8	1.34-1.39	280-1 200	10-18	10-50
Polyethylene (PE)	25-1 000	0.96	80-600	5.0	12-100
Polyethylene (HPPE)	-	0.97	4 100-3 000	80-150	2.9-4.1
Polypropylene (PP)	10-200	0.90-0.91	310-760	3.5-4.9	6-15.0
Polyvinyl acetate (PVA)	3-8	1.2-2.5	800-3 600	20-80	4-12
<b>Natural - organic</b>					
Cellulose (wood)	15-125	1.50	300-2 000	10-50	20
Coconut	100-400	1.12-1.15	120-200	19-25	10-25
Bamboo	50-400	1.50	350-50	33-40	-
Jute	100-200	1.02-1.04	250-350	25-32	1.5-1.9
<b>Natural - inorganic</b>					
Asbestos	0.02-25	2.55	200-1 800	164	2-3
Wollastonite	25-40	2.87-3.09	2 700-4 100	303-530	-

#### 2.2.4. Fibre Terminology

Various terms are used in fibre reinforced concrete to characterize fibres. These terminologies do not depend on the fibre type or material properties but on their geometries (Löfgren, 2005). Some of them are;

- **Aspect ratio:** this is the ratio of the length to diameter of a fibre strand

- **Volume fraction:** this is the percentage of fibre in a fibre-reinforced concrete mix. Volume fraction ranges from 0.25% and 3% (Trub, 2011).
- **Multifilament:** many continuous filaments or strands of fibre. Usually natural or synthetic.
- **Monofilament:** a continuous fibre with a large diameter usually greater than 100 $\mu$ m.
- **Fibrillated:** a continuous networks of fibres with individual fibrils of fibres.
- **Bundled:** strands consisting of various filaments of microfibres.
- **Micro-fibres:** fibres with length less than maximum aggregate size in a matrix and cross-section diameter similar to cement grains.
- **Macro-fibres:** opposite of micro-fibres. That is with a length greater than maximum aggregate size.

## 2.2.5. Mechanical Properties of FRC

### 2.2.5.1. Compression

Compression strength of FRC is only slightly higher than its plain concrete counterpart. This increase is usually up to 15% for 1.5% fibre content for steel fibres. Polypropylene synthetic fibres show no effect on compressive strength with minor differences reported to be as a result of variations in experimental work, air contents and unit weights. The known difference was observed to be in the mode and mechanism of failure of specimens when

subjected to compression forces as they show a ductile pattern due to their ability to absorb energy. This was also observed for steel fibres (Kooiman et al., 2000; Lim and Nawy, 2005). The addition of fibres also are able to sustain loads and endure deformation without shattering (ACI Committee 544.1R, 2002).

Fibre orientation was also observed to affect compressive strength, with a reduction in crack propagation and higher strength observed for fibres oriented perpendicularly to the loading direction (Fanella and Naaman, 1985; Homrich & Naaman, 1987; Ezeldin et al., 1992; Barnes, 2007; Li & Mishra, 1992). A 50% increase in compressive strength was observed when the fibres were oriented randomly (Balaguru and Najm, 2004). A common consensus is that a strength increase is observed when fibres are not oriented parallel to the direction of the force. Neves et al. (2005) reported a slight decrease in the elastic modulus of concrete with addition of steel fibres to a matrix and attributed this decrease to the voids created from addition of fibres. A schematic of the compressive behaviour is also shown in Figure 2.7.

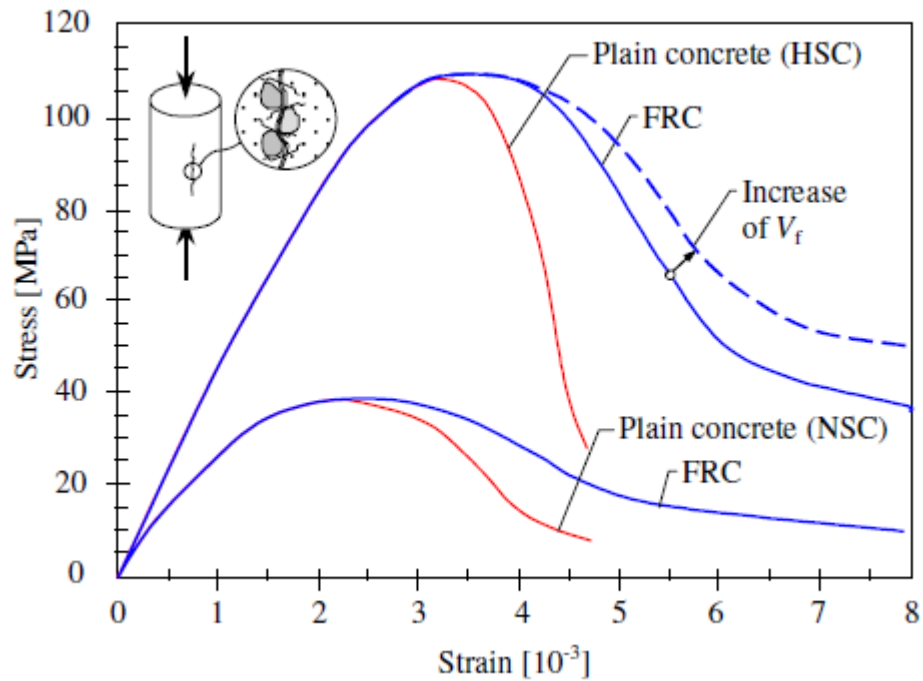


**Figure 2.7: Compressive behaviour of concrete (Löfgren, 2005).**

### 2.2.5.2. Tension

The primary reason for adding fibres to plain concrete is to improve its ductility and post-cracking capacity resulting in improved crack arrest and crack bridging mechanism (Oikonomou-Mpegetis, 2013). Addition of steel fibres increases the tensile strength of concrete (Homrich & Naaman, 1995; Balaguru & Najm, 2004). Barnes (2007) reported an increase in tensile cracking strength of about 10% with volume fraction of 1 to 2%. Gray and Johnston (1978), Williamson (1974) reported a 30-40% increase in strength for 1.5% volume fraction. As pointed out in Section 2.2.1, the behaviour of FRC in tension can be

either tension hardening or tension softening. When cracks develop, the fibres crossing the cross-section of the crack resist further opening by a bridging effect. If the fibres are pulled out or broken during cracking and cannot carry further stresses, the first crack strength in that case will be the ultimate strength which is characterized by the opening of a single crack. This is referred to as tension softening and it occurs mostly when low volume fraction of fibres are used. On the other hand, if the fibres are not broken and are able to carry more loads after the formation of the first crack, it results in the development of multiple cracks and this behaviour is tension or strain hardening (Löfgren, 2005; RILEM TC, 2002). Addition of synthetic fibres only slightly increases the tensile strength (Tameemi and Lequesne, 2015).

### **2.2.5.3. Flexure**

The addition of fibres to plain concrete can substantially increase its flexural response. Addition of fibres also increases fracture toughness and an increase in volume fraction results in an increase in fracture toughness (Oikonomou-Mpegetis, 2013). Deformed steel fibres were observed to be more effective in increasing flexural first cracking strength than synthetic fibres because of the low modulus of elasticity of synthetic fibres (Yurtseven, 2004; Naaman and Chandrangsou, 2003; Balaguru and Khajuria, 1996). Yurtseven (2004) reported that the flexural strength of FRC depends on the aspect ratio and volume fraction with higher volume fractions giving higher flexural strengths. Barnes (2007) reported a 10

to 80% increase in concrete flexural strength with fibre aspect ratios ranging from 30 to 120. Fibre geometry also has an effect on the flexural strength of concrete with deformed and hooked end steel fibres showing better post cracking strength than straight steel fibres due to the excellent bond between the deformed and hooked fibres and concrete matrix (Bentur & Mindess, 1990; Balaguru & Shah,1992). The effect of polypropylene fibres on the flexural strength have been reported to increase slightly at volume fraction of as low as 0.1% when fibrillated fibres are used (Ramakrishnan et al., 1987; Zollo, 1984).

#### **2.2.5.4. Shear**

Allos (1989) observed an increase in shear capacity of concrete with the addition of fibres. An increase in volume fraction also increases the shear strength and residual shear stress at different slip limits (Barragán, 2002). Darwish (1987) and Swamy and Bahia (1985) reported an increase in shear resistance with the addition of steel fibres. A number of researchers have investigated the use of steel fibres as a replacement for stirrups and found an increase in ultimate shear resistance and capacity with addition of fibres and increase fibre volume fraction (Yang et al., 2011; Hockenberry and Lopez 2012).

#### **2.2.6. FRC Testing Methods**

A number of test methods have been used to characterize directly or indirectly the behaviour of fibre reinforced concrete. These will be briefly introduced here. The following criteria should be considered when deciding an appropriate test method (Kooiman, 2000):

- The ease or complexity of test set-up, preparation of sample and execution of test
- The ability to reproduce the tests
- The cost and suitability in practice
- Reliability of test results and acceptance of test method by researchers.

#### **2.2.6.1. Direct Tension Test**

Also referred to as the uniaxial tension test, the direct tension test is proposed by RILEM TC162-TDF (2002). This is the most efficient and direct method to determine the uniaxial behaviour of fibre reinforced concrete. This test method is not easy to carry out as it requires more preparation time, relies on highly experienced personnel and is expensive when compared to other test methods (Kooiman, 2000). It is a suitable method to directly derive the stress-crack width relation of concrete (De Oliveira, 2010; Dupont, 2003). The test specimen is usually a cylinder with a notch at mid-height showing the point of least tensile strength and crack initiation. For a review of uniaxial test method, see Dupont (2003) and Löfgren, (2005). Figure 2.8 shows the test set-up of uniaxial test.

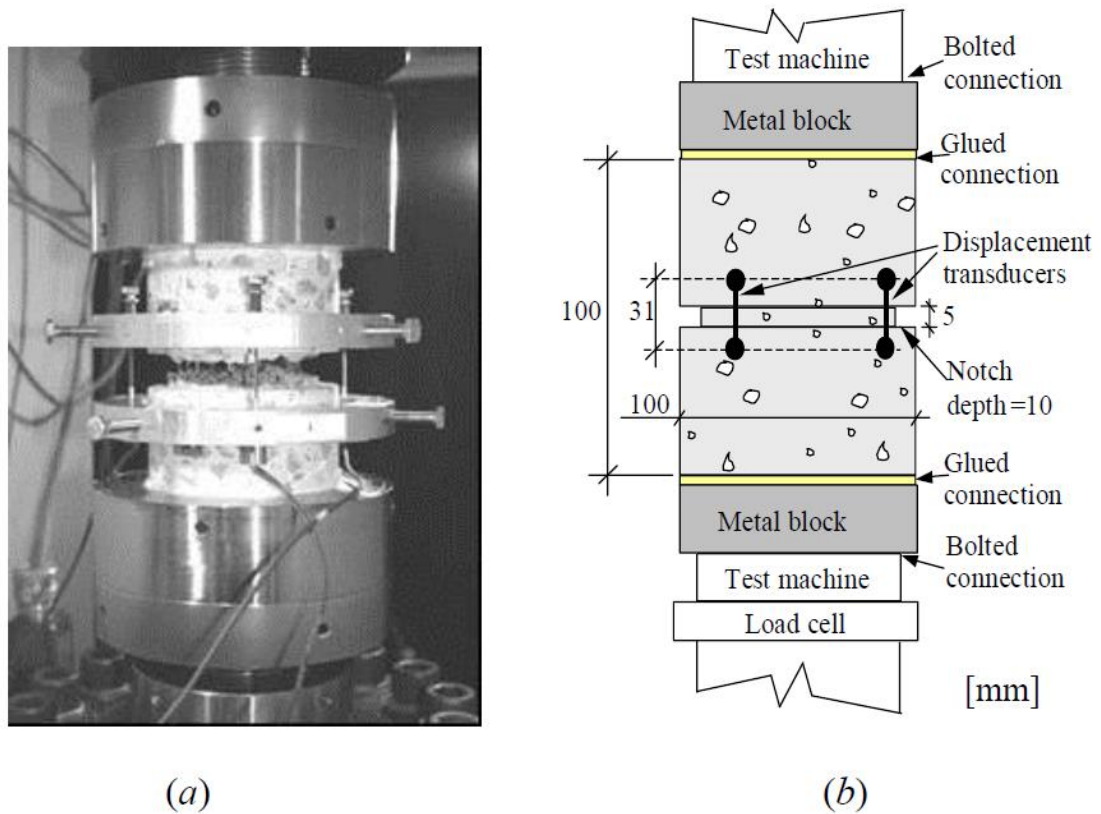


**Figure 2.8: Test set-up for uniaxial tension test (a) photo (b) schematic (Jansson, 2011).**

### 2.2.6.2. Flexural Bending Test

Flexural tests are performed on prisms (beams) in either three or four-point bending. This test method is widely used in various national and international standards such as JCI-SF4 (Japan), UNI U73041440 (Italy), ASTM C1018, ASTM C78, ASTM C1609, EN14845-1, RILEM TC162-TDF (Löfgren, 2005). Three or four-point bending tests are easier to carry

out than the uniaxial test. The time required to perform a bending test is less than the time to perform a uniaxial test (Dupont, 2003). The test specimen is a beam of length 500 to 600 mm with width and depth 150 to 155 mm and the span length is 500 mm. A notch of 25 to 45 mm is usually created at the center of the specimen mostly in three-point bending test for deflection softening FRC to create a path for the formation of a crack which forces the beam to fail at the notch. A notch is usually important when crack mouth opening displacement is measured during testing, however, a notch is not necessarily needed in four-point bending tests. Results from these tests are obtained as load-deflection curves. Figure 2.9 and 2.10 shows the test set-up for 3 and 4 point bending tests respectively.

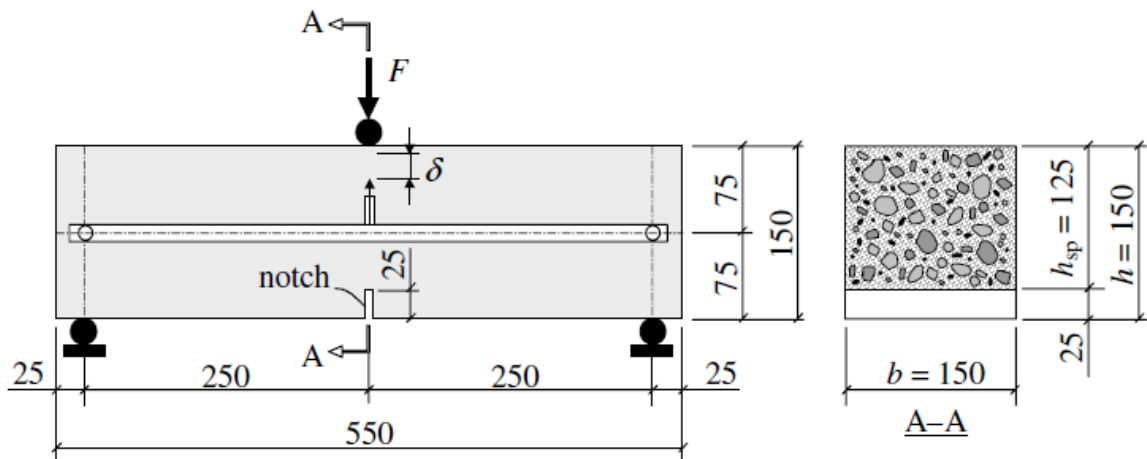


**Figure 2.9: Test set-up for three-point bending test (Löfgren, 2005).**

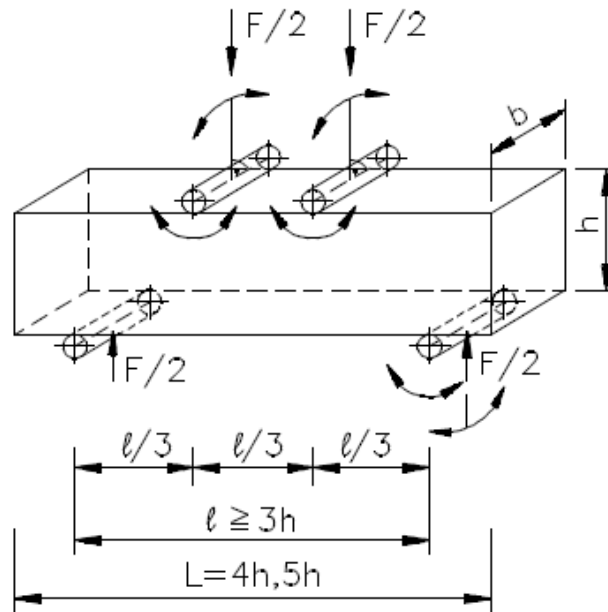


**Figure 2.10: Test set-up for four-point bending test (Dupont, 2003).**

### 2.2.6.3. Wedge Splitting Test

The wedge splitting test was originally proposed by Linsbauer and Tschegg (1986) and modified by Bruhwiler and Wittmann (1990). It is performed on 150 mm cubic specimens with a groove on one side and a notch at the middle of the groove to create a path for crack initiation. Two steel loading angles are placed on the corners of the groove and the specimen is loaded by forcing a wedge between the loading angles. A clip gauge is fixed over the notch to measure CMOD (Dupont, 2003). See Figure 2.11 for a schematic of this test set-up. The wedge splitting test does not directly give the stress-crack width relationship. To get this relationship, inverse analysis has to be carried out. For practical

and experimental use of wedge splitting test, see Jansson (2011), Jansson (2008), and Löfgren (2005).

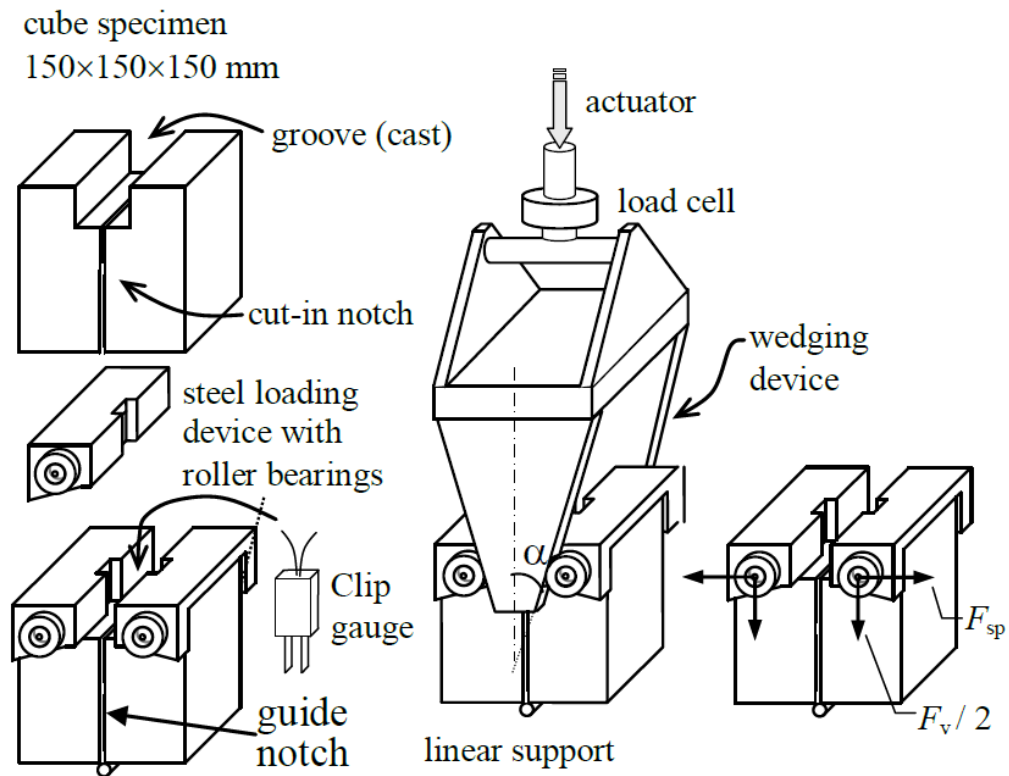


**Figure 2.11: Test set-up for wedge-splitting test (Löfgren, 2005).**

#### 2.2.6.4. Plate Tests

Plate tests (or panel tests) can be used as a substitute to beam tests. ASTM C1550 (2012), European Federation of Producers and Applicators of Specialist Products for Structures (EFNARC, 1996) and BS EN 14488 (2006) are methods of carrying out plate tests. ASTM C1550 uses molded round panels supported on three symmetrically arranged pivots and

subjected to a central point load through a hemispherical-ended steel piston going at a defined displacement rate. The fracture or flexural toughness is the area under the load-deflection curve and represents the energy absorbed by the panel. Panels experience bi-axial bending and the mode of failure is considered similar to the *in-situ* behaviour of structures and is categorized as a statically determinate test. The diameter of the test specimen is 800 mm with 75 mm depth. Figure 2.12 and 2.13 shows a schematic and photo of the test set-up respectively. EFNARC and BS EN 144488 are categorized as statically indeterminate and use square panels with dimension of 600 x 600 x 100 mm supported on each side with a clear span of 500 mm. The fracture toughness is also obtained similarly to the ASTM method by measuring the area under the load-deflection curve (Oikonomou-Mpegetis, 2013). Lambrechts (2007) observed the crack pattern to be unpredictable during tests using plates.

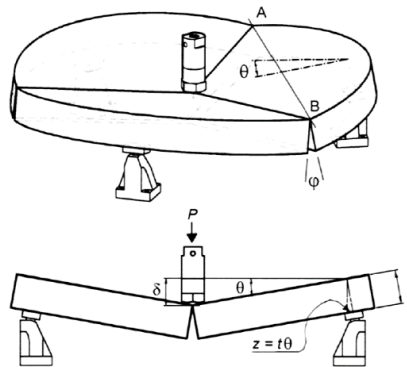


**Figure 2.12: Schematic of panel test according to ASTM C1550 (Bernard, 2005).**



**Figure 2.13: Photo of test set-up for panel test (Oikonomou-Mpegetis, 2013).**

### **2.2.7. Analysis, Design and Modelling of Fibre Reinforced Concrete**

The benefits and increased use of fibre reinforced concrete has given rise to the need for a suitable and reliable design model. Modelling of post-cracking behaviour of fibre reinforced concrete is based on several methodologies of existing constitutive laws (De Oliveira, 2010; Oikonomou-Mpegetis, 2013) including non-linear fracture mechanics and

finite element analysis. The mechanics of crack formation and crack propagation in materials is known as fracture mechanics (RILEM TC 162-TDF, 2000).

The behaviour of FRC in tension can be classified into the pre-cracking stage and the post-cracking stage. In the pre-cracking stage the effects of fibres are negligible with the stress-strain or load-displacement curve largely linear up until the first crack which is the point the tensile capacity is reached. The second and post-cracking stage is the stage of crack formation and softening behaviour mostly influenced by fibres (Dupont, 2003; De Oliveira, 2010). This softening behaviour can generally be modelled by various constitutive laws categorized according to their philosophy as; stress-crack width method, stress-strain method or crack band width theory (Kooiman, 2000; Oikonomou-Mpegetis, 2013).

#### **2.2.7.1. Stress-Crack Width**

The stress-crack width law assumes the existence of a cohesive zone to transfer stresses over a crack and is rooted on the fictitious crack model proposed by Hillerborg et al., 1976 (De Oliveira, 2010). Hillerborg et al. (1976) proposed for plain concrete that cracking is represented by a process zone and localized crack, with the localized crack consisting of aggregate interlock and traction free crack (also referred to as macro-crack) zones (Oikonomou-Mpegetis, 2013). This concept is illustrated with Figure 2.14.

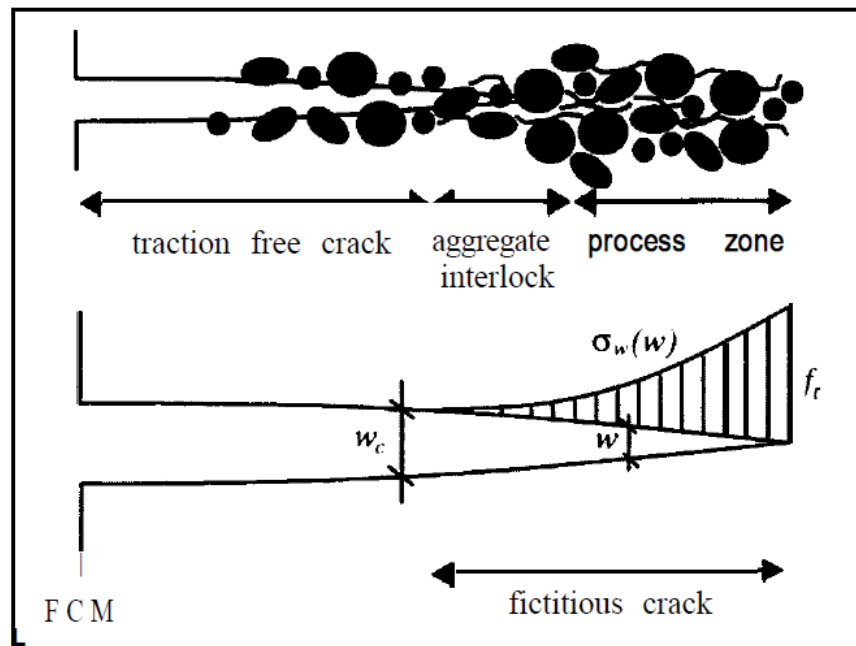


**Figure 2.14: Crack propagation in plain concrete (RILEM TC 162-TDF, 2002).**

Hillerborg et al. (1976) considered the stress-displacement,  $\sigma - \delta$  relationship as a stress-strain relation,  $\sigma - \varepsilon$  outside the fracture zone (pre-cracking) and a stress-crack width relation,  $\sigma - w$  within the fracture zone (post-cracking). This model assumes that over a length from the crack tip, a cohesive zone exists and stresses can be transferred over the cohesive zone till the critical crack width  $w_0$  is attained as shown in Figure 2.15. The length of the crack bridged by fibres determines the length of the cohesive zone (Kooiman, 2000). A crack is referred to as fictitious as long as stress transfer occurs as opposed to a real crack with no stress transfer (Jansson, 2008).

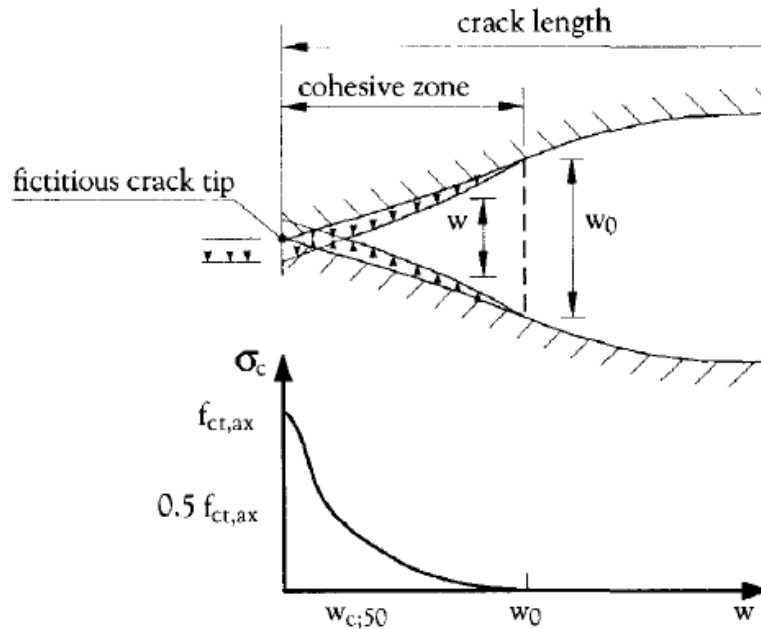


**Figure 2.15: Fictitious crack model (Hillerborg et al., 1976).**

Hillerborg (1980) went further to characterize fibre reinforced concrete behaviour with the fictitious crack model by considering the crack arrest and crack bridging mechanism from fibres. The fictitious crack model in fibre reinforced concrete consists of a process zone, aggregate interlock and fibre bridging (De Oliveira, 2010; Oikonomou-Mpegetis, 2013; RILEM TC 162-TDF, 2002) as shown in Figure 2.16. Hillerborg categorized the response of fibres into those that are fully anchored having an embedded length on both sides equal or greater than the critical fibre length  $l_f$  and those which the embedded length on one side is less than the critical fibre length  $l_f$  (Oikonomou-Mpegetis, 2013).

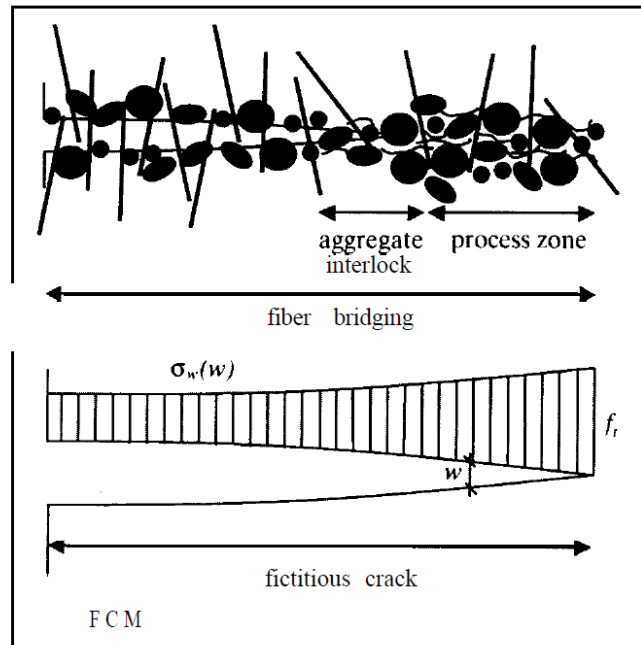


**Figure 2.16: Crack propagation in FRC (RILEM TC 162-TDF, 2002).**

Löfgren (2005) noted a combined bridging effect of aggregate and fibres and considered three distinct zones in fibre cracking; a traction free zone, a bridging zone with stress transfer by aggregate bridging and fibre pull-out and a zone of micro-cracking and micro-crack growth as shown in Figure 2.17.

Using the fictitious crack model and micro-mechanics concept, Li et al., (1993) developed a semi analytical modelling procedure from analyzing fracture process in uniaxial tension tests to derive the post-cracking properties of FRC.

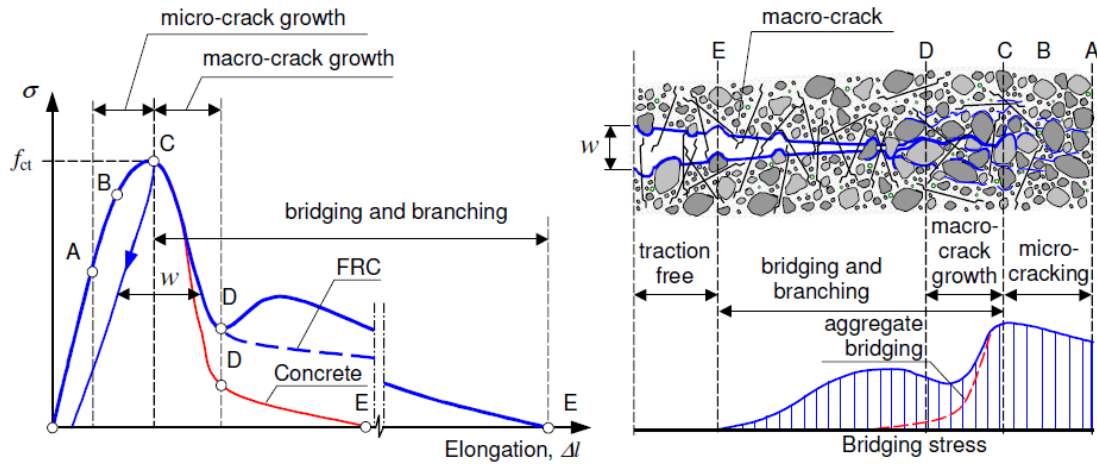


**Figure 2.17: Zones of fracture process in fibre reinforced concrete (Löfgren, 2005).**

#### 2.2.7.1.1. Inverse Analysis

Characterization of the softening branch may be done by using a direct or indirect inverse approach. A direct way of determining the stress-crack opening relationship is by uniaxial tensile tests. Inverse analysis is an alternative indirect method of determining the stress-crack opening relationship. It is also referred to as parameter or function estimation. The inverse approach has been used in modeling tensile behaviour of plain concrete (Roelfstra and Wittman, 1986) and this use was subsequently extended to SFRC (Barros and Figueiraas, 1999; Souse and Gettu, 2006). It involves a series of back calculations and iterations to fit experimental data so as to derive the parameters that define an assumed shape for the constitutive diagram using either the stress-strain or stress-crack width

relationship whereas the direct approach uses experimental values to obtain the parameters needed (Oikonomou-Mpegetis, 2013; De Oliveira, 2010; Kooiman, 2000).

Löfgren (2005) made the following recommendations when performing inverse analysis on FRC;

- The tensile strength should be derived from separate experiments but can also be obtained from previous data. When splitting tests are used to derive the tensile strength, it should be done on a plain concrete mix of the same properties but not including fibres.
- The slope of the first descending part for a deflection softening FRC should be steep and sufficient points used to define the remaining parts
- Information about the behaviour of the fibre being used and how they affect the shape of the stress-crack relationship is needed
- The right fitting interval should be chosen carefully with the purpose of fitting the most important part of the experimental curve. A particular stress-crack width relationship may be better for a test with lesser deflection but may not be suitable for another test with larger values of deflection.

Some of the disadvantages or drawbacks of inverse analysis as outlined by De Oliveira (2010) include:

- The need for experimental characterization

- Due to different production methods, batch size, etc. the fibre reinforced concrete properties used in experiments are likely to vary from the ones in actual applications.
- Knowledge of a materials post cracking behaviour can only be gained by trial and error.
- The deviation tolerance and convenience of the chosen shape of the constitutive diagram determines the appropriateness of the experimental fitting
- The procedure gives debatable constitutive models because the numerical method gives the parameters that best fit an already assumed shape for the diagram.

#### **2.2.7.1.2. Design Relationships for Stress-Crack Opening**

Stress-crack width relationships can be determined directly through uniaxial tension tests and can be divided into fibre and concrete contributions. The shapes of these relationships for FRC, however, are affected by factors such as the fibre type and volume fraction in the mix (RILEM TC 162-TDF, 2002). A softening stress-crack opening relationship defines the concrete contribution of the unreinforced concrete and the fibre contribution consists of an ascending and slowly descending part. The combined responses of the fibre and concrete can be summed up by a descending part followed by an ascending part and finally a descending or softening part as shown in Figure 2.18 (Amin et al. 2014). These

relationship based on their shapes are introduced in the following sections (RILEM TC 162-TDF, 2002).

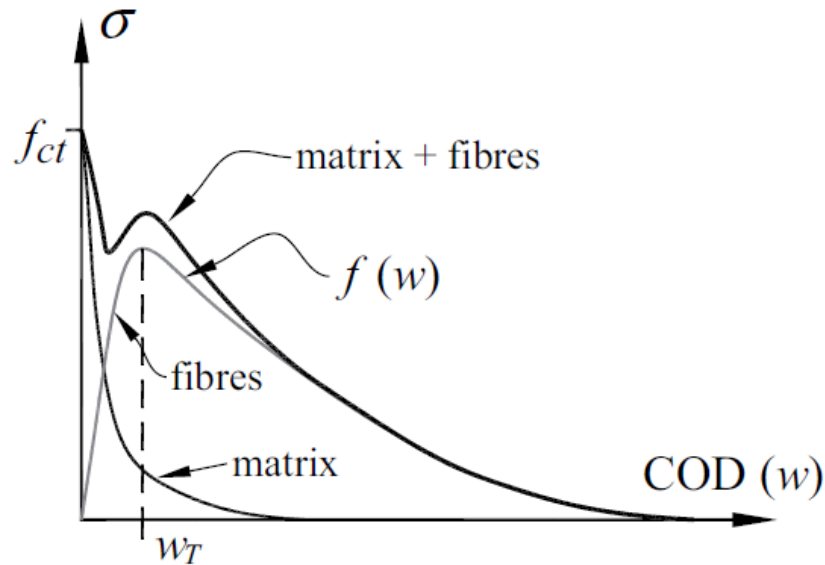


**Figure 2.18: Stress vs crack width relationship for SFRC (Amin et al. 2014).**

#### 2.2.7.1.2.1. Bi-Linear Relationship

A bilinear relationship may be used to define the stress-crack width relationship. When using this approach, four material parameters are required (RILEM TC 162-TDF, 2002) or five when  $E_c$  (Young's modulus) is considered (Jansson, 2008). They are the tensile capacity of the matrix ( $f_{ct}$ ), the slope of the first branch ( $a_1$ ), the slope of the second branch ( $a_2$ ) and the point where the second branch crosses the y-axis ( $b_2$ ). For examples using this relationship see Roelfstra and Wittmann (1986), Bolzon et al (2002), Østergaard (2003). This relationship is shown in Figure 2.19.

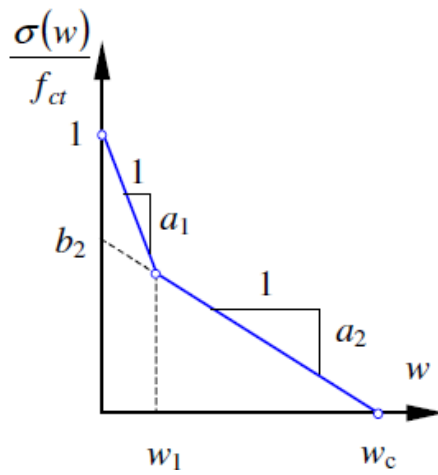


**Figure 2.19: Bi-linear relationship (Löfgren, 2005).**

#### **2.2.7.1.2.2. Poly-Linear or Multi-Linear Relationship**

Poly-linear (multi-linear) relationships are shown in Figure 2.20. An assumption when using this approach is that the tensile strength is never attained a second time after softening has occurred. See Nanakorn and Horri (1996b), Kitsutaka (1997) for examples of poly-linear relationships in FRC.

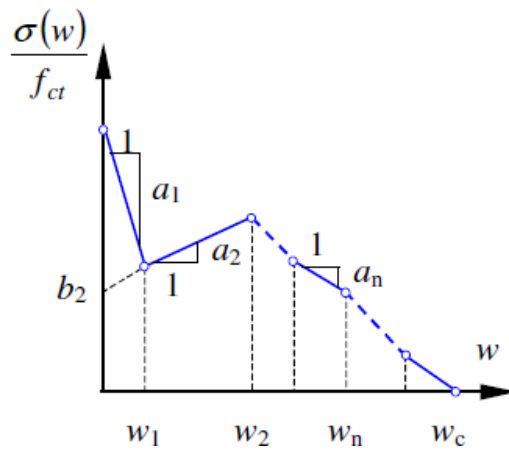


Figure 2.20: Multi-linear relationship (Löfgren, 2005).

### 2.2.7.1.2.3. Drop-Constant Relationship

In the drop-constant relationship approach, three material parameters are needed to describe the stress-crack width relationship. It is a more simple representation from a design standpoint and is illustrated in Figure 2.21 with the constant stress level as the residual strength (RILEM TC 162-TDF, 2002).

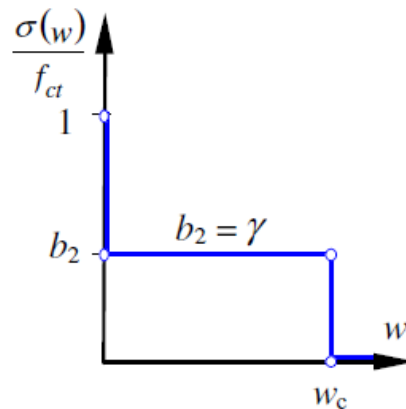


Figure 2.21: Drop-constant relationship (Löfgren, 2005).

Other forms of relationships that exist include the exponential relationship proposed by Hordijk (1991), the free form relationship (RILEM TC 162-TDF, 2002) and the simple constant relationship which neglects the tensile strength.

#### **2.2.7.2. Stress-Strain Law**

Stress-strain modelling procedures have been proposed for the German stress-strain model (DBV 1992) and the RILEM TC 162 (2002) modelling method. A general advantage of the stress-strain model is that the complete uniaxial behaviour of the material is modelled in one diagram making it easy to use in cross-sectional analysis (Kooiman, 2000). Another advantage of the stress-strain model is that it can easily be used in structural design applications as a result of the compatibility of the strain concept in design with other material types and its resemblance to traditional reinforced concrete design procedure (De Oliveira, 2010). Using the stress-strain relation also makes it possible to characterize the material both in tension and compression. Using this approach, the tensile stress is calculated with regard to strain (Oikonomou-Mpegetis, 2013).

The German concrete society (DBV 1992) was the first design guideline to make use of the stress-strain relation. It uses experiments from four-point bending tests to model the stress-strain behaviour (Kooiman, 2000). Figure 2.22 shows the stress-strain concept according to the German method.

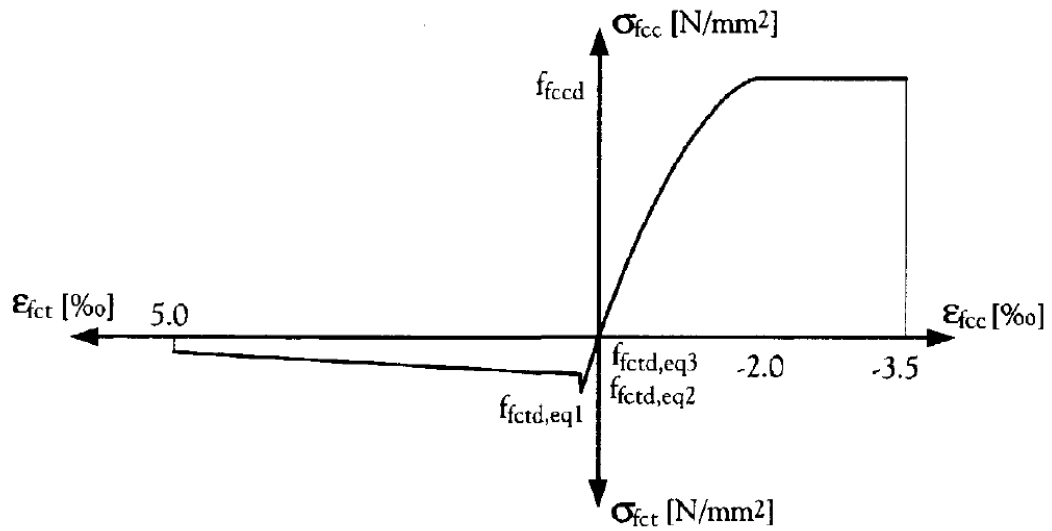
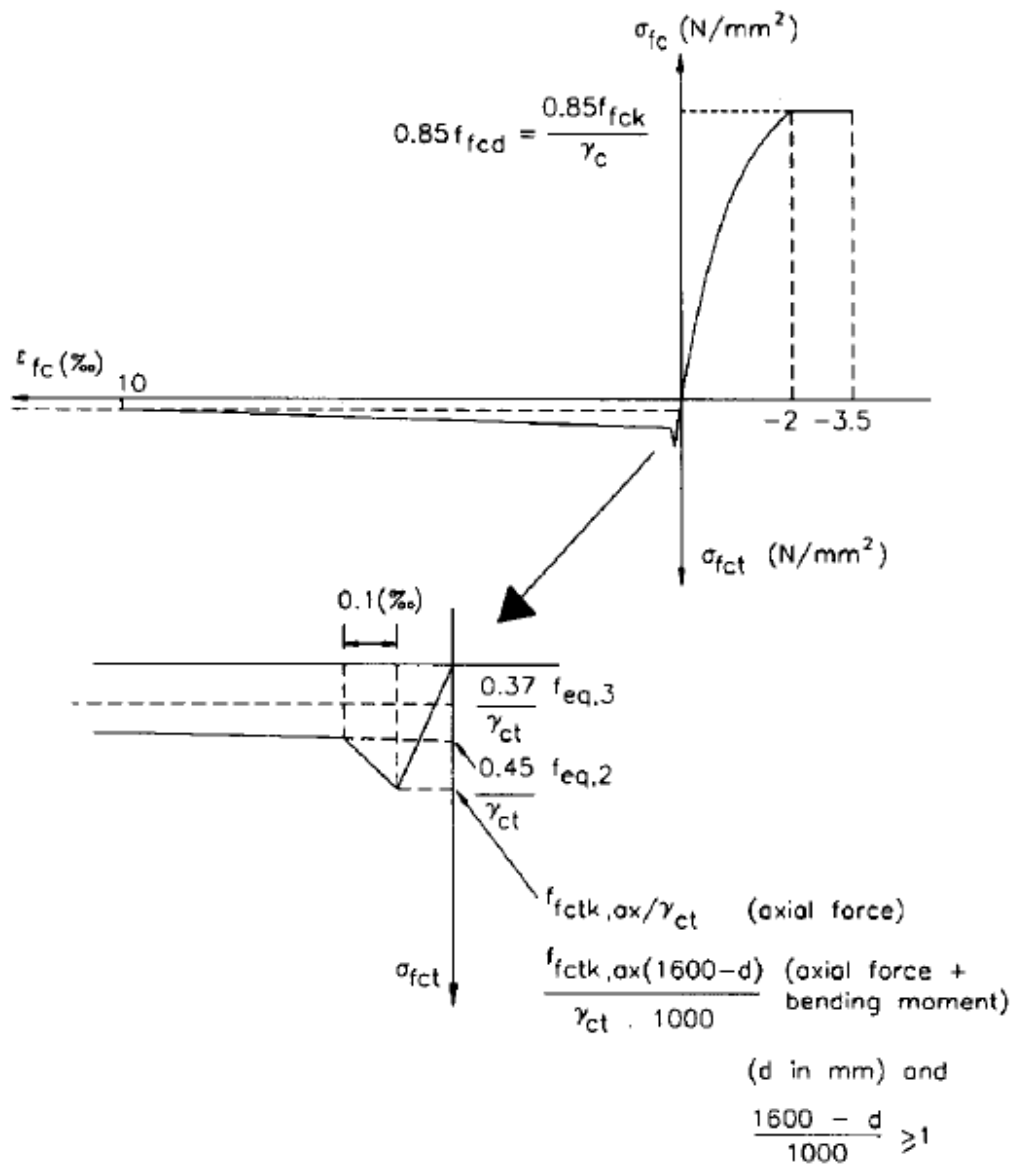


**Figure 2.22: Stress-strain diagram according to (DBV, 1992).**

The RILEM TC 162 (2002) method is quite similar to the German model. They both make use of a trilinear stress-strain relation and equivalent flexural tensile strengths to characterize post-cracking behaviour but differs in the use of three point bending tests and its use in all types of structural loadings conditions and applications. Another difference is the introduction of a factor of 0.85 accounting for time dependent behaviour and a partial factor of safety to create a design value. It also does not show a rapid drop in peak load in the tension region (Kooiman, 2000). This concept is shown in Figure 2.23.



$\gamma_c$  : partial safety factor for steel fiber reinforced concrete in compression  
 $\gamma_{ct}$  : partial safety factor for steel fiber reinforced concrete in tension

**Figure 2.23: RILEM stress-strain diagram (RILEM TC 162-TDF, 2002).**

### 2.2.7.3. Crack Band Width

The crack band width theory was initially developed by Bazant and Oh (1983) and is somewhat similar to the stress-crack width philosophy. It is based on the assumption that rupture in a heterogeneous material can be modelled as a strip of parallel, closely distributed micro cracks as against the stress crack width models where a singular line crack is presumed (Kooiman, 2000). Bazant and Oh (1983) stated that if the relation of the normal stress ( $\sigma_{ct}$ ) and the relative displacement ( $\delta$ ) across a line crack is the same as the relationship of the normal stress and displacement  $\delta = \epsilon_c \cdot l_{cb}$  obtained by summing the strains due to micro cracking over the crack band width  $l_{cb}$ , then the line crack model and the crack band model are similar. In this theory, a stress-strain relationship is developed for a crack by converting the width of the crack to strain. It is used mostly with finite element modelling and is associated with the smeared crack approach of finite modelling of plain or reinforced concrete (Kooiman, 2000; Oikonomou-Mpegetis, 2013). This concept is shown in Figure 2.24.

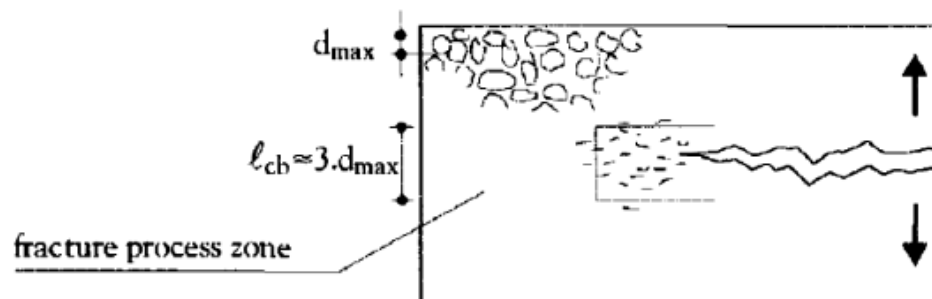


**Figure 2.24: Crack-band theory by Bazant and Oh (Kooiman, 2000).**

### 2.2.8. Pull-out Behaviour of Steel Fibres

The crack bridging abilities of fibres is provided through a bond-slip mechanism between the fibres and the matrix (De Oliveira, 2010). Guerrero and Naaman, (2000) highlighted that in spite of all the research done thus far, there was no available standard method used to measure the bond in fibre reinforced composites. This bond has been measured by indirect methods of single fibre pull-out experimental tests. Pull-out of fibres depend on the geometrical and mechanical properties of the fibre and also chemical affinity of the fibre to the matrix (e.g. whether a chemical bond can develop between the fibre and cement/matrix). Pull-out energy increases with increased fibre embedment length but if the embedment length is too long the fibre breaks (Löfgren, 2005). The pull-out tests that exist in literature are classified according to their geometry as hooked and straight fibres. Figure 2.25 shows various configurations of the pull-out tests.

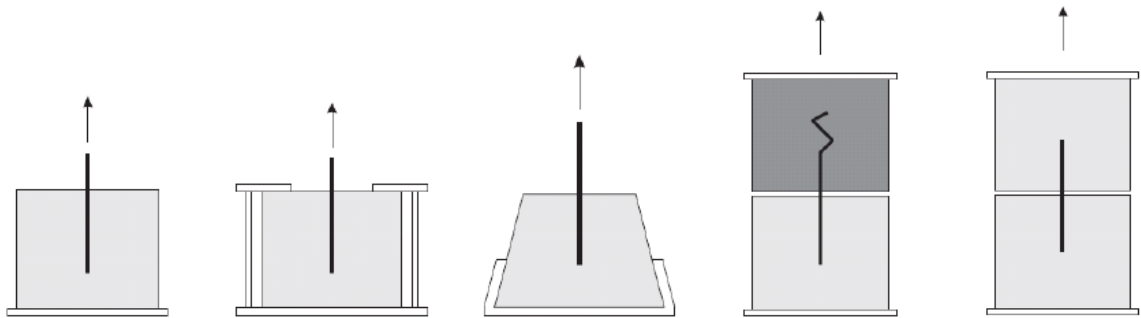


**Figure 2.25: Pull-out test configurations (Cunha et al., 2007).**

### **2.2.8.1. Straight Fibres**

Early experimental work on pull-out tests were carried out by Naaman and Shah (1976), Shannag et al., (1997) and Guerrero and Naaman, (2000). Researchers have developed models to predict the pull-out curve from an assumed bond-slip relationship (Naaman et al 1991, Banholzer et al 2005). Fibre orientation and inclination angle is however a factor in the pullout and bond-slip relations (De Oliveira, 2010; Löfgren, 2005). Naaman and Shah (1976) observed that it required more work to completely pull-out an inclined fibre than a fibre aligned with the load direction. They also observed the peak pull-out load of an inclined fibre was almost similar to an aligned fibre. Fibre bending, matrix spalling and local friction effects are considered in modelling the pull-out of fibres (De Oliveira, 2010). Several modelling approaches are based on energy failure criteria or cohesive interface model. It is difficult to measure the critical interface debonding energy (Shah and Ouyang, 1991). In the cohesive interface model, heavy numerical iterations are required because bond properties need to be measured in each case and cannot be generalized (Shah and Ouyang 1991; Fantilli and Vallini 2007).

Morton and Groves (1974) modelled the bridging force accounting for bending of a fibre and were able to predict the maximum force required to produce a given deflection of an elastic or perfectly plastic fibre in an epoxy matrix. They neglected friction and debonding in their assumptions thus making the model inapplicable to cementitious composites. Li et al. (1990) simulated fibre pullout on an elastic matrix as a beam bending and deformation

was assumed to occur at the exit point of the fibre. Cailleux et al. (2005) developed an analytical model for the pullout of inclined fibres based on strength of materials. Fibre bending, matrix spalling and concentrated friction load at matrix exit point were considered in their model. A typical pullout curve of a straight fibre is shown in Figure 2.26. The initial part of the curve 0-A represents elastic or adhesive bond, point A-B represents initiation of debonding, point B represents full debonding and point B-F represents complete pull-out of the straight fibre (Löfgren, 2005).

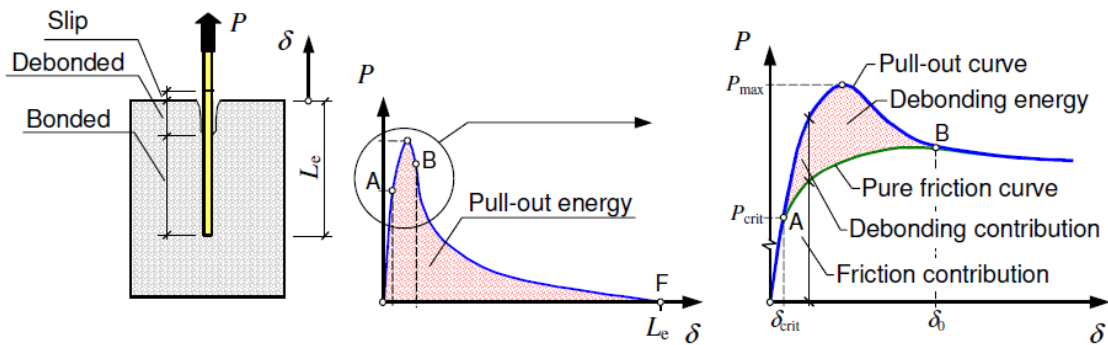


**Figure 2.26: Pull-out of straight fibre (Löfgren, 2005).**

### 2.2.8.2. Deformed Fibres

The need to improve the bond-slip relationship between fibres and cement gave rise to the advent of deformed fibres. The introduction of hooked and deformed fibres shifted the focus on modelling pullout behaviour from straight fibres to hooked fibres. Van Gysel (2000) developed a procedure based on the principle of conservation of energy and accounts for fibre debonding, plastic deformations and additional frictional forces due to

the hook. Alwan et al. (1999) developed a model based on frictional pulley and two plastic hinges to simulate hook action. Sujivorakul et al., (2000) developed a new model based on the concept of non-linear springs to represent the effects of the hook. The focus on these models are on the effects of the hooks on the pull-out response. Other researchers have focused on the influence of fibre inclination angle and embedded length on the pull-out behaviour (Banthia and Trottier, 1994; Armelin and Banthia 1997; Robbins et al 2002). Figure 2.27 shows a comparison between hooked and straight steel fibres on pull-out behaviour. The initial/ascending part of the curve OA represents elastic or adhesive bond, point A-B represents initiation of debonding, point B represents full debonding, in the case of hooked fibre BC represents increase in load due to mechanical anchorage, CD represents slip and progressive deformation from the matrix is represented by DE. EF represents a frictional decaying phase when the end anchor has been completely pulled out and straightened (Löfgren, 2005).

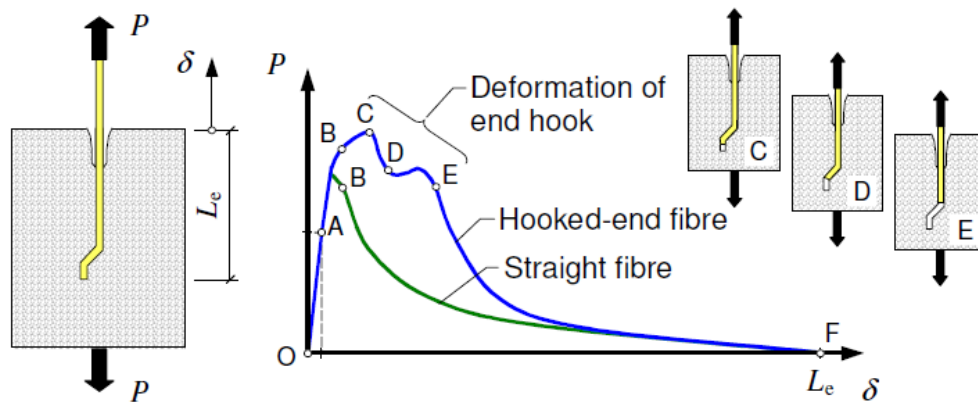


**Figure 2.27: Pull-out behaviour of hooked and straight fibres (Löfgren, 2005).**

### **2.2.9. Fibre Distribution**

The post-cracking response of fibre reinforced concrete to an extent depends on the distribution and orientation of fibres (Oikonomou-Mpegetis, 2013). Factors such as geometry, placement method, equipment used (e.g. pumping), and properties of fresh concrete (resistance against fibre segregation) influence the orientation and distribution of fibres (Löfgren, 2005). Oikonomou-Mpegetis (2013) quantified the effects of fibre distribution on structural behaviour by dividing a beam of hardened FRC into three zones. They observed a varied concentration of fibres at these zones and a slight difference in the structural responses of one of the beams which was attributed to the relatively low fibre count in the bottom third.

### **2.2.10. Finite Element Modelling**

Finite element (FE) modelling involves choosing a stress-opening relationship and using it as a material input and performing trials until FE results agree with experimental results with enough accuracy. Software such as DIANA can be used to perform these analysis on FRC (Jansson, 2008). For examples on the use of finite element modelling of FRC see Hemmy et al. (2002), Kanstad and Døssland (2003). Several methods of finite element modelling involving smeared crack concept and discrete crack approach exists but is not within the scope of this study.

### **3.0. EVALUATION OF FLEXURAL BEHAVIOUR OF LOW-DENSITY FIBRE-REINFORCED CONCRETE USING DIGITAL IMAGE CORRELATION.<sup>1</sup>**

Ibeawuchi, John, Moffatt, Edward and Lloyd, Alan

**Abstract:** Over the years, fibre-reinforced concrete has gained popularity in structural applications through studies on its behaviour. Despite these studies there is a need to fully understand the flexural behaviour of fibre-reinforced concrete (FRC). This paper presents the results of an experimental program to investigate the mechanical properties and post-cracking behaviour of FRC beams under four-point loading using digital image correlation (DIC) to monitor strain, displacement, and cracking. Expanded polystyrene low-density fibre-reinforced concrete prisms with steel and polypropylene fibre types at replacement levels of 0% and 0.5% by volume for each fibre type were cast and tested in flexure in accordance to ASTM C1609/C1609M-12. This experimental work detects the initiation and propagation of cracks on the specimens. It shows the failure mechanism, neutral axis shift and compression strain field of each prism. Results from the experiments showed that SFRC produced a slight increase in compressive strength. However, flexural strength and post-peak ductility were significantly higher with the addition of either steel or plastic

<sup>1</sup>Chapter 3 is adapted from CSCE 2018 conference proceedings.

fibres. Steel-fibre mixtures showed deformation hardening behaviour while synthetic-fibre mixtures exhibited deformation softening behaviour and a significant drop in peak load after first crack, which is a result of rapid crack propagation due to the low stiffness of the plastic fibres. DIC was used to measure displacement and strain fields and the observed values correlates well with traditional LVDT measurements.

### **3.1. Introduction**

Concrete is the most widely used building material in the world and this is attributed to its availability and economy. The use of conventional plain concrete can sometimes be limited because of its brittle nature and low tensile properties. To improve the tensile properties, it has become common practice to use reinforcement to carry the tensile stresses that may develop in concrete. Concrete reinforcement affects crack development and propagation as it bridges the cracks and improves the behaviour of the concrete in flexure. Recent developments and research have given an alternative to the use of reinforcement bars in the form of fibre reinforcement for crack control, which involves the addition of discontinuous discrete reinforcing fibres of different types and geometry to the concrete matrix. In some cases, fibre reinforcement can be used to replace traditional reinforcement such as welded fabric in non-structural applications. However, it can also be used in combination with steel reinforcement. Various forms and types of fibres are available, however, steel and synthetic are the most common for a wide range of structural

applications including but not limited to slabs on grade, mining, tunnelling and excavation support applications and rock slope stabilization (ACI 544-2010).

Many researchers have studied the effects of test method, fibre geometry, aspect ratio, fibre type and volume fraction of the use of fibres in concrete and on the post-cracking strength of fibre reinforced concrete (FRC). In hybrid construction containing both steel and synthetic fibres, the concrete has been shown to improve in both strength and flexural toughness (Wu et al., 2003). Rizzutti and Bencardino (2014) analyzed the effects of fibre volume fraction on the mechanical properties of steel FRC. They observed that the addition of fibres does not significantly affect the compressive strength of concrete. Song and Hwang (2004) observed that the compressive strength of fibre reinforced concrete reached a maximum strength at a replacement of 1.5% by volume with no significant strength gain above 1.5%. They also observed that the flexural strength of fibre reinforced concrete improved with increasing fibre volume fraction. Others have attempted to model the pull-out behaviour of fibres in order to predict the flexural response of FRC. The property/quality of the concrete matrix, the fibre type, content and geometry determine the mechanical properties of FRC (Robins et al., 2002). These mechanical properties can be characterized from the analysis of load-deflection plots of the FRC. The primary reason for adding fibres in concrete is to improve the ductility and post-peak behaviour.

The use of strain gauges, extensometers and linear variable differential transducer (LVDT) sensors have been well used in experimental research for measuring the displacements and

strains of concrete. These techniques are not very accurate in the estimation of strain fields or early crack detection and local failure processes in structural members. An alternative technique is the use of digital image correlation (DIC) analysis.

DIC is one of the full field non-contact optical techniques used in measuring displacements and strains in experimental mechanics. Other techniques include photo-elasticity, geometric moiré, moiré interferometry, holographic interferometry, speckle interferometry (ESPI), and the grid method (Grédiac, 2004). These methods are, however, expensive, difficult to use and often cannot typically be used in outdoor conditions compared to DIC. DIC can be used in structural monitoring and inspections by capturing images and making comparisons/analysis to identify differences in the behaviour of a member under consideration. DIC is also a better alternative to methods like dye penetration in measuring crack opening (McCormick and Lord, 2010).

This paper presents an investigation into the behaviour of steel and polypropylene synthetic lightweight FRC in flexure at a replacement level of 0.5% by volume. Behaviours were compared with a non-fibre low-density concrete mixture. This experimental work also validates the use of DIC in the measurement of displacement and strains as opposed to traditional methods of measurement. Low-density concrete containing expanded polystyrene (EPS) beads was used in the study.

### 3.2. Materials

All concrete mixtures were prepared with a CSA A3000 General Use Portland cement with a density of 3150 kg/m<sup>3</sup>. Concrete specimens were cast using a water/cementitious materials ratio (W/CM) of 0.35 in addition to a normal density gravel as the coarse aggregate with a nominal maximum size of 9.5 mm and a standard lab grade sand. In order to maintain a low W/CM and reach a suitable strength, a moderate dosage of a high-range naphthalene-based superplasticizer was used to achieve a workable slump. Two types of fibres were studied including hooked-end steel fibres glued together in bundles by a water soluble glue and polypropylene synthetic fibres (see Table 3.1). The density of all mixtures, except the control, were reduced through the use of expanded polystyrene (EPS) beads with a nominal diameter of 3 to 5 mm and density range of 11 to 32 kg/m<sup>3</sup>.

**Table 3.1: Properties of fibres**

Fibre Type	Diameter (mm)	Length (mm)	Aspect ratio ( $L_f/d_f$ )	Tensile strength (Mpa)	Elastic Modulus (Gpa)
Steel	0.5	30	60	1500	200
Synthetic	1.0	30	30	800	8.0

Note:  $L_f$  = Length of fibre,  $d_f$  = diameter of fibre

### 3.3. Mix Proportions

Concrete mixtures were designed in accordance with ACI-211.2 and were modified by incorporating EPS beads. The expanded polystyrene beads were batched by volume as it was not accurate to batch by weight due to the low density of the beads. Two fibre volume contents of 0% (control) and 0.5% by volume were used. Table 3.2 presents the mix proportions of the various concrete mixes.

**Table 3.2: Concrete mix proportions**

Mix	Mix Designation	W/CM	Coarse Aggregate (kg/m <sup>3</sup> )	Fine Aggregate (kg/m <sup>3</sup> )	EPS Beads (m <sup>3</sup> )	Cement (kg/m <sup>3</sup> )	HRWRA (mL/100kg)	Fibre Volume (%)
Control	NFRNWC*	0.35	875	693	-	550	975	-
Control	NFRLDC**	0.35	451	350	0.3	550	-	-
Steel	SFRLDC***	0.35	451	350	0.3	550	198	0.5
Polypropylene	PFRLDC****	0.35	451	350	0.3	550	-	0.5

\*NFRNWC: Non-Fibre Reinforced Normal Weight Concrete

\*\*NFRLDC: Non-Fibre Reinforced Low-Density Concrete

\*\*\*SFRLDC: Steel Fibre reinforced Low-Density Concrete

\*\*\*\*PFRLDC: Polypropylene Fibre reinforced Low-Density Concrete

### 3.4. Specimen Preparation

All concrete specimens were cast and cured in accordance with ASTM C192. A total of 5 specimens including three 101.6 x 203.2 mm cylinders and two 152.4 x 152.4 x 530 mm prisms were prepared for each mixture. The mixing procedure consisted of firstly mixing

all aggregates (fine and coarse) for 30 seconds in a drum mixer and batch size of 50L. This was followed by the addition of cement, EPS beads, and fibres, which were then mixed for 30 seconds, 1 minute and 2 minutes, respectively. Water was then added and left to mix for another 3 minutes. The superplasticizer was finally added to achieve the desired workability. Concrete specimens were then cast and compacted with tamping rods as per ASTM C192 specifications for each specimen type, after which the specimens were covered in wet burlap and plastic for 24 hours. The specimens were then demoulded and placed in a fog room (100% relative humidity) at room temperature ( $22\pm 2^{\circ}\text{C}$ ) until they were tested.

### **3.5. Test Setup and Procedure**

#### **3.5.1. Compression Test**

The compressive strength test was performed on 101.6 x 203.2 mm end-grinded cylinders in accordance with ASTM C39 at a loading rate of 0.24 MPa/s (35 psi/s). Compressive strength was measured at an age of 28 days.

#### **3.5.2. Flexural Test**

The flexural strength (average of two specimens) was measured on 152.4 x 152.4 x 530 mm prisms under four-point loading configuration in accordance with ASTM C1609/C1609M-12 by orienting the specimen with the form finished sides facing up and down. Two LVDTs were mounted on a jig at mid-span, one on each side in order to

measure the displacement. The jig was clamped to the prism directly above the supports with a span of 450 mm. The tests were carried out at a constant loading rate of 0.1 mm/min in accordance with Table 1 in ASTM C1609/C1609M-12 before and after a net deflection of  $L/900$  (where  $L = 457.2$  mm) had been reached. A photograph of the test setup is presented in Figure 3.1.

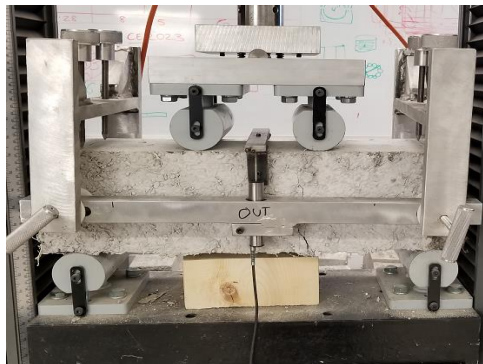


**Figure 3.1: Test setup for flexural test.**

### **3.5.3. Digital Image Correlation**

DIC is a non-contact optical full-field deformation measurement system. A commercial 3D acquisition and analysis software was used for this research (Correlated Solutions Vic-3D and Vic Snap). DIC was used to measure the displacement and strain on the specimens. The setup consists of two cameras with a resolution of 5 megapixels positioned 300 mm apart on a tripod and 1000 mm away from the specimen in such a way that the specimen fills the field of view of both cameras. An external light source was used to illuminate the field of view. Necessary adjustments to focus, aperture and exposure time were made to

ensure higher image quality. Prior to testing, the specimen surface in view of the camera was painted white and speckled with random black dots. The system was then calibrated as specified by Vic-3d testing guide. Images were captured at one frame per second. Applied force data was also recorded with a data acquisition system coupled to the DIC software during testing. Analysis and post-processing of data was done with image analysis software with a subset size of 35 pixels. Figures 3.2 and 3.3 presents the speckled specimens prior to testing and the DIC test setup, respectively.

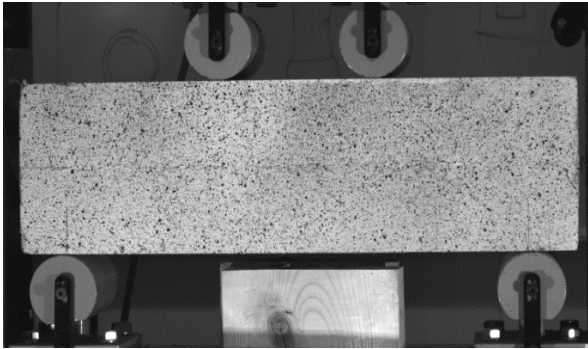


**Figure 3.2: Speckle pattern on specimen.**



**Figure 3.3: DIC setup.**

### **3.6. Results and Discussions.**

#### **3.6.1. Fresh Concrete Properties (Slump)**

The workability of each mixture was determined by measuring the slump in accordance with CSA A23.2-5C. The results are presented in Table 3.3 and show that the workability decreased with addition of fibres and improved with higher content of superplasticizer.

### 3.6.2. Density

The density of each mixture was determined using hardened cylinders in accordance with CSA A23.2-11C and the results are presented in Table 3.3. The addition of fibres is shown to have negligible effect on the hardened concrete density, which is not surprising considering the volume fraction was less than 1%. The density of the low-density mixes show a 20% decrease from the normal weight concrete mix due to the addition of EPS beads and not due to the fibres. It should be noted that bulk volume replacement of EPS at 30% is actually lower due to voids created by EPS that is filled up with paste. Thus, 30% volume replacement in the mix design is not equal to 30% drop in density.

**Table 3.3: Concrete properties**

Concrete	Density (kg/m <sup>3</sup> )	Compressive Strength (MPa)	M.O.R (MPa)	Slump (mm)
NFRNWC	2408	65	3.79	45
NFRLDC	1930	31	2.71	65
SFRLDC	1933	33	3.87	70
PFRLDC	1929	30	3.14	25

### 3.6.3. Compressive Strength

The compressive strength after 28 days of age is also presented in Table 3.3. The results show that the addition of steel fibres slightly increases the compressive strength. However,

the addition of synthetic fibres showed a 3% decrease in 28-day compressive strength. This decrease can be attributed to the tendency of synthetic fibres to ball in the mix, which can introduce air voids in the specimen. The addition of fibres also showed an improvement in post peak ductility capacity of the concrete specimens. The results show a 50% drop in strength of the low-density concrete compared to the normal density concrete due to the addition of EPS lightweight aggregate.

#### **3.6.4. Flexural Strength**

The flexural strength was determined and calculated in accordance with ASTM C1609 and are presented in Table 3.3. It was observed that the addition of fibres increased the flexural strength. However, the use of steel fibres gave a significantly higher flexural strength when compared with the synthetic fibre and non-fibre mixes as expected. Typical flexural load-deflection curves for the different mixes used in this study are presented in Figure 3.4 to 3.6, which compares the load-deflection plots of the DIC and that from the LVDT. The increase in flexural strength beyond a displacement of 1.5 mm is attributed to deflection hardening due to the effects of fibres. Both curves correspond with each other and demonstrates the validity and reliability of the use of DIC to measure displacement and strain values. The DIC was used for measurement on one of the prisms while the LVDT was used for the other. Both methods were not combined as the jig holding the LVDT was in the view of the camera. The deformation was controlled by only movement of the cross-

head up until the point of first cracking. The data for normal weight non fibre-reinforced concrete was not included in flexure but was only compared in compression.

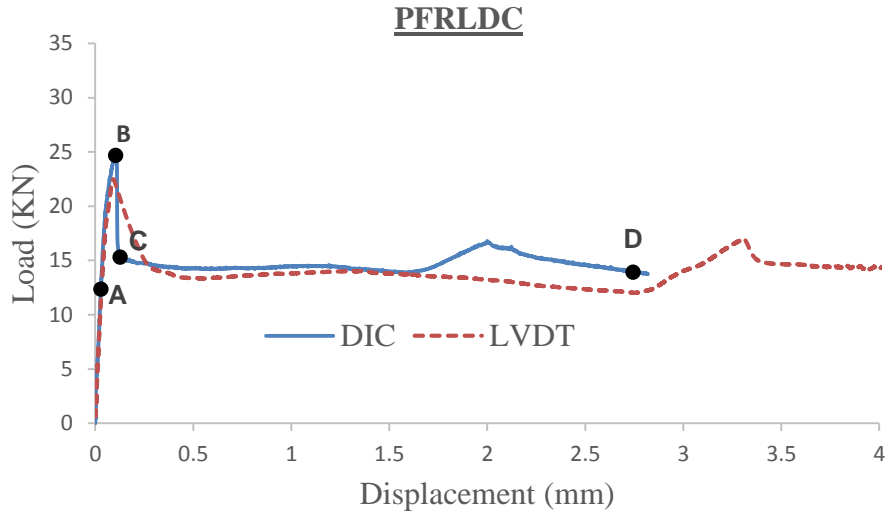


**Figure 3.4: Load-Displacement curve for polypropylene fibre reinforced low-density concrete.**

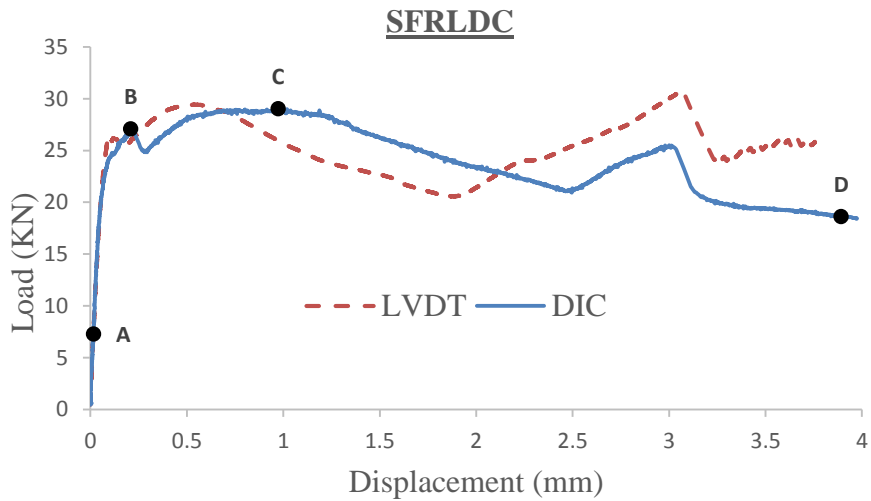


**Figure 3.5: Load-Displacement curve for steel fibre reinforced low-density concrete.**

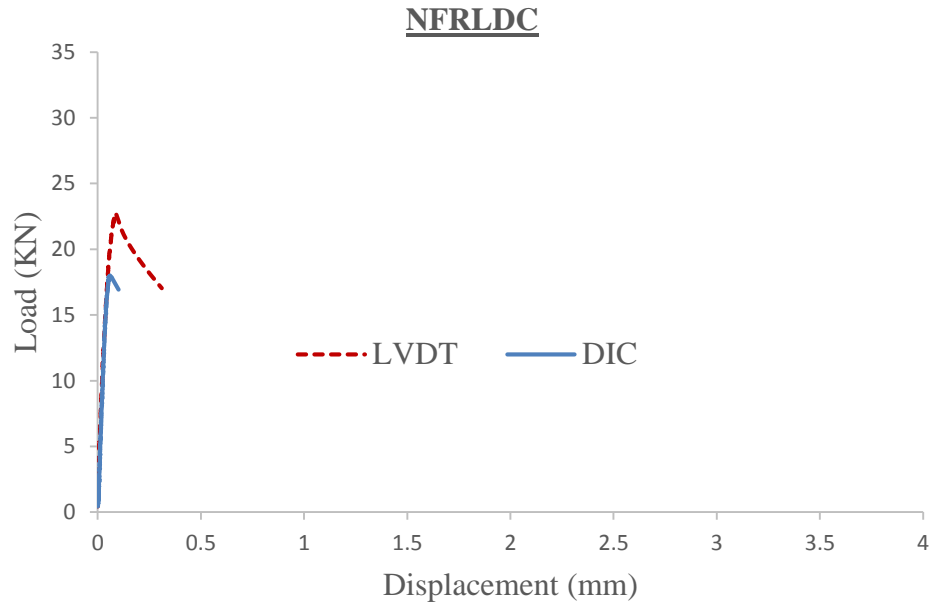


**Figure 3.6: Load-Displacement curve for non-fibre low-density concrete.**

### 3.6.5. Crack Detection

Cracking in concrete is most times a sign of failure. This can be seen when a concrete specimen is subjected to constant loading. Due to these loads it is capable of reaching its capacity, which inevitably leads to cracking and in certain cases failure. In bending tests, as cracks propagate, there is a decrease in load and increase in crack width. It is assumed that the point of divergence from linearity of load-deflection curves is the point of first crack (Bensaid et al., 2014). Although this assumption holds value, it is still difficult to identify these cracks especially in cases where multiple cracks exist. In bending tests, these cracks develop in the tensile region of the specimen and propagate upwards towards the

loading surface. With the aid of DIC, the cracks were immediately detected and their propagation was monitored until failure as presented in Figure 3.7. The figure shows the longitudinal (strains due to flexure) strain fields overlaid on the prisms at various times as the flexural test proceeded to specimen failure. Regions on the beam indicated by red show high strain concentrations and existence of cracks, whereas purple indicates low strain values (compression). From the image analysis, it was observed that SFRLWC (Figure 3.7 left) had more than one crack. The primary (first) crack corresponds with the deviation from linearity on the load deflection curve and was bridged by fibres. A secondary crack developed after first crack which led to the ultimate failure of the beam. Figure 3.7 shows the detection and propagation of cracks on the steel and plastic fibre concrete mixes studied. Figure 3.7A represents the strain distribution in the linear-elastic region. Figure 3.7B represents the first crack and initiation of cracks. Figure 3.7C shows the propagation of crack and Figure 3.7D shows the fracture at failure of the specimens. These can also be seen in the load-deflection plots in Figures 3.4 and 3.5.

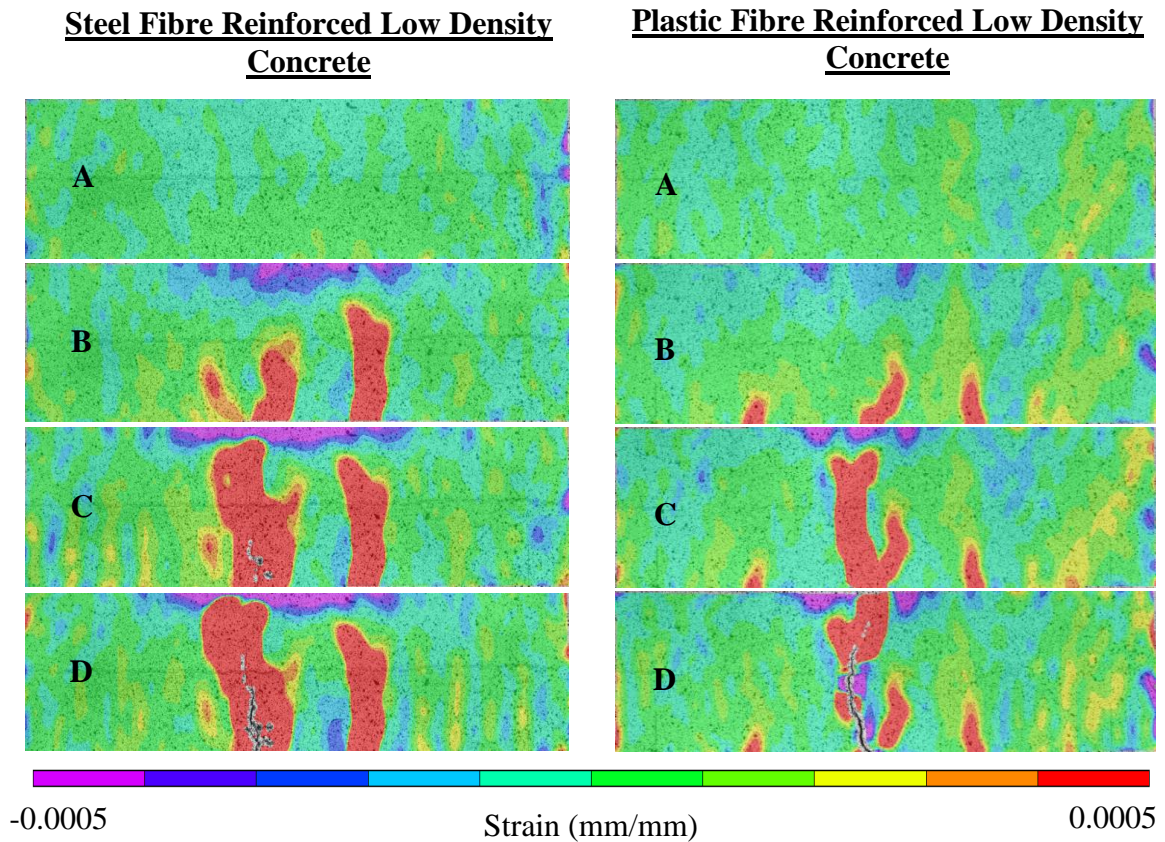


**Figure 3.7: Contour diagram showing longitudinal strain distribution.**

### 3.6.6. Neutral Axis Movement

The neutral axis is defined as an axis in the cross-section of a beam where axial stresses and strains are zero. If the beam cross-section is symmetric and the material is homogeneous and isotropic, the neutral axis would be at the centre. However, when concrete specimens are loaded, cracks develop causing the material to be anisotropic and the neutral axis shifts. By using image analysis, the shift of neutral axis of the concrete

beams was observed. It was observed that the synthetic fibre mix showed a high jump in the neutral axis position when cracks developed when the sectional strain was measured at the crack location. This can also be seen in the load-deflection curve (Figure 3.4) where there was a rapid drop in load after first crack. However, the movement of the neutral axis in the SFRLDC mix was gradual as a result of the fibres arresting the crack and the high flexural strength of the matrix. When cracks developed, the neutral axis moved up and was measured to be 49.4 mm from the compression face of the beam at yield strength as shown in Figure 3.9. This movement was gradual until failure and was measured to be 33.2 mm at fracture. The neutral axis position in the non-fibre mix is not presented in this work. From Figures 3.8 and 3.9, it can be seen that the strain distribution of the compression side remained largely linear. The strain distribution in the tension side is not representative of the real material strains due to the formation of cracks in the tension zone and are not used. From the movement of the neutral axes, strain diagrams were plotted considering only compression strain values with line of best fit extending into the tension region and are presented in Figure 3.10 and 3.11. The plots show the gradual movement of the neutral axis of the steel fibre specimen and a more rapid movement for the synthetic fibre specimens.

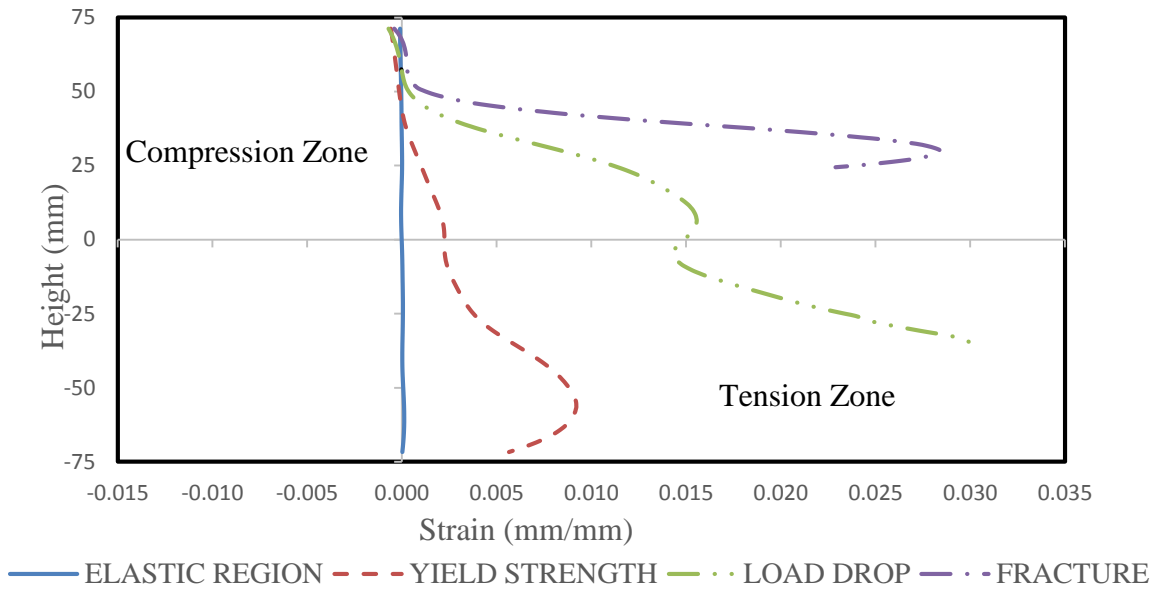


**Figure 3.8: Neutral axis movement of PFRLDC shown from DIC.**

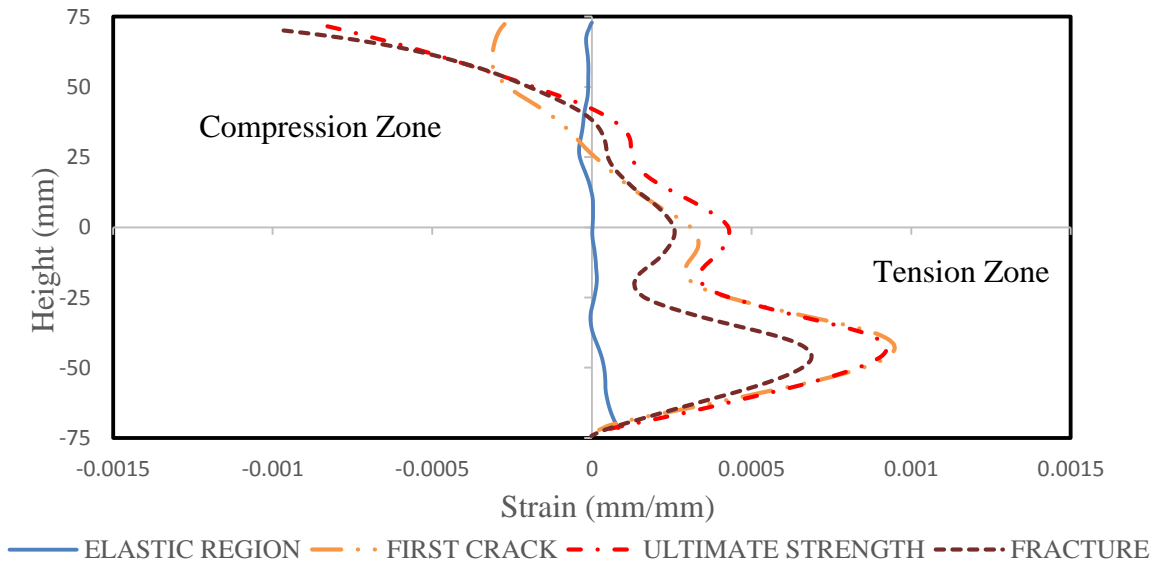


**Figure 3.9: Neutral axis movement of SFRLDC shown from DIC.**

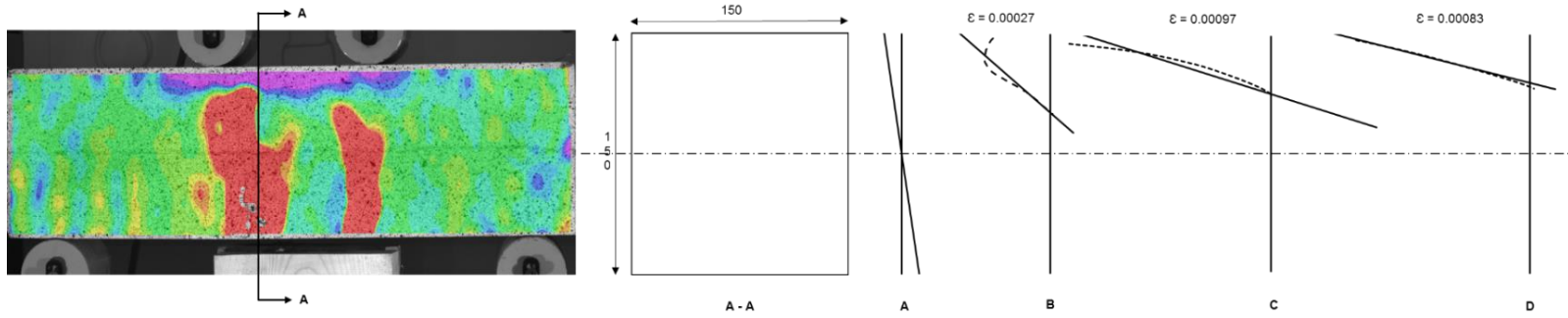


**Figure 3.10: Neutral axis movement of SFRLDC plotted from DIC.**

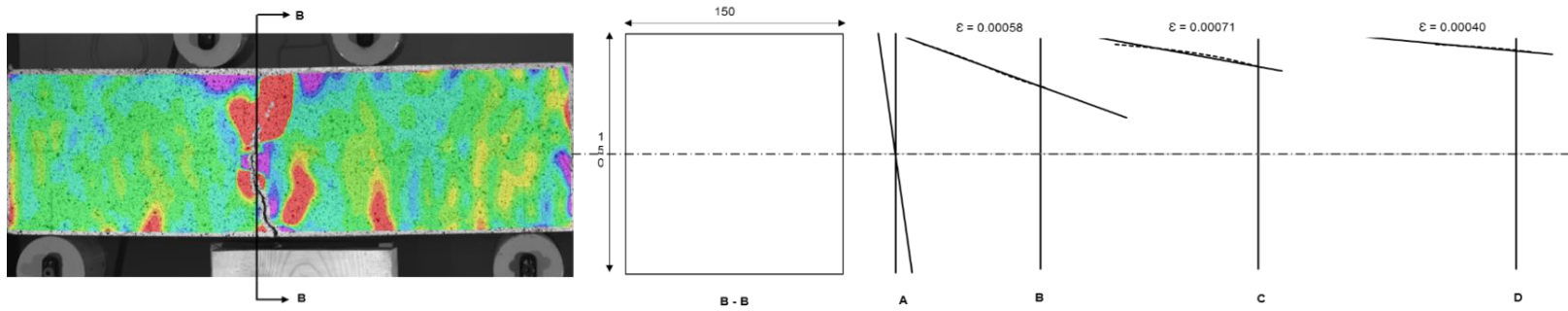


**Figure 3.11: Neutral axis movement of PFRLLDC plotted from DIC.**

**Table 3.4a: Neutral axis position for SFRLDC**

Point	Position	Distance* (mm)
A	Elastic region	75
B	Yield Strength	49.40
C	Ultimate Strength	36.85
D	Fracture	33.20

**Table 3.4b: Neutral axis position for PFRLDC**

Point	Position	Distance* (mm)
A	Elastic region	75
B	Yield Strength	31.08
C	Load Drop	18.14
D	Fracture	8.08

\* Distance measured from the compression face of the specimen

### 3.7. Conclusions

Based on the results presented within this paper, the following conclusions can be drawn:

- The effectiveness of steel fibres in arresting cracks is more pronounced than synthetic fibres for the same dosage. This can be seen from the neutral axis plots where the steel fibre mix showed a gradual shift in neutral axis position compared to polypropylene fibre, which showed a more rapid movement.
- Steel fibre of low aspect ratio and volume fraction as low as 0.5% produces tensile hardening properties when used in low density concrete.
- The use of steel fibres slightly improved the compressive strength and greatly improved the flexural strength and ductility of the matrix.
- Digital image analysis measured similar deformation response as LVDT while providing more information on cracking and strain distribution.

**Note:** Experimental work and technical paper carried out solely by John Ibeawuchi. Alan Lloyd and Edward Moffatt provided supervision in all stages.

### 3.8. References

American Concrete Institute. Committee 211. (2004). “Standard practice for selecting proportions for structural lightweight concrete.” ACI 211.2, Farmington Hills, MI.

American Concrete Institute. Committee 544. (2010). “State of the art report on fibre reinforced concrete.” ACI 544.1R, Farmington Hills, MI.

ASTM C1609/C1609M. (2012). “Standard test method for flexural performance of fibre-reinforced concrete (using beam with third-point loading).” *ASTM International*. West Conshohocken, PA, United States.

Bensaid B., Mostefa H., Mohamed C. and Sofiane A. (2015). “Failure mechanism of fibre reinforced concrete under splitting test using digital image correlation.” *Materials and Structures*, Vol. 48, No. 8: 2713–2726.

Correlated Solutions. (2016). “Vic-3D v7.2.6 Testing guide”. [www.correlatedsolutions.com](http://www.correlatedsolutions.com).

Correlated Solutions. (2016). “Vic-3D v7.2.6 Reference Manual”. [www.correlatedsolutions.com](http://www.correlatedsolutions.com).

CAN/CSA-A23.2-5C. (2014). “Slump and slump flow of concrete.” *Standards Council of Canada*. Mississauga, ON. Canada.

CAN/CSA A23.2-11C. (2014). “Water content, density, absorption, and voids in hardened concrete, grout, or mortar.” *Standards Council of Canada*, Mississauga, ON. Canada.

CAN/CSA A3001 (2018). "Cementitious materials for use in concrete." *Standards Council of Canada*, Mississauga, ON. Canada.

Grédiac, M. (2004). "The use of full-field measurement methods in composite material characterization: Interest and limitations." *Applied Science and Manufacturing*, Vol. 35, No. 7-8:751-761.

McCormick, N. and Lord J. (2010). "Digital Image Correlation." *Materials Today*, Vol. 13, No. 12: 52–54.

Rizzuti, L. and Bencardino, F. (2014). "Effects of fibre volume fraction on the compressive and flexural experimental behaviour of SFRC." *Contemporary Engineering Sciences*, Vol. 7, No. 8: 379-390.

Robins, P., Austin, S. and Jones, P. (2002). "Pull-out Behaviour of Hooked Steel Fibres." *Materials and Structures*, Vol. 35, No. 7: 434–42.

Song, P. S and Hwang, S. (2004). "Mechanical Properties of High-Strength Steel Fibre-Reinforced Concrete." *Construction and Building Materials*, Vol. 18, No. 9: 69–73.

Wu, Y., Jie, L., and Keru W. (2004). "Mechanical Properties of Hybrid Fibre-Reinforced Concrete at Low Fibre Volume Fraction." *Cement and Concrete Research*, Vol. 33, No. 1: 27–30.

## **4.0. POST-CRACKING SECTIONAL ANALYSIS OF LOW-DENSITY FIBRE REINFORCED CONCRETE USING DIGITAL IMAGE CORRELATION (DIC)**

### **4.1. Introduction**

Unlike conventional concrete, fibre reinforced concrete (FRC) is concrete containing discrete and randomly oriented fibres. FRC is known for enhanced post-cracking strength and toughness over plain concrete since it requires energy in debonding and pulling out of fibres. In comparison, plain concrete, which is characterized by its weakness in tension and low ductility, shows no significant post-cracking response as the strength quickly reduces to zero after cracking.

The traditional method for enhancing the tensile capacity and ductility of plain concrete is by adding reinforcement bars to carry tensile forces after cracking or by prestressing so that a majority of the concrete remains in compression. An alternative to this is the use of fibre reinforcement in full replacement of distributed reinforcement steel for low moment applications such as in slabs on grade, walls and foundations or in combination with reinforcement bars for high moment applications such as in beams or slabs (Löfgren, 2005; Oikonomou-Mpegetis, 2013). These fibres bridge the cracks and transmit tensile forces across them resulting in enhanced post-cracking tensile behaviour (Amin et al., 2015). In contrast to conventional reinforcement, fibres are relatively short, closely spaced and generally distributed throughout a cross-section whereas reinforcement bars are not closely

spaced, are continuous and are placed only where needed (Löfgren, 2005). When fibre reinforced concrete members are subjected to flexural loads, failure occurs when the strain in the extreme tensile fibre is greater than the ultimate rupture strain value, but in plain concrete this failure occurs when the concrete strain reaches its ultimate tension value at cracking (Singh, 2014).

This addition of fibres has an effect on both the serviceability and ultimate limit states of concrete structures. The effects on serviceability is on controlled crack propagation and subsequent reductions in crack width and spacing and an increase in flexural stiffness. In the ultimate limit state, it provides an increased load resistance and improved ductility (Löfgren, 2005). This resistance of FRC to cracking is achieved by fibres arresting micro-cracks, preventing their propagation to macro cracks and also by bridging cracks once macro cracking has occurred. These are referred to as micro-crack arrest mechanisms and crack bridging mechanisms, respectively (Oikonomou-Mpegetis, 2013).

The use of any material, regardless of its potential structural benefit, requires thorough research into its material behaviour, analysis models and structural reliability (Singh, 2014). In recent years, there has been considerable development in the design, modelling and analysis methods of fibre reinforced concretes (Hillerborg, 1980; RILEM TC 162-TDF, 2002). Despite these methods there is a lack of consistency in design, testing, and interpretation of test results that has hindered a widespread use of FRC in structural applications (Löfgren, 2005).

Sectional analysis involves analyzing a critical section (cracked section) to determine its response in terms of applied moment versus curvature, strain or crack opening. Structural analysis, on the other hand, is done to derive the global behaviour such as the load-deflection relationship (Löfgren, 2005). Available analytical methods for cross-sectional analysis are based on assumptions on whether the cracked surface remains plane or not (kinematic models) and stress-crack width relationship in tension or stress-strain relationship in compression (constitutive models) (RILEM TC 162-TDF, 2002). A method was proposed by Nanakorn and Horrii (1996) to determine the tensile strength carried by fibres based on fracture mechanics of concrete. They were able to predict the sectional capacity and forces of FRC tunnel linings with different thicknesses. Lok and Pei (1998) in their work on flexural response of steel fibre reinforced concrete proposed a constitutive model using a bilinear strain softening curve and were able to calculate the flexural moment-curvature relationship from the model. Lok and Xia (1999) went further to demonstrate how the flexural first crack strength can be derived from a constitutive stress-strain model. An analytical algorithm was developed by Ezeldin and Shiah (1995) to evaluate the moment-curvature and load-deflection behaviour of steel fibre reinforced concrete (SFRC) beams containing traditional reinforcement. Ahmadi et al. (2012) derived a simple model to predict the behaviour of SFRC under four point bending tests (FPBT). They calculated the moment capacity and all forces in the beam critical section by satisfying equilibrium and making necessary assumptions regarding the stress-strain

behaviour for concrete in compression, the uncracked tension region of the concrete and the stress-crack opening for the cracked region.

This paper presents cross-sectional analysis carried out on low density (light-weight) concrete reinforced with steel and polypropylene synthetic fibres at 0.5%, 1.0% and 1.5% volume fraction with the aim of contributing to the ongoing research effort in composite materials for structural use. Digital image correlation (DIC) was used to measure the strain values along the specimens. The position of the neutral axis and their corresponding values at various loading stages was also obtained using DIC. Through the analysis, the equivalent location of the tension and compression forces and their magnitudes were found.

## **4.2. Experimental Work**

An experimental investigation was carried out using hooked end steel fibres and polypropylene synthetic fibres as fibre reinforcement in low-density concretes made using expanded polystyrene (EPS) beads as the light weight aggregate. All tests were conducted using corresponding American and Canadian standard test guidelines.

### **4.2.1. Materials**

All concrete specimens were produced with a water-cement ratio of 0.35. Fine aggregates and normal density gravel with an average size of 9.5 mm was used as coarse aggregate. Commercially available ordinary Portland cement conforming to CSA A3000 was used as a binder for all mixes. Expanded polystyrene beads with nominal diameter 3-5 mm were

used to reduce the density of the concrete. Polypropylene synthetic fibre and hooked end steel fibres glued together using water soluble glue were used as fibre reinforcement. A polycarboxilate based high range water reducing admixture was added in the mix to achieve a workable mixture. The property of the fibres used is shown in Table 4.1.

**Table 4.1: Properties of fibres**

Fibre Type	Diameter (mm)	Length (mm)	Aspect ratio ( $L_f/d_f$ )	Tensile strength (Mpa)	Elastic Modulus (Gpa)
Steel	0.5	30	60	1500	200
Synthetic	1.0	30	30	800	8.0

Note:  $L_f$  = Length of fibre,  $d_f$  = diameter of fibre

#### 4.2.2. Mix Design

Six different concrete mixes were used in this experimental work. The six mixes are classified into two main categories; steel fibre low density and synthetic fibre low density fibre reinforced concrete mixes, all designed in accordance with ACI 211.2 (2004). The main variables that were changed to determine the influence on the behaviour of the FRC composites were fibre type and fibre content. The cement content of all concrete mixes was kept constant at  $550 \text{ kg/m}^3$ . Fine and coarse aggregate represented 14% and 17% of the total aggregate volume in concrete respectively while EPS represented another 30% of the

total volume of the low density concrete. The maximum dosage of the high range water reducing admixture used was specified at 975 mL/100 kg of cement but was added to the mixtures as required to achieve desired workability. All mixes were reinforced at fibre volume fractions of 0.5%, 1.0% and 1.5% for both steel and polypropylene fibres. The mix details are shown in Table 4.2.

**Table 4.2: Mix design details**

Mix Designation	W/C	Cement (kg/m <sup>3</sup> )	Fine Aggregate (kg/m <sup>3</sup> )	Coarse Aggregate (kg/m <sup>3</sup> )	EPS (m <sup>3</sup> )	HRWRA (mL/100kg)	Fibre Volume	
							%	kg/m <sup>3</sup>
SFRLDC0.5	0.35	550	350	451	0.3	198	0.50	39.25
SFRLDC1.0	0.35	550	350	451	0.3	-	1.00	78.50
SFRLDC1.5	0.35	550	350	451	0.3	198	1.50	117.75
PFRLDC0.5	0.35	550	350	451	0.3	-	0.50	4.55
PFRLDC1.0	0.35	550	350	451	0.3	-	1.00	9.10
PFRLDC1.5	0.35	550	350	451	0.3	790	1.50	13.65

\*SFRLDC: Steel Fibre Reinforced Low-Density Concrete

PFRLDC: Polypropylene Fibre Reinforced Low-Density Concrete

#### 4.2.3. Preparation of Test Specimens

Test samples were produced by mixing constituents in a 100L drum mixer. Three cylinders (101.6 mm diameter by 203.2 mm length) and two prisms (152.4 mm x 152.4 mm x 530

mm) were prepared for each mixture. All constituents of the mix with the exception of EPS were batched by weight. Due to the low density of the EPS beads, it was difficult to batch accurately by weight therefore it was batched by volume using a graduated cylinder. The constituent materials were first mixed dry without fibres for approximately 2 minutes. The fibres were added in small amounts to prevent agglomeration and to ensure the concrete mixture was homogenous and of uniform consistency. After the addition of fibres, the mixing was done for an additional 2 minutes to ensure the fibres were well distributed in the mixture. Water was added and high range water reducing admixture added to achieve good workability. Additional mixing time was needed for mixtures with over 1.0% volume fraction of fibres to ensure distribution of the fibres. Cylinders and prisms were then cast and compacted using tamping rods in accordance to ASTM C192 (2016). Specimens were covered with wet burlap and plastic for 24 hours to prevent loss of moisture. Following 24 hours, specimens were removed from molds and kept in a fog room of 100% relative humidity at a temperature of  $22\pm 2^{\circ}\text{C}$  until testing.

#### **4.2.4. Digital Image Correlation**

Digital image correlation (DIC) is a full field non-contact optical method used to measure the strains, global and relative displacements, and examine fracture of specimens or structures in experiments or structural monitoring. It works by considering behaviour or motion of an area of interest in a series of digital deformed images in relation to a reference

and initial undeformed image of the specimen or structure being considered (Dutton 2012, McCormick and Lord 2010). DIC was extensively used throughout this work in monitoring and measuring displacements and strains in a particular region of interest of a specimen in both flexural and compression tests using two high resolution 5 mega pixel cameras sitting on a tripod. The cameras were positioned approximately 1 meter away from the specimen surface. Normal LED white light was used as an external light source to provide uniform light intensity across the surface of the cylindrical and prismatic specimens. A consistent cover of a thin layer of matte white paint was applied on the surface of the specimen in view of the cameras and a sprayed-on random speckle pattern of black dots was created using black mist paint to achieve adequate contrast in the gray-scale of individual objects. The system was calibrated before testing using a calibration plate placed in front of the specimen and calibration images captured at different positions of the plate. Adjustments to aperture, focus and exposure time were made to ensure high quality images were captured during testing. Digital images were recorded/captured at a rate of 4 frames per second (fps) for flexure and 1 frame per second (fps) for compression. Commercially available 3D image acquisition and analysis softwares (Correlated solutions Vic-3D, 2016) were used in this research for post-processing image analysis and for recording data during the loading process, respectively. A DIC test setup in compression is shown in Figure 4.1 and Figure 4.2 shows the random speckle pattern on the cylinder and prism specimens.



**Figure 4.1: DIC test set-up.**

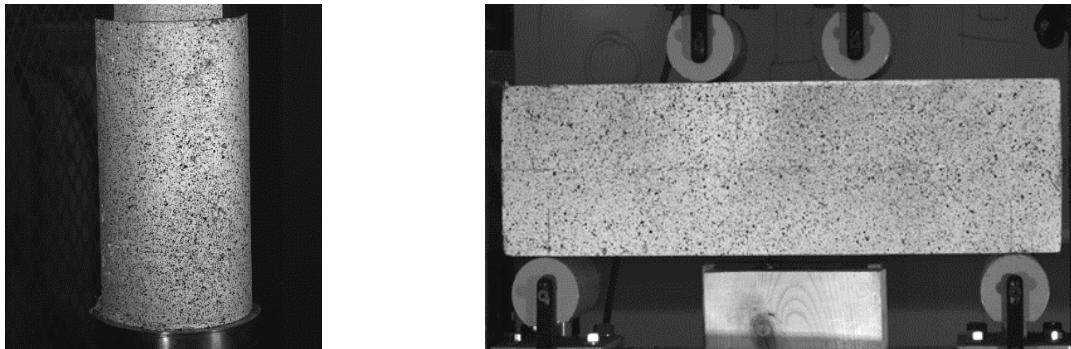


**Figure 4.2: Speckle pattern on cylinder and prism.**

### **4.3. Experimental Test and Results**

#### **4.3.1. Density and Slump**

The densities of all mixes were determined in accordance with ASTM C642 and are presented in Table 4.3. Slump was measured to determine the workability in accordance to CSA A23.2-5C and is also presented in Table 4.3. The density results show no significant

difference in density of both fibre specimens. Slump results show a decrease in workability with increase in volume fraction of fibres with synthetic fibre at volume fraction of 1.0% showing the lowest slump value. The addition of synthetic fibres gave the highest reduction in slump and workability.

#### **4.3.2. Compression**

Following 28 days of curing, the cylindrical specimens were tested in compression in accordance with ASTM C39 at a loading rate of 0.24 MPa/sec. A 2500 kN SATEC, servo-controlled compressive testing machine was used. The results obtained showed an increase in compressive strength with increase in fibre volume fraction. An observation of the surface of failed specimen showed that the failure zone consisted of longitudinal cracks parallel to the direction of the load and the specimens were not completely shattered/crushed even after failure. DIC was used to obtain the strain in the concrete cylinders by placing multiple virtual extensometers of height 100 mm at a location on the specimen measured from a distance of 50 mm from the top of the specimen to 50 mm from the bottom as shown in Figure 4.3. The location of the extensometers were selected to bypass any confinement due to the test supports close to the point of application of loads. The compression stress-strain relationship obtained for a typical specimen of each mixture group is shown in Figure 4.4 with corresponding images from the DIC showing the strain distribution on the specimen at various loading stages shown in Figure 4.5. Point 1

represents pre-cracking, point 2 represents the strain distribution at the peak and point 3 represents the longitudinal strain distribution at failure. Compression results show that the strain corresponding to peak stress is slightly increased by increase in content of fibres. Also the slope of the descending, post-peak response decreased gradually showing a ductile behaviour as a result of the fibres resisting crack growth for the FRC. Average compression results for three cylinders for each mix is presented in Table 4.3.

**Table 4.3: Concrete properties**

Mix Designation	Compressive strength (MPa)	Modulus of Rupture (MPa)	Slump (mm)	Density (Kg/m <sup>3</sup> )
SFRLDC0.5	33	3.87	70	1933
SFRLDC1.0	35	6.32	30	1936
SFRLDC1.5	40	6.53	50	1934
PFRLDC0.5	30	3.14	25	1929
PFRLDC1.0	35	3.00	20	1929
PFRLDC1.5	42	3.22	45	1930

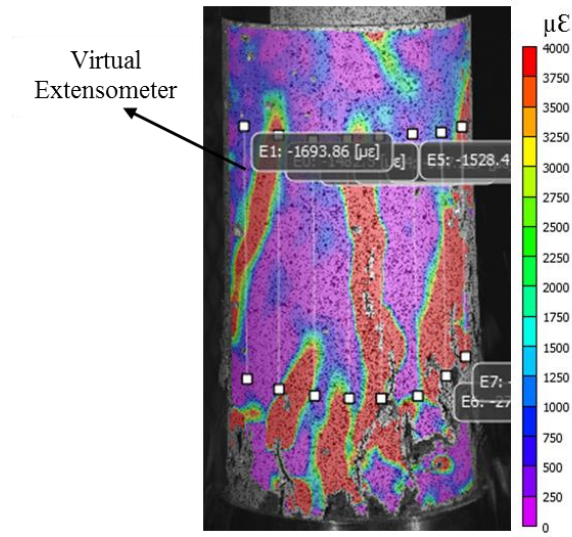
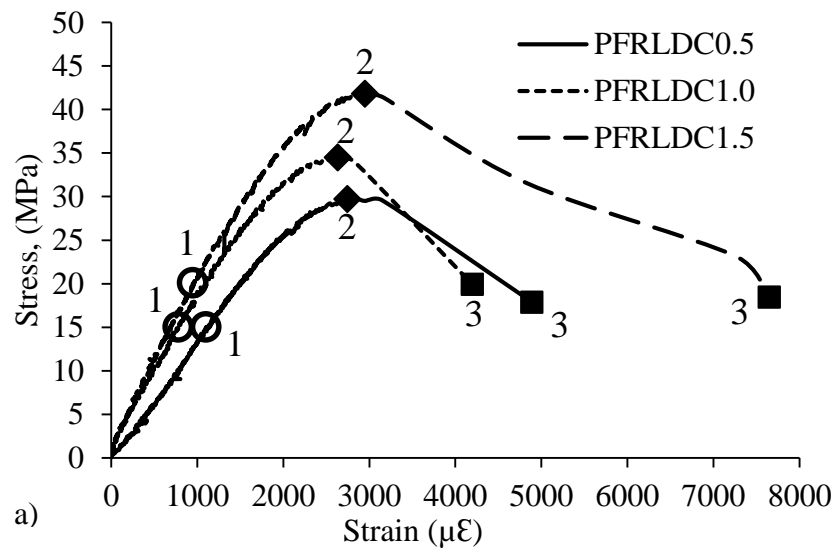
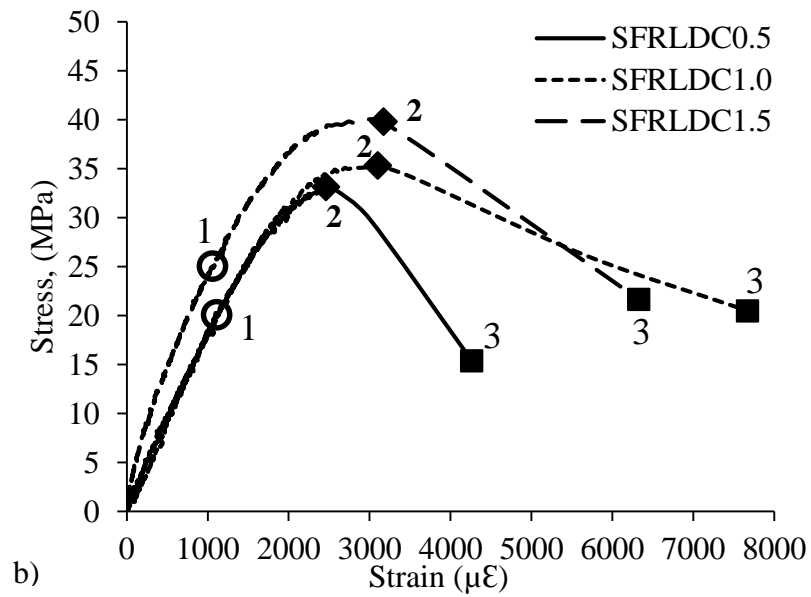
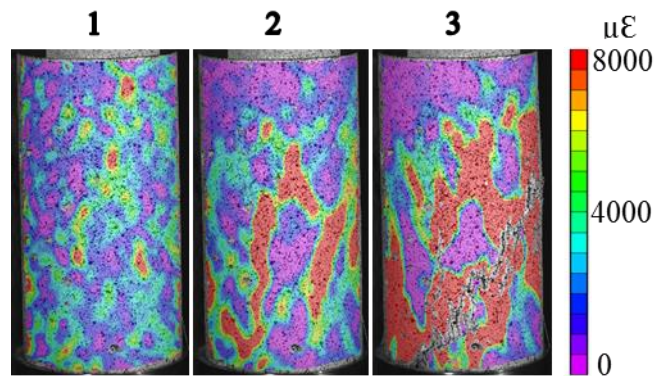


Figure 4.3: Virtual extensometers shown on SFRLDC0.5 specimen.





**Figure 4.4: Stress-strain relationship in compression: a) polypropylene fibre mix, b) steel fibre mix.**

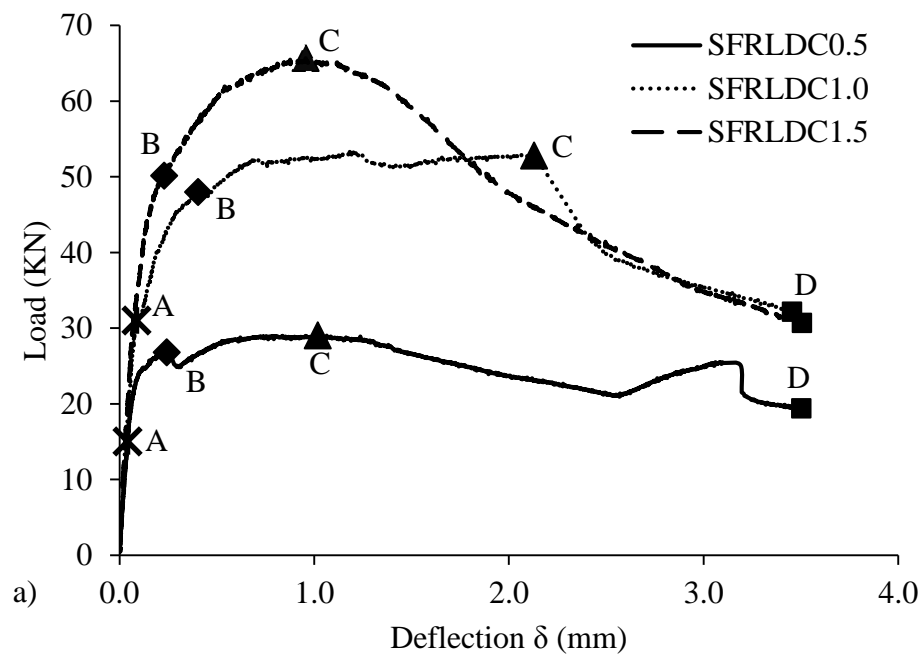


**Figure 4.5: Longitudinal strain on SFRLDC0.5 specimen for various loading stages.**

### **4.3.3. Flexure**

Test methods for determining the material properties (flexural response) of concrete specimens that exist include three and four point prism bending tests, square and round panel tests, wedge splitting tests and uniaxial tension tests. For the purpose of this research, the flexural behaviour of the FRC was assessed by performing four point bending test on 152.4 x 152.4 x 530 mm prisms in accordance with recommendations of ASTM C1609/1609M-12 using an Instron universal testing machine with a capacity of 2500 kN and a constant cross-head movement of 0.1 mm/min. Load-deflection curves were obtained using data from DIC and are presented in Figure 4.6. Contact displacement sensors such as LVDTs were not used in any of the measurements as the DIC displacement measurements had been validated for accuracy in this application in a previous study (Ibeawuchi et al., 2018). Results from the four point bending test showed a measure of post-peak ductility for all FRC concrete mixes. Steel fibre mixes (Figure 4.6a) exhibited higher load carrying capacity after first cracking when compared to synthetic fibre mixes (Figure 4.6b) of the same volume fraction. This is attributed to the higher stiffness of steel fibres and the bridging stress arresting crack opening and propagation. This increase was also observed with an increase in fibre content for both fibre types. The deflection values at first crack also increased with increase in fibre content with the steel fibre mixes having a greater increase in comparison to the synthetic fibre mixes. The ultimate flexural strength was observed to be almost doubled when the fibre content was doubled with a higher steel

fibre content. Synthetic fibre mixes (Figure 4.6b) generally exhibited a reduction in load-carrying capacity after first cracking. At 0.5% synthetic fibre content (Figure 4.6b), a significant drop in peak load/loss in capacity after first crack occurred (point C) and deflection hardening behaviour followed after a net deflection of 2 mm. At 1.0% synthetic fibre content (Figure 4.6b), a drop in load (point C) was also observed but deflection hardening occurred almost immediately with a gradual increase reaching a maximum at 2 mm deflection. At 1.5% synthetic fibre content, a gradual drop in load was observed. The average modulus of rupture values obtained from the flexural tests are presented in Table 4.3. The tests were not conducted under displacement control.



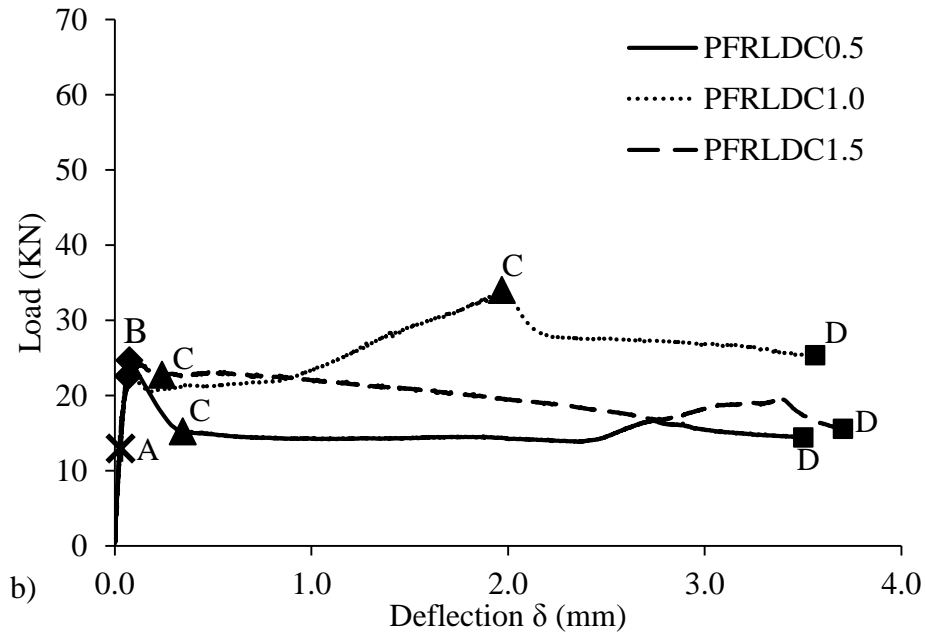


**Figure 4.6: Load vs deflection curves: a) steel fibre mix b) polypropylene fibre mix.**

Point A on the load deflection curve represents the elastic region, point B represents the point of first crack and points C and D represents the peak load and failure point respectively. For the PFRLDC0.5 and PFRLDC1.5, point C represents the point of rapid drop in load.

The contour diagram showing the longitudinal strain distribution for PFRLDC1.5 and SFRLDC1.5 prisms obtained using DIC for points A, B, C, D of the load-deflection curve is shown in Figure 4.7. For both specimens, image A shows the strains, location of the four point bending loads with two rollers on each end and two above applying the loads. Image B shows the formation of cracks with multiple tension cracks in the steel fibre specimen as

indicated by red. These multiple tension cracks shows the ability of the steel fibres to bridge cracks and further distribute forces with less crack opening due to their higher stiffness when compared to the polypropylene fibre specimen. This is further evident in points C and D with well distributed high strain region over the midsection of the beam under constant moment with one dominant crack leading up to failure. The polypropylene fibre specimen had a single crack from initiation to failure.

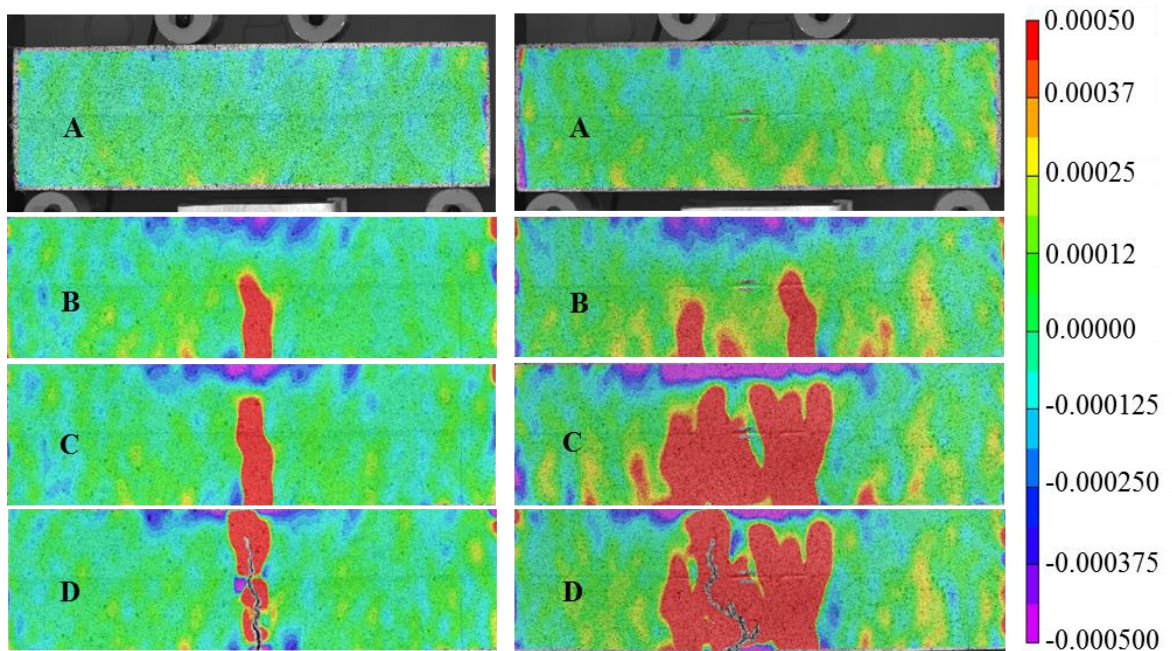


**Figure 4.7: Contour diagram from DIC showing longitudinal strains along the prisms at various stages of loading (Left: PFRLDC1.5 Right: SFRLDC1.5).**

#### **4.4. Post-Cracking Sectional Analysis**

Having found the compressive stress-strain relationship and applied moment, sectional analysis for post-cracking behaviour of the critical (cracked) section was carried out on all concrete mixes following four point bending tests to derive the values of the tension and compression force and the location of these forces as the prism is loaded to failure.

Using DIC, the position of the neutral axis and compression strain values at various loading stages were obtained. As cracks propagated, the neutral axis depth decreased, moving up the compression face with an increase in deflection. The neutral axis movement/behaviour was influenced by the fibre type and fibre content. Prisms with steel fibres showed a gradual decrease until failure while prisms with synthetic fibres showed a more rapid movement especially at a low fibre content of 0.5%. Curvature was subsequently calculated using the obtained neutral axis positions and top compression strain values, and is represented as the ratio of compressive fibre strain to the depth of neutral axis. Moment was computed from the force acting on the specimen. The moment-curvature diagrams generated for the various mixtures are shown in Figure 4.8a and 4.9a. Figure 4.8b and 4.9b show the response of the elastic region. This shows a linear response that begins to plateau prior to crack formation at point B. The total curvature capacity of the polypropylene fibre specimens was observed to be greater than that of the steel fibre specimens. This is further explained by the images from DIC in Figure 4.7 that shows a single crack for the synthetic fibre specimen with higher curvature over the single crack location compared to the steel

fibres which are better in distributing stress over the constant moment region. Prior to first cracking, the neutral axis is at the centroid of the specimen with a linear moment-curvature relationship and the tension and compression stress is assumed to be linear, becoming non-linear as the loading and depth of crack increases. Table 4.4 gives values for the various points labeled on the moment-curvature curve diagram in Figure 4.8a and 4.9a.

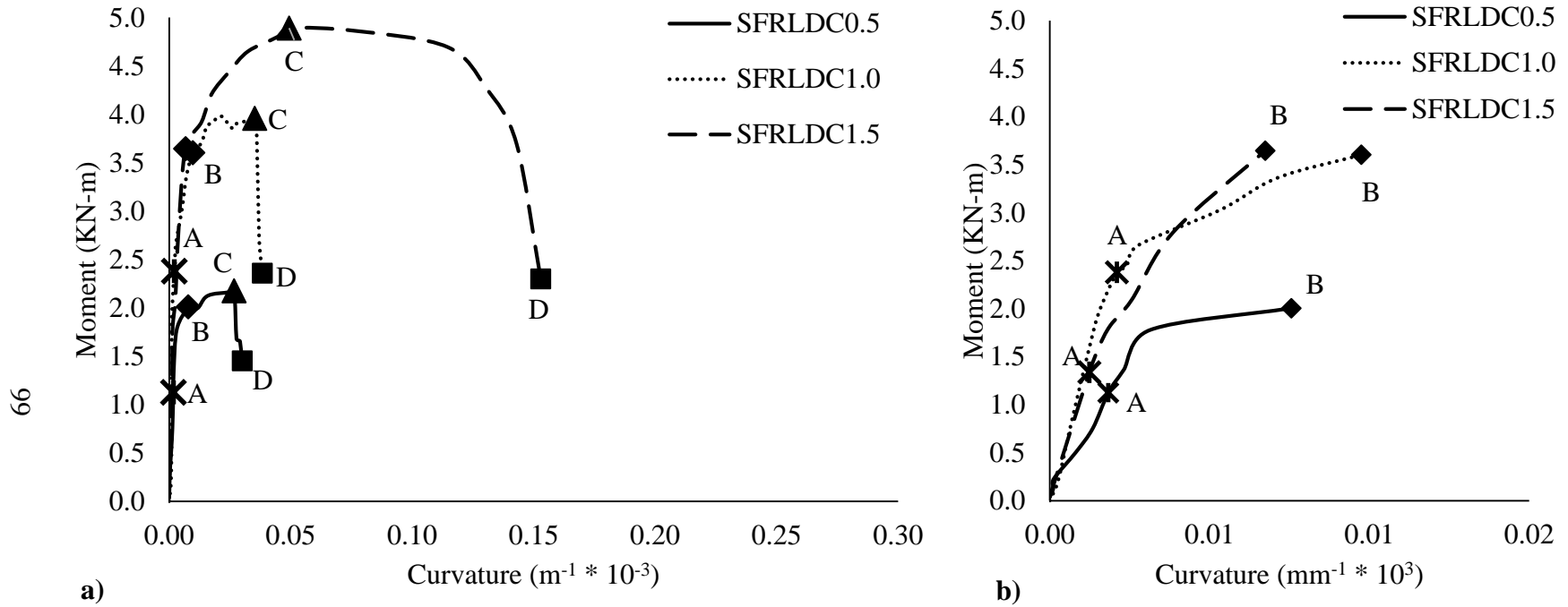
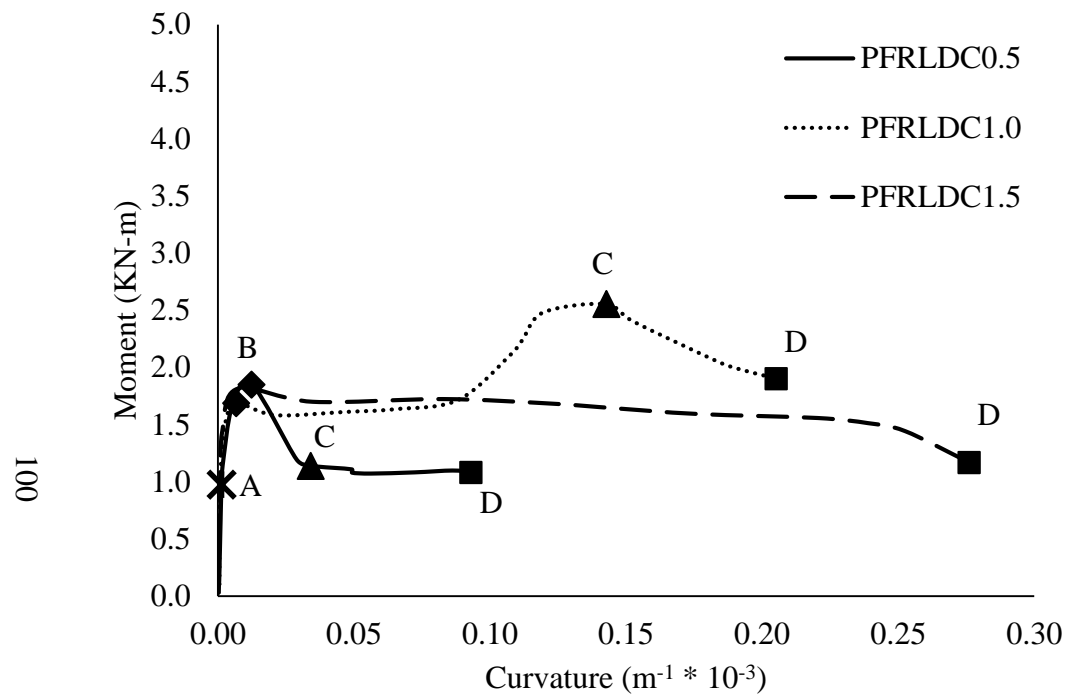
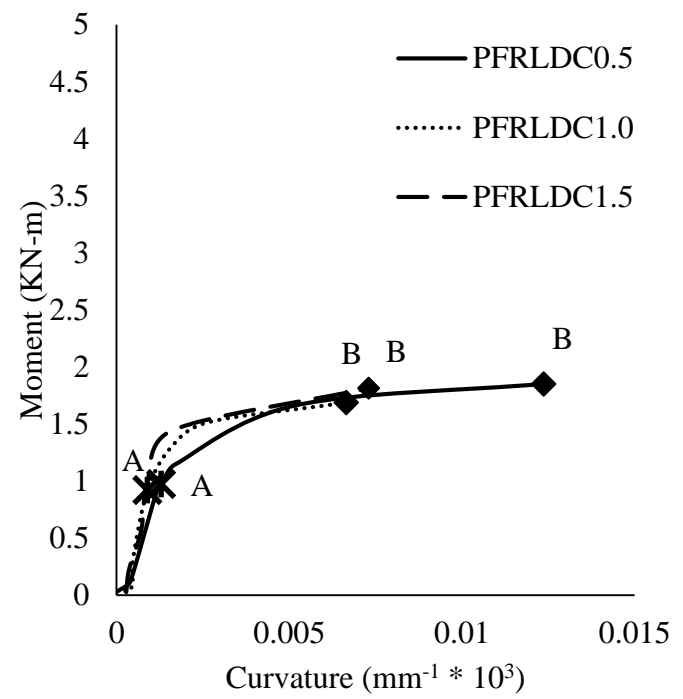


**Figure 4.8: Moment vs curvature relationship for the steel fibre mix: a) Full response of the specimen b) Elastic region response.**



a)



b)

**Figure 4.9: Moment vs curvature relationship for the polypropylene fibre mix: a) Full response of the specimen b) Elastic region response.**

**Table 4.4: Values corresponding to points A, B, C, D.**

Mix designation	Point	Load (kN)	Deflection (mm)	Moment (kN-m)	Curvature (m <sup>-1</sup> )
SFRLDC0.5	A	15.01	0.04	1.13	1.14E-04
	B	26.81	0.24	2.01	7.79E-03
	C	29.02	1.02	2.18	2.67E-02
	D	19.40	3.50	1.44	3.00E-02
SFRLDC1.0	A	31.01	0.09	2.33	2.11E-03
	B	47.97	0.40	3.60	9.75E-03
	C	52.78	2.13	3.96	3.59E-02
	D	32.16	3.45	2.41	3.83E-02
SFRLDC1.5	A	15.01	0.04	1.13	1.25E-03
	B	50.15	0.23	3.76	6.75E-03
	C	65.68	0.96	4.93	4.93E-02
	D	30.68	3.50	2.30	1.53E-01
PFRLDC0.5	A	12.98	0.03	0.97	1.29E-03
	B	24.67	0.07	1.85	1.24E-02
	C	15.18	0.35	1.14	3.41E-02
	D	14.43	3.50	1.08	9.29E-02
PFRLDC1.0	A	12.98	0.26	0.97	4.94E-04
	B	22.62	0.07	1.70	6.65E-03
	C	34.05	1.97	2.55	1.43E-01
	D	25.37	3.56	1.90	2.05E-01
PFRLDC1.5	A	12.96	0.02	0.97	8.98E-04
	B	24.18	0.13	1.81	7.30E-03
	C	22.78	0.24	1.71	3.48E-02
	D	15.59	4.34	1.17	2.76E-01

To carry out the sectional analysis, the beam depth was divided into  $n$  number of layers of height ( $\Delta_i$ ) in compression and tension (see Figure 4.11). The constitutive behaviour of concrete in compression was then modeled by curve fitting a polynomial trendline on the experimentally obtained stress-strain diagrams and an equation for the relationship obtained. The curve fitting is comprised of two regions, the first region depicts a parabolic trendline stress-strain relationship up until ultimate strain  $\epsilon_0$  while the second region represents a linearly decreasing stress-strain relation beyond  $\epsilon_0$  as shown in Figure 4.10.

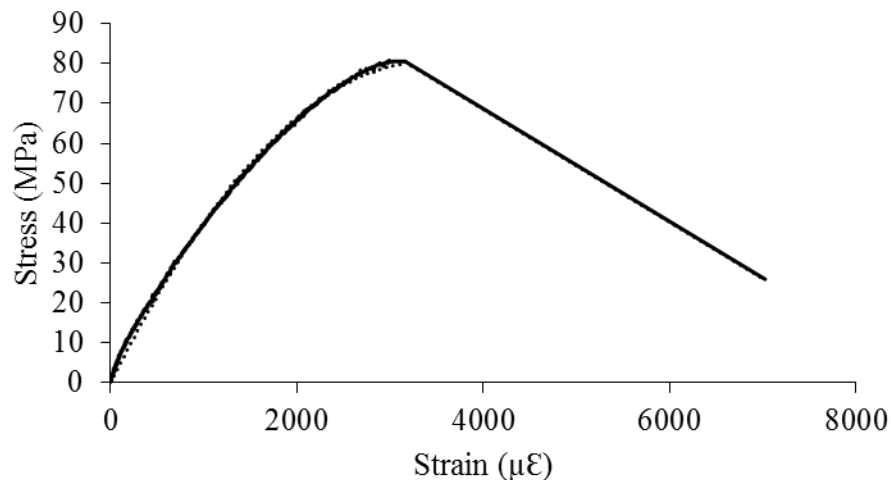


**Figure 4.10: Modelled compressive stress-strain behaviour.**

The stress in each layer is determined from the obtained stress-strain equation for the corresponding value of strain along the depth of the beam for each specimen. The compressive force of the uncracked section was obtained using the Equation 4.1.

$$C = \sum_{i=1}^n (\sigma_i \times \Delta_i \times b) \quad (4.1)$$

The moment associated with the compression force was calculated by summing moments generated by concrete in compression about a known location as described in Equation 4.2.

$$M_c = \sum_{i=1}^n (\sigma_i \times \Delta_i \times b \times h_i) \quad (4.2)$$

Where  $h_i$  is the distance between the extreme tension face of the cross section and the  $i^{\text{th}}$  layer,  $\sigma_i$  is the stress corresponding to the  $i^{\text{th}}$  layer and  $b$  is the width of the specimen.

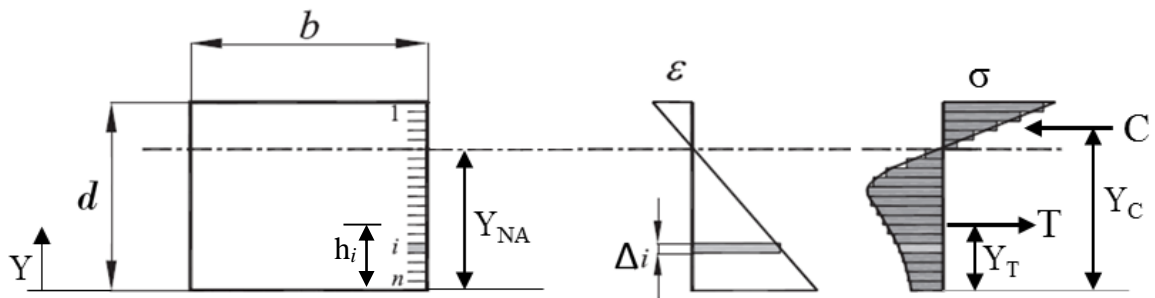


**Figure 4.11: Cross-section of beam showing stresses and strain profile (adapted from fib Model Code 2010).**

The location of the tension and compression forces were determined through the sectional analysis and are shown in Table 4.5 for points B, C, D corresponding to points on the moment-curvature and load-deflection curves. From the results, it was observed that for

both fibre types, the compression force was high up the section above the neutral axis and it increased continuously from cracking to failure of the specimen. The magnitude of the compression force also showed an increase with increase in load with maximum at the peak load (point C) for all specimens with the exception of the SFRLDC1.5 mix. This exception can be attributed to fibre agglomeration due to the higher fibre content of the mix. At failure (point D), the force magnitude dropped. A comparison of compression force values for both fibre types show that the steel fibre had higher force values than the polypropylene fibre. Only the post-cracking behaviour of the specimens were observed. Point A was not analyzed as the cracks had not developed yet and the neutral axis was assumed to be at the centroid of the specimen.

The tension force location also increased linearly for the steel fibre specimens. The polypropylene fibre specimens showed inconsistency in the position of the tension force as it was observed to increase up till the point C and dropped at fracture. This movement of the compression and tension force is plotted against curvature and is shown in Figure 4.12 for all six mixes.

**Table 4.5: Neutral axis and force locations corresponding to points on the Moment vs Curvature plots**

Mix designation	Point	$Y_{NA}$ (mm)	$Y_T$ (mm)	$Y_C$ (mm)	C (N)
SFRLDC0.5	B	103.9	72.9	133.4	33222
	C	115.3	103.0	137.2	63574
	D	118.2	114.3	138.1	61060
SFRLDC1.0	B	95.9	77.5	129.5	69272
	C	112.6	104.2	136.1	123996
	D	115.5	110.4	137.0	114351
SFRLDC1.5	B	91.8	32.8	134.5	35863
	C	109.2	82.3	136.4	90437
	D	115.5	105.3	138.0	106904
PFRLDC0.5	B	120.9	52.7	137.4	21851
	C	133.9	103.8	140.4	31094
	D	143.9	34.5	143.8	9906
PFRLDC1.0	B	102.9	55.2	135.0	24965
	C	139.1	84.5	143.5	43318
	D	141.9	94.4	143.7	38593
PFRLDC1.5	B	104.4	65.3	104.4	26068
	C	130.2	83.7	128.2	29303
	D	142.5	33.2	140.5	10569

Note: Neutral axis location, tension force and compression force location is measured from the bottom of the prism

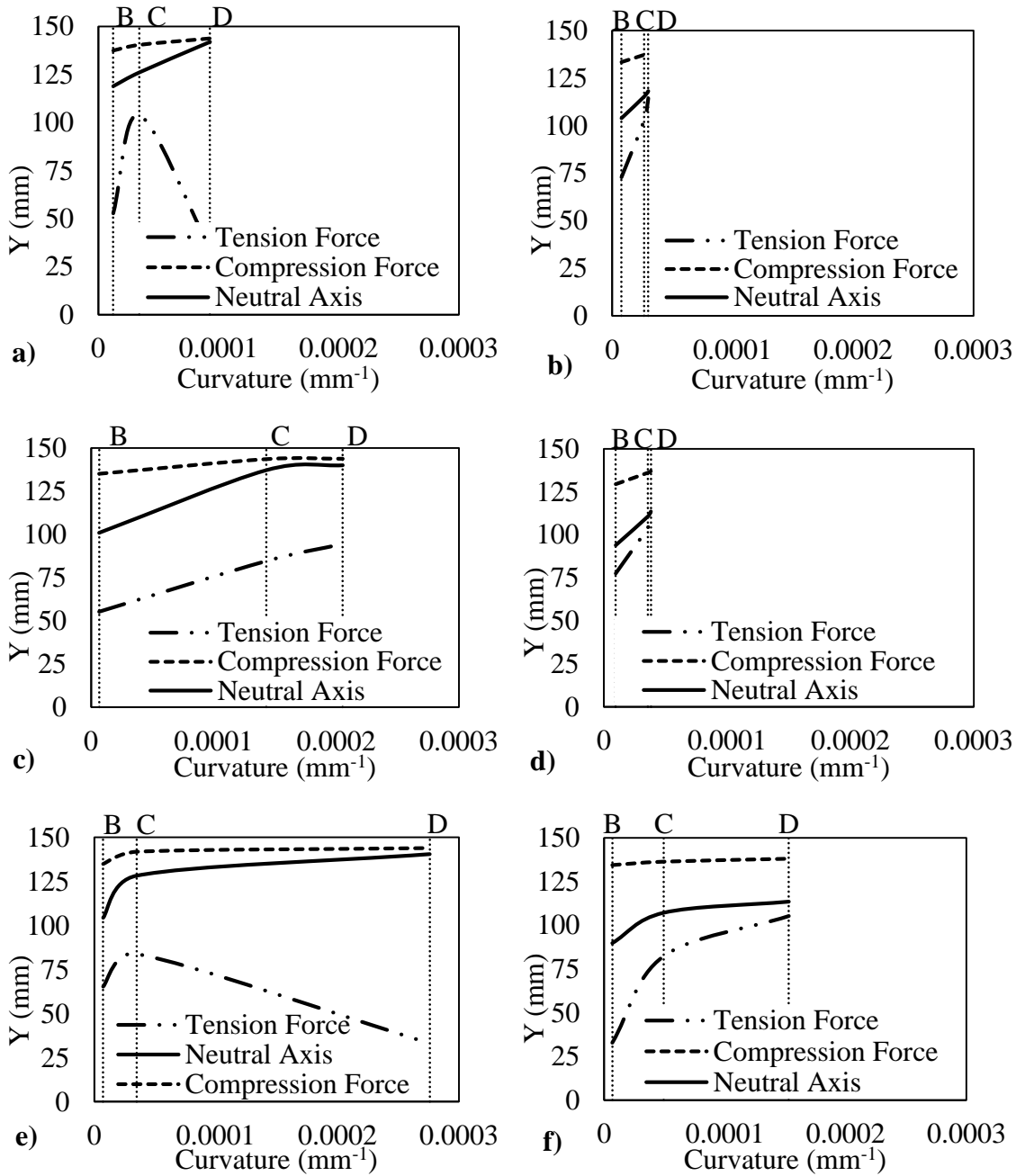


**Figure 4.12: Force location versus curvature (a) PFRLCD0.5 (b) SFRLCD0.5 (c) PFRLCD1.0 (d) SFRLCD1.0 (e) PFRLCD1.5 (f) SFRLCD1.5.**

#### 4.5. Conclusions

In order to improve the knowledge and use of lightweight FRC in structural applications, a series of tests were carried out in this work to study the post cracking behaviour of polypropylene and steel fibre reinforced concrete at different volume fractions. Compression tests were carried out and a stress-strain relation needed to carry out the sectional analysis was derived for each specimen mixture. DIC was used to obtain strain data at the cracked section and in order to further evaluate the flexural behaviour of the cracked section, sectional analysis was carried out to determine the magnitude of the forces in the section and their location. Based on the results obtained from the experimental program, the following conclusions were made:

- Compression results show an increase in peak strain and compressive strength with increase in fibre content for both fibre mixes.
- Both steel and polypropylene synthetic fibre types were observed to give good ductility when used in low density concrete with steel fibre giving higher load carrying capacity.
- From the sectional analysis it was found that the compression force was more likely to be at approximately 64% of the neutral axis height above the neutral axis.
- For the mixes investigated, 1.0% volume fraction was observed to be the optimum fibre content for synthetic fibre as results show a higher magnitude of compression force, better ductility, deflection hardening behaviour immediately after first crack,

higher load capacity at first crack and gradual neutral axis movement when compared to mixes of same fibre type with 0.5 and 1.5% fibre content. As counter intuitive as it may seem, the better performance of polypropylene fibre at 1.0% over 1.5% is attributed to the fibre balling when higher contents are used. The same was observed for steel fibre reinforced concrete mixes.

- Synthetic fibre showed a higher curvature capacity than steel fibre with curvature increasing with increase in fibre content for both fibre types.
- A gradual shift in neutral axis position was observed for steel fibre mixes. On the other hand, synthetic fibre mixes showed a higher neutral axis position at failure when compared to steel mixes. An increase in fibre content showed an increase in neutral axis position at different loading stages for all fibre types with the exception of PFRLDC1.5. This exception is attributed to the balling effects of higher polypropylene fibre content.
- Increase in fibre content also showed an increase in tension force location for steel fibre mixes. Polypropylene fibre mixes on the other hand showed a drop in tension force location at point D (fracture).

Further testing is recommended to be carried out using DIC in direct tension testing of FRC. Only flexural and compression tests were performed in this program, therefore further work should be done to completely understand the behaviour of a cracked section when subjected to direct tension.

#### 4.6. References

American Concrete Institute. Committee 211. (2004). “Standard practice for selecting proportions for structural lightweight concrete.” ACI 211.2, Farmington Hills, MI.

Ahmadi, R. et al. (2011).” A precise solution for prediction of fibre-reinforced concrete behaviour under flexure.” *Journal of Zhejiang University-Science (Applied Physics & Eng.)*, Vol. 12, No. 7: 495-502.

Amin, A., Foster, S. J., & Muttoni, A. (2015). “Derivation of the  $\sigma$ -  $w$  relationship for SFRC from prism bending tests.” *Structural Concrete*, Vol. 16, No. 1: 93–105.

ASTM C39/C39M. (2017). “Test method for compressive strength of cylindrical concrete specimens.” *ASTM International*. West Conshohocken, PA, United States.

ASTM C192/C192M. (2016). “Practice for making and curing concrete test specimens in the laboratory.” *ASTM International*. West Conshohocken, PA, United States.

ASTM C1609/C1609M. (2012). “Standard test method for flexural performance of fibre-reinforced concrete (using beam with third-point loading).” *ASTM International*. West Conshohocken, PA, United States.

ASTM C642. (2013). “Standard test method for density, absorption and voids in hardened concrete.” *ASTM International*. West Conshohocken, PA, United States.

CAN/CSA-A23.2-5C (2014). “Slump and slump flow of concrete.” *Standards Council of Canada*. Mississauga, ON. Canada.

CAN/CSA A23.2-11C. (2014). “Water content, density, absorption, and voids in hardened concrete, grout, or mortar.” *Standards Council of Canada*. Mississauga, ON. Canada.

CAN/CSA A3001 (2018). "Cementitious materials for use in concrete." *Standards Council of Canada*. Mississauga, ON. Canada.

Correlated Solutions. (2016). "Vic-3D v7.2.6 Testing guide". [www.correlatedsolutions.com](http://www.correlatedsolutions.com).

Correlated Solutions. (2016). "Vic-3D v7.2.6 Reference Manual". [www.correlatedsolutions.com](http://www.correlatedsolutions.com).

Dutton, M. (2012). "Digital image correlation for evaluating structural engineering materials." *M. Sc. Thesis*. Queen's University, Canada.

Ezeldin, A. S. and Shiah, T. W. (1995). "Analytical immediate and long-term deflections of fibre-reinforced concrete beams." *Journal of structural engineering*, Vol. 121, No. 4: 727-738.

*fib* - International Federation for Structural Concrete (2010). *Model Code: final draft. Vol. 1 for Concrete Structures*.

Hillerborg, A. (1980). "Analysis of fracture by means of the fictitious crack model, particularly for fibre reinforced concrete." *International journal of cement composites*, Vol. 2, No. 4: 177-184.

Ibeawuchi, J. C. et al. (2018). "Evaluation of flexural behaviour of low-density fibre reinforced concrete using digital image correlation." *6<sup>th</sup> International materials specialty conference, Canadian society for civil engineering annual conference*. Fredericton, NB. Canada.

Löfgren, I. (2005). "Fibre-reinforced concrete for industrial construction- a fracture mechanics approach to material testing and structural analysis." *Phd thesis*. Chalmers University of Technology, Sweden.

Lok, T. S. and Pei, J. S. (1998). "Flexural behaviour of steel fibre reinforced concrete." *Journal of Materials in Civil Eng.*, Vol. 10, No. 2: 86-97.

Lok, T. S. and Xiao, J. R. (1999). "Flexural strength assessment of steel fibre reinforced concrete." *Journal of Materials in Civil Eng.*, Vol. 11, No. 3: 188-196.

McCormick, N. and Lord, J. (2010). "Digital image correlation." *Materials Today*, Vol. 13, No. 12: 52-54.

Nanakorn, P. and Horii, H. (1996). "A fracture-mechanics-based design method for SFRC tunnel linings." *Tunnelling and underground space technology*, Vol. 11, No. 1: 39-43.

Oikonomou-Mpegetis, S. (2013). "Behaviour and design of steel fibre reinforced concrete slabs." *PhD thesis*. Imperial College London.

RILEM TC 162-TDF. (2002). "Test and design methods for steel fibre reinforced concrete: design of steel fibre reinforced concrete using  $\sigma - w$  method: principles and applications." *Materials and Structures*, Vol. 35: 262-278.

Singh, H. (2014). "Flexural modelling of steel fibre-reinforced concrete members: analytical investigations." *Practice periodical on structural design and construction* Vol. 20, No. 4: 1943-5576.

## **5.0. MODELLING OF POST-CRACKING BEHAVIOUR OF STEEL FIBRE REINFORCED LOW DENSITY CONCRETE**

### **5.1. Introduction**

The adoption of fibre reinforced concrete in real life practice is wide spread because of the various benefits of fibres that includes improved ductility, post-cracking flexural capacity, impact resistance, crack control, and superior energy absorption. These have established fibre reinforced concrete as a favorable material for structures subjected to severe loading conditions like blasts, impacts and earthquake (Yoo et al., 2015a). Three or four point bending tests are commonly used to derive flexural parameters in order to make a performance-based classification of fibre reinforced concrete for structural design purposes (Soetens and Matthys, 2014). The post-cracking behaviour is an important consideration when designing fibre reinforced concrete structural members (Amin and Foster, 2016) and this post-cracking tensile behaviour of fibre reinforced concrete can be grouped into hardening and softening behaviour (Soetens and Matthys 2014). The improvement of the post-cracking response over that of plain concrete is caused by fibres transmitting tensile forces across the cracks and is referred to as fibre bridging (Amin et al., 2015; Yoo et al., 2015b; fib Model Code, 2010). When cracks occur in plain concrete, crack bridging action is provided solely by aggregate interlock but with the addition of fibres, the bridging effect is achieved by a combination of fibres and aggregates, resulting in an increase in stress

carried along the crack (Li et al., 1993). The importance of crack-width control in structures can never be overlooked. There is a correlation between crack width and durability of structures as there are certain limits to crack widths that can be allowed for a structure to be considered safe in service. The use of fibres is known to improve the serviceability behaviour by reducing crack widths and crack spacing (*fib* Model Code, 2010; Li et al., 1993).

The advantages of FRC has led to its increased use and has further given rise to a demand for better modelling and design rules. Various FRC material models exist in literature and a number of standards (RILEM TC 162-TDF, 2002; Li et al., 1993) have also given guidelines and recommendations for modelling the post-cracking behaviour of FRC. The *fib* model code (2010) characterizes this behaviour using a simplified rigid-plastic model and a more detailed bi-linear constitutive model as shown in Figure 5.1.

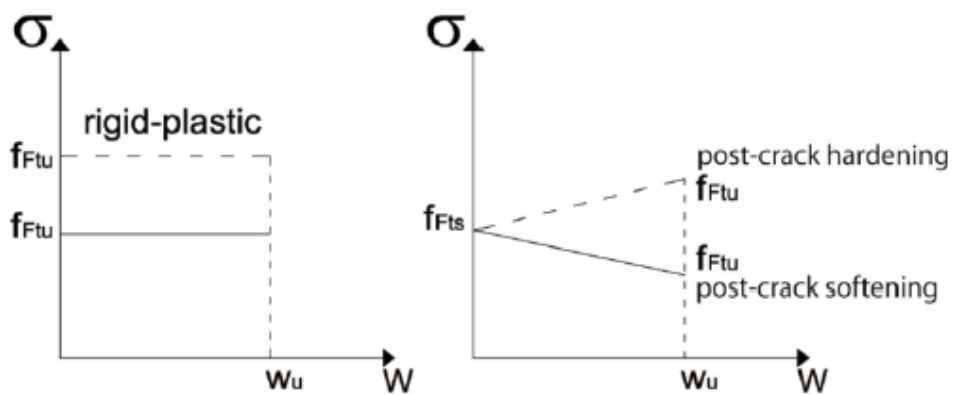


**Figure 5.1: Simplified post-cracking constitutive law (*fib* Model code, 2010).**

The post cracking behaviour of FRC is expressed in terms of stress-crack width or crack opening displacement and can be obtained directly from direct uniaxial tests. However these tests are time consuming, quite complex, requires much effort and are expensive (Amin et al., 2015; Kooiman, 2000; Dupont, 2003). Also, flexural tests do not put the section under constant tension stress. As an alternative to direct tension tests, various researchers have attempted to model the post cracking behaviour of FRC by inverse analysis. Inverse analysis normalizes flexural stress to be comparable with tension tests and corresponding tension properties. Some researchers have also tried modelling this behaviour from the pull-out response of fibres (Hugo and Banthia, 1997; Lee et al., 2013; Soetens and Matthys, 2014). Others have modelled the post-cracking behaviour using a fracture mechanics based inverse analysis (Kooiman et al., 2000; Kurihara et al., 2000). Soetens and Matthys (2014) modelled the post-cracking behaviour from fibre pull-out tests and were able to calculate the axial crack bridging ability of FRC. Their proposed model follows closely the axial pull-out model developed by (Soetens et al., 2013). They also developed a model based on inverse analysis of bending test results and later finite element analysis to characterize the post-cracking behaviour. Barros et al. (2005) performed numerical research and inverse analysis to evaluate the post-cracking stress-strain and stress-crack width relationship and analyzed the suitability of the RILEM TC 162-TDF (2002) stress-strain modelling approach. From their work they obtained a relationship between post-cracking strain ( $\epsilon^{pct}$ ) and crack opening displacement ( $w$ ) as  $\epsilon^{pct} = w/L_p$  where

$L_p$  is the length of the fracture process zone. They observed a correlation between the equivalent flexural tensile strength and residual flexural strength proposed by RILEM TC 162-TDF (2002) but argued that the equivalent flexural tensile strength is more suitable for design purposes than the residual flexural strength. Li et al., (1993) proposed a micromechanics based model used to predict the stress-crack width relationship of steel and polypropylene fibres in the post-cracking region by accounting for interface debonding, fibre pre-stress, aggregate and fibre bridging effects. Their model was verified with results obtained experimentally. Lee et al., (2013) calculated the stress-crack width relationship using a simplified diverse embedment model which considers frictional bond and mechanical anchorage effects. Obtaining the properties such as pull-out slip curve, fibre orientation etc. requires complex equations and much effort thereby making the fracture mechanics-based inverse analysis a simpler method to model the post-cracking tensile behaviour of FRC (Yoo et al., 2015a).

In this chapter, four-point bending tests were carried out as per ASTM C1609 (2012) and the post-cracking behaviour of steel FRC beams with various compressive strengths, densities and fibre volume fractions were predicted using inverse analysis, to generate the stress-crack width relationship from experimental load-deflection data.

## 5.2. Experimental Program

In this experimental program, the test parameters include fibre dosage and concrete type (normal weight and low-density). Expanded polystyrene beads were used as lightweight aggregates to reduce the density of the mixes and a high range water reducing admixture was added to increase workability of the mixes as required. All specimens were prepared in accordance with ASTM C192 (2016) and cured in a fog room at a constant temperature of  $22\pm 2^{\circ}\text{C}$  and 100% relative humidity until testing.

Table 5.1 shows the mix composition that was used in this experimental work. Compression strength tests were performed after 28 days of curing in accordance with ASTM C39 (2017) on 101.6 mm diameter by 203.2 mm long cylinders for each mix. A servo-controlled SATEC universal testing machine was used to apply uniaxial compressive load at a rate of 0.24MPa/sec in order to get the complete post-peak and pre-peak curves.

Four-point bending tests based on ASTM C1609 (2012) were conducted in order to obtain the flexural properties and investigate the bending behaviour of steel fibre reinforced prisms with nominal dimensions 152.4 mm x 152.4 mm x 530 mm. The steel fibre used was a hooked end type. A summary of the fibre properties is presented in Table 5.2. The prism span length is 450 mm and the distance between the loading positions is a third of the span length (i.e. 150 mm). The tests were conducted until reaching a drop in load of about 70% of the peak load or a crack mouth opening displacement of at least 3 mm.

Digital image correlation (DIC) was used to measure the crack mouth opening deflection (CMOD), deflection and strains for both tests. The test setup for flexure is shown in Figure 5.2.

**Table 5.1: Mix proportions**

Mix	Mix Designation	W/C	Cement (Kg/m <sup>3</sup> )	Fine Aggregate (Kg/m <sup>3</sup> )	Coarse Aggregate (Kg/m <sup>3</sup> )	EPS (m <sup>3</sup> )	HRWRA (mL/100Kg)	Fibre Volume	
								%	Kg/m <sup>3</sup>
Steel	SFRNWC0.5	0.35	550	693	875	0.0	975	0.50	39.25
Steel	SFRLDC0.5	0.35	550	350	451	0.3	198	0.50	39.25
Steel	SFRLDC1.0	0.35	550	350	451	0.3	-	1.00	78.50
Steel	SFRLDC1.5	0.35	550	350	451	0.3	-	1.50	117.75

\***SFRNWC**: Steel fibre reinforced normal weight concrete \***SFRLDC**: Steel fibre reinforced low density concrete

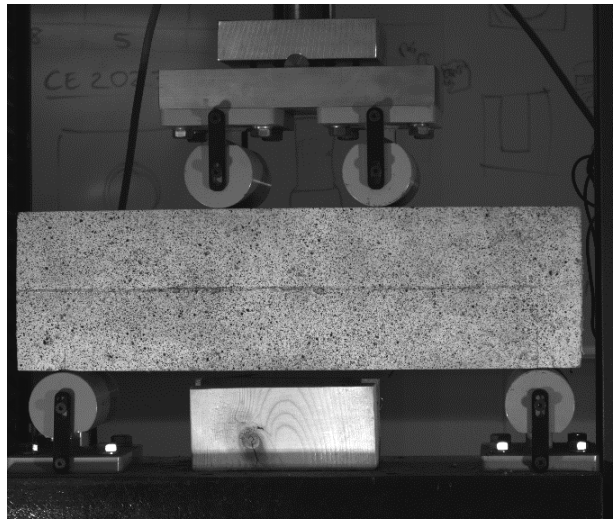


**Figure 5.2: Test setup for flexural test**

**Table 5.2: Properties of Fibres**

Fibre Type	Diameter (mm)	Length (mm)	Aspect ratio ( $L_f/d_f$ )	Tensile strength (MPa)	Elastic Modulus (GPa)
Steel	0.5	30	60	1500	200

Note:  $L_f$  = Length of fibre,  $d_f$  = diameter of fibre

### 5.3. Experimental Results

The workability of each mix was measured as per CSA A23.2-5C (2014) by measuring the slump. The workability of all fibre mixes were generally poor but was improved with the addition of a high range water reducing admixture (HRWRA). Comparing the mixes without HRWRA, results show that addition of fibre reduces slump with the higher fibre content mixes having lower slump values.

Results from the compression tests show little improvement in compressive strength with the addition of fibres. The most notable difference in compressive strength is seen when comparing the strength of low-density mixes to normal weight concrete mix.

For all four-point bending test series, the complete load-crack mouth opening deflection curves are shown in Figure 5.4 and average results from bending tests are summarized in Table 5.3. It was observed that an increase in strength of the matrix resulted in an increase in load carrying capacity. The increase in fibre content also increased the load carrying capacity. This agrees with the findings of (Yoo et al., 2015b). The deflection at peak load

also showed an increase with increase in fibre content. All beams showed an increase in load carrying capacity after first crack. The steel fibre mixes at 0.5% volume fraction showed deflection hardening behaviour for the low-density concrete but a softening behaviour for the normal weight concrete. From this behaviour it can be deduced that low fibre contents are ineffective in normal weight concrete compared to their low-density counterpart. It is recommended that fibres with higher aspect ratio, modulus of elasticity and deformed geometry be used to achieve deflection hardening and more ductility in normal weight concrete.

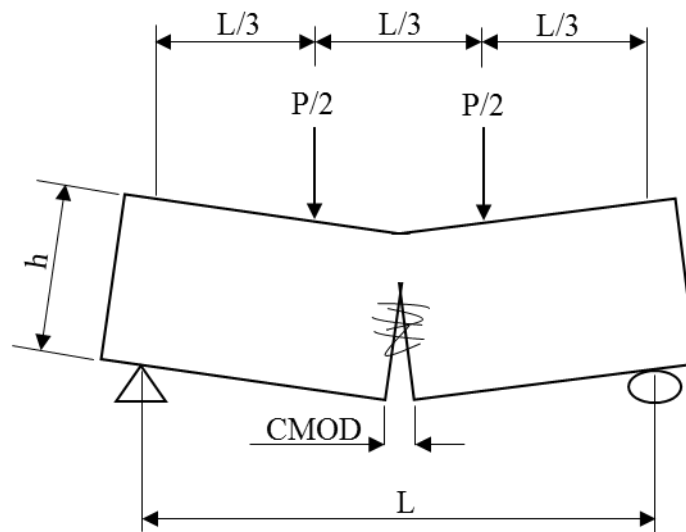
The flexural tests curves can be described by phases of elastic behaviour up to first crack, hardening up to peak load and a reduction in load with increase in CMOD. CMOD (as shown in Figure 5.3) is the crack mouth opening displacement at the bottom of the prism and was measured using the equation proposed by (Vandawalle & Dupont, 2002) and is given by Equation 5.1 below. CMOD was also measured using DIC and it was observed that DIC measurements gave higher values of CMOD compared to Equation 5.1. It should be noted that similar to Equation 5.1, these values apply only to the post-crack region. Measurements in the uncracked region are as a result of micro-cracking picked up by DIC and long extensometer gauge length used in measurement. However, the calculated values were used for the inverse analysis to be consistent with the inverse analysis method and because the neutral axis shifts, computing crack width ( $w$ ) was not feasible using DIC. Vandawalle & Dupont (2002) performed a series of experimental verifications on various

material behaviours in both plain and SFRC and averaged the results to derive Equation 5.1 with  $\beta$  as a constant which is independent of the fibre content and concrete strength.

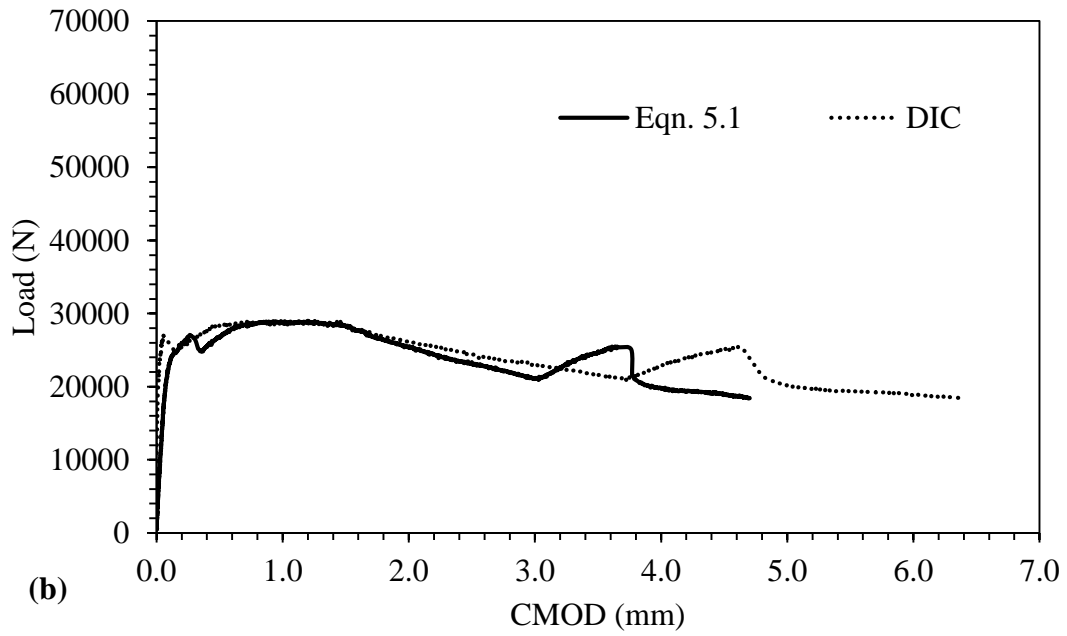
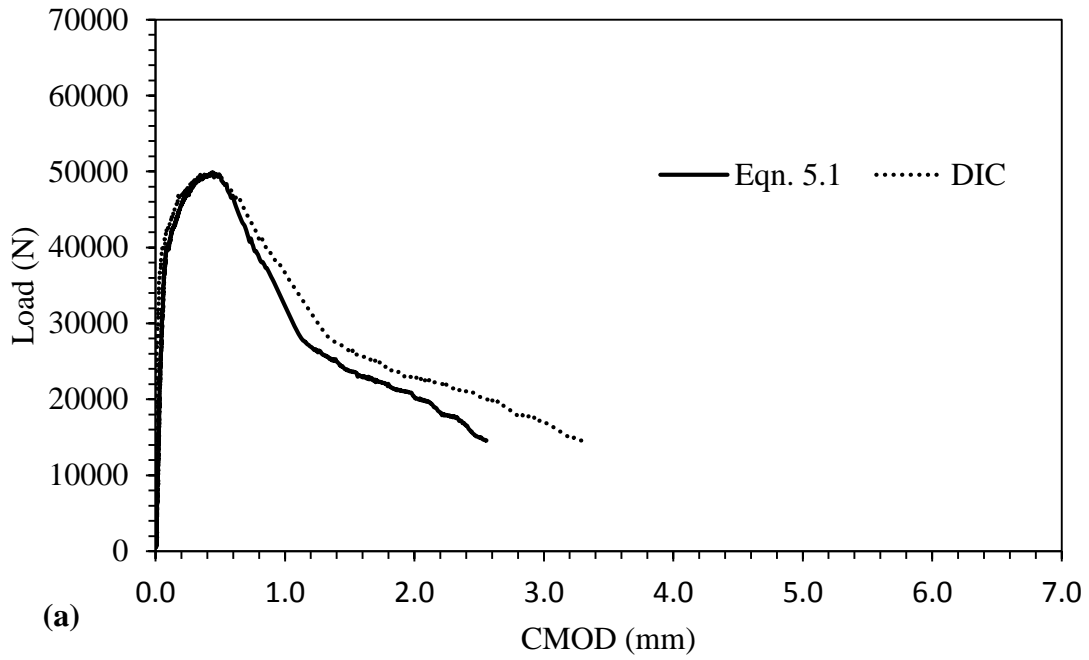
$$CMOD = 1.18\delta + \beta \quad \text{with } \beta = -0.0416 \quad (5.1)$$

**Table 5.3: Summary of results**

Mix Designation	Compressive strength (Mpa)	Modulus of Rupture (Mpa)	Slump (mm)	Density (Kg/m <sup>3</sup> )	Maximum Load (KN)	Deflection at Max. Load (mm)
SFRNWC0.5	84	6.39	240	2430	49.86	0.3676
SFRLDC0.5	33	3.87	70	1933	29.02	1.0184
SFRLDC1.0	35	6.32	50	1936	53.45	1.1822
SFRLDC1.5	40	6.53	30	1934	65.68	0.9561



**Figure 5.3: Crack mouth opening deflection shown in four-point bending.**



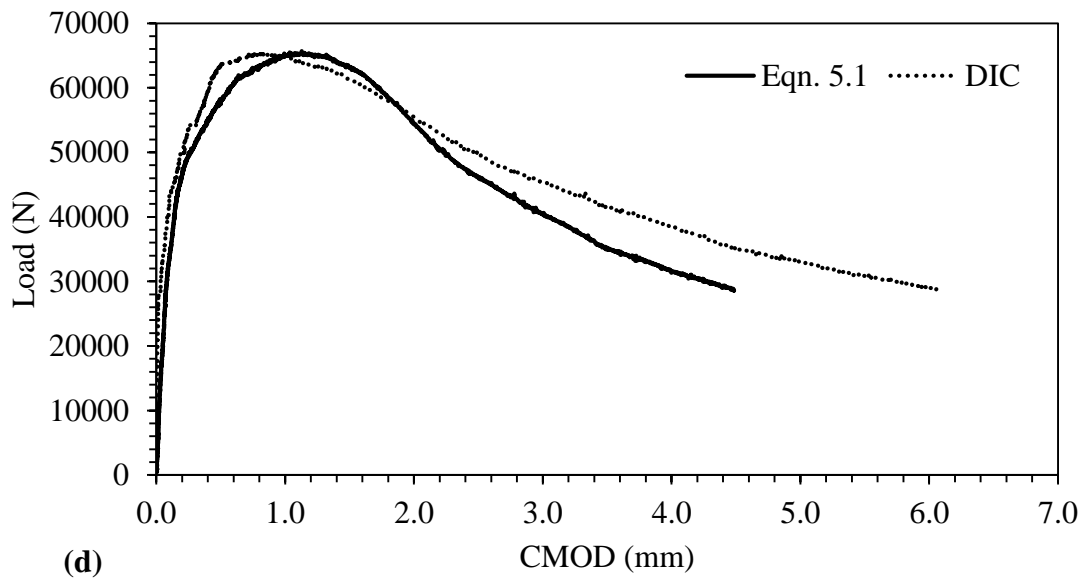
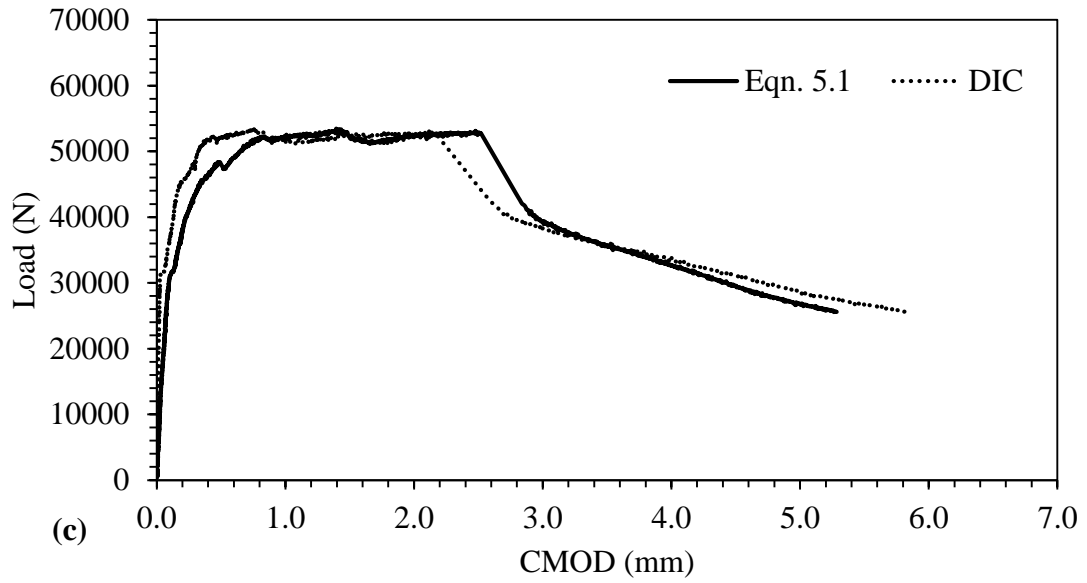


**Figure 5.4: Load – CMOD relationships for (a) SFRNWC0.5 (b) SFRLDC0.5 (c) SFRLDC1.0 (d) SFRLDC1.5.**

#### 5.4. Determination of Post-Cracking Stress-Crack Width Relationship

The post cracking tensile properties of FRC are measured using either direct tension tests or inverse analysis on bending test results. Various analytical and computer models have been developed to determine the stress-crack width relationship of FRC through inverse analysis (De Oliveira & Gettu, 2006; Zhang & Stang, 1998; Planas et al., 1999). In this study, inverse analysis was done on the obtained load – CMOD curves to obtain the tensile crack opening relationship using the model proposed by Amin et al., (2015) for conversion of prism bending test data to  $\sigma$ - $w$ . Using the model, the strength for a given crack width was determined from the individual stress carried by the fibres and concrete from Equation 5.2.

$$\sigma(w) = \sigma_c(w) + \sigma_f(w) \quad (5.2)$$

where  $\sigma_c(w)$  is the stress carried by the concrete for a given crack width,  $\sigma_f(w)$  is the stress carried by the fibres.

The concrete stress  $\sigma_c(w)$  is derived from Equation 5.3 as

$$\sigma_c(w) = c_1 f_{ct} e^{-c_2 w} \quad (5.3)$$

where  $f_{ct}$  is the tensile strength of concrete,  $c_1$  is a coefficient that accounts for beneficial effects of fibres on peak strength of matrix and is taken as unity,  $c_2$  is a coefficient and is given by equation 5.4 and 5.5 for different aggregate size. It is influenced by the volume of fibres and composition of the matrix and controls the steepness of the descending branch.

$$c_2 = 30 / (1 + 100\rho_f) \text{ for } a_g \leq 10 \text{ mm} \quad (5.4)$$

$$c_2 = 20 / (1 + 100\rho_f) \text{ for } a_g > 10 \text{ mm} \quad (5.5)$$

where  $a_g$  is the maximum size of aggregate in matrix and  $\rho_f$  is the fibre volume fraction.

In this work 9.5 mm maximum aggregate size was used.

The fibre component  $\sigma_f(w)$  is given by Equation 5.6

$$\sigma_f(w) = f_w \zeta(w) \quad (5.6)$$

where  $\zeta(w)$  is a transition function given by Equation 5.7, representing a transition zone between cracking point and a point corresponding to where the influence of uncracked concrete are considered insignificant.

$$\zeta(w) = \begin{cases} \sqrt{1 - \frac{(w_T - w)^2}{w_T^2}} & \text{if } w < w_T \\ 1 & \text{if } w \geq w_T \end{cases} \quad (5.7)$$

$w_T$  represents the point of maximum effectiveness of fibres usually the crack width corresponding to the maximum post-cracking load.

$f_w$  is the tensile stress carried by fibres and for ASTM four point bending test it is given by Equation 5.8 (Foster et al., 2018)

$$f_w = 0.4f_{R2} + 1.2(f_{R4} - f_{R2})\xi(w) \geq 0 \quad (5.8)$$

where  $\xi(w) = \frac{w}{3} - \frac{1}{4}$  for four-point bending test without a notch.

In accordance with EN 14651 (2007),  $f_{R,j}$  ( $f_{R2}$  and  $f_{R4}$ ) is defined by Equation 5.9

$$f_{R,j} = \frac{3F_j a}{bd^2} \dots j = 1, 2, 3, 4 \quad (5.9)$$

where  $a$  is the shear span =  $l/3$  for four-point bending test and  $F_j$  is obtained from the bending test and represents the values of load corresponding to CMOD of 0.5, 1.5, 2.5 and 3.5 mm, respectively (see Figure 5.5). Values corresponding to 0.5 and 2.5 mm CMOD can also be used. When modelling, one can decide to use any two values of  $f_{R,j}$  in the post cracking region but care should be taken to make sure that the selected values are far apart from each other and from the crack in order to get the full response.

The crack opening displacement or crack width ( $w$ ) for four point bending test without a notch is taken as  $CMOD/2$ . Results from the modelling are shown in Figure 5.6.

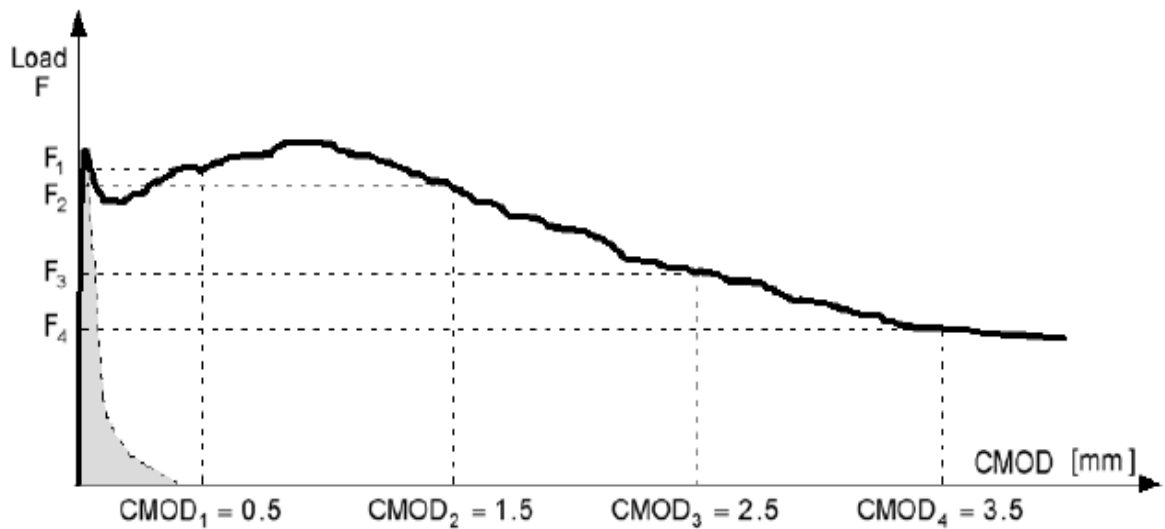


**Figure 5.5: Key points on Load-CMOD curve (fib Model code 2010).**

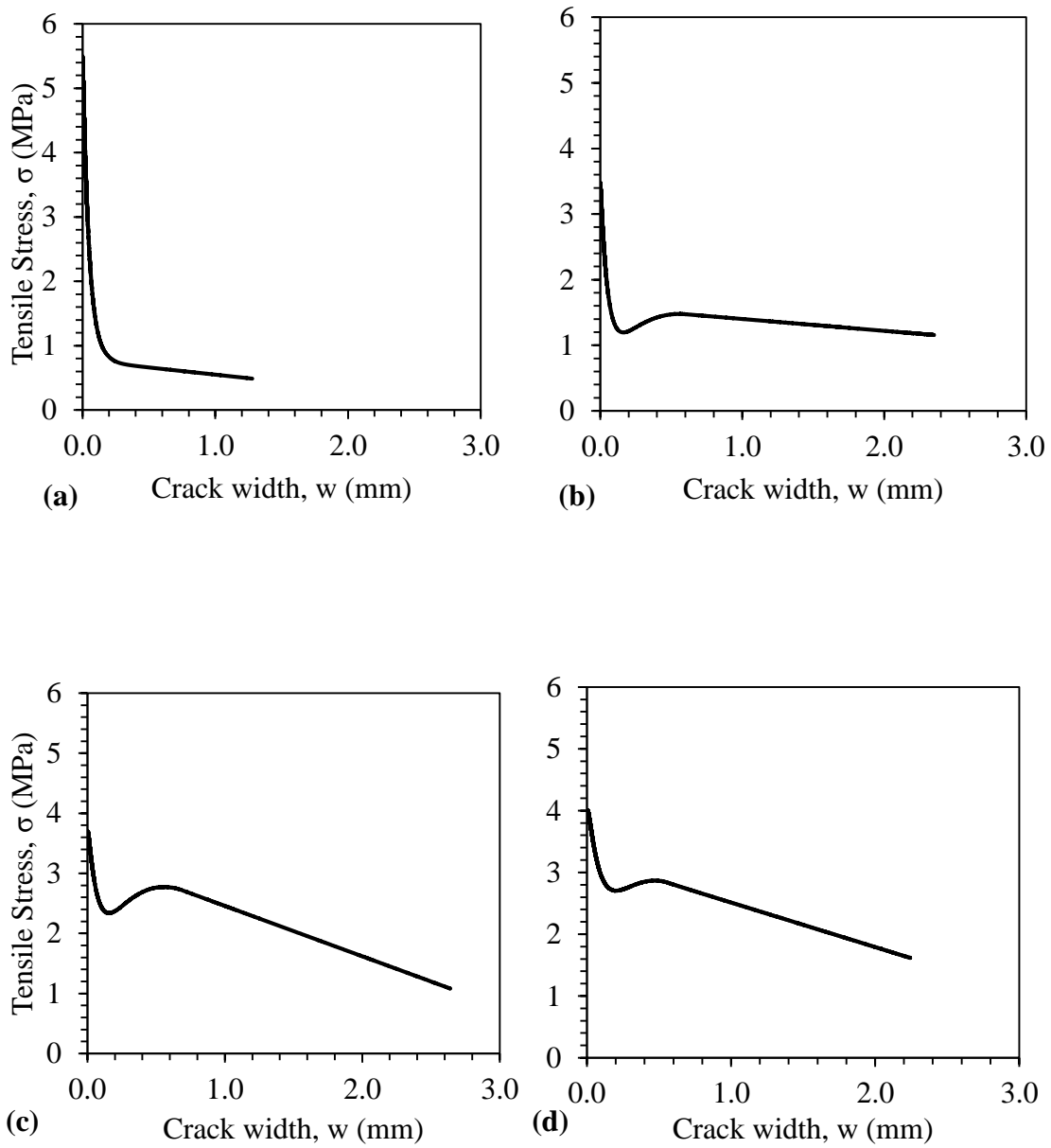


**Figure 5.6: Tensile stress vs crack width ( $\sigma - w$ ) curves obtained from inverse analysis for (a) SFRNWC0.5 (b) SFRLDC0.5 (c) SFRLDC1.0 (d) SFRLDC1.5.**

## **5.5. Discussion of Results**

Results from the inverse analysis modelling show a multi-linear relationship for all low density mixes and a bilinear relationship for the normal weight concrete mix. These results show a distinction between tension hardening and deflection hardening. Looking at both SFRLDC0.5 and SFRLDC1.0 deflection results, one would observe a hardening behaviour in deflection but in reality it is a softening behaviour as the tensile strength is not attained a second time following initial softening as shown by the stress-crack width curves. Figure 5.6 show that the tensile stress drops at crack for all specimens with the SFRLDC1.5 specimens showing less drop compared to the other specimens. This shows the effectiveness of higher fibre volume fraction. The results also show an increase in tensile strength with increase in fibre content and a reduction in tensile strength of the low density mixes when compared to the normal weight mix. The tensile stress corresponding to first crack was also observed to increase with increase in fibre content and was measured at 0.8, 1.2, 2.4 and 2.7 MPa for the normal weight concrete mix, 0.5%, 1.0% and 1.5% fibre mixes, respectively. The low-density concrete specimens showed more ductile behaviour than the normal weight concrete specimen.

## **5.6. Conclusion**

The inverse analysis model used in this work has already been verified by Amin et al. (2015) to conform to direct tension test results for normal weight concrete. Further work

may be needed to validate its use in lightweight concrete. This model was used in this work to show the post-cracking behaviour of normal weight and low-density steel fibre reinforced concrete. It is shown from the study that the stress-crack width relationship is a better way of understanding the behaviour of fibres without relying solely on bending tests. Bending tests can be useful in providing the deflection behaviour and capacity of fibres and various mixes but can't be used as a design basis in providing the tensile behaviour.

## 5.7. References

ASTM C192/C192M. (2016). "Practice for Making and Curing Concrete Test Specimens in the Laboratory." *ASTM International*. West Conshohocken, PA, United States.

ASTM C39/C39M. (2017). "Test Method for Compressive Strength of Cylindrical Concrete Specimens." *ASTM International*. West Conshohocken, PA, United States.

ASTM C1609/C1609M. (2012). "Standard Test Method for Flexural Performance of Fibre-Reinforced Concrete (Using Beam with Third-Point Loading)." *ASTM International*. West Conshohocken, PA, United States.

Amin, A., & Foster, S. J. (2016). "Predicting the flexural response of steel fibre reinforced concrete prisms using a sectional model." *Cement and Concrete Composites*, Vol. 67: 1–11.

Amin, A., Foster, S. J., & Muttoni, A. (2015). "Derivation of the  $\sigma$ - $w$  relationship for SFRC from prism bending tests." *Structural Concrete*, Vol. 16, No. 1: 93–105.

Barros, J. A. O., Cunha, V.M.C.F., Ribeiro, A.F. & Antunes J.A.B. (2005). "Post-cracking behaviour of steel fibre reinforced concrete." *Materials and Structures*, Vol. 38: 47-56.

CAN/CSA-A23.2-5C (2014). “Slump and slump flow of concrete.” *Standards Council of Canada*. Mississauga, ON. Canada.

Dupont, D. (2003). “Modelling and experimental validation of the constitutive law ( $\sigma - \varepsilon$ ) and cracking behaviour of steel fibre reinforced concrete.” *PhD Thesis*, Catholic University of Leuven.

De Oliveira e Sousa, J. L. A., & Gettu, R. (2006). “Determining the tensile stress-crack opening curve of concrete by inverse analysis.” *Journal of Engineering Mechanics*, Vol. 132, No. 2: 141–148.

De Oliveira e Sousa, J. L. A., Barrag, B. E. & Gettu, R. (2002). “An inverse analysis of the notched beam response for determining the  $\sigma - w$  curve for plain and fibre reinforced concretes.” *Journal of fracture mechanics*, Vol. 19: 393 - 398.

EN 14651 (2007). “Test method for metallic fibre concrete - measuring the flexural tensile strength (limit of proportionality (LOP), Residual).” *European Committee for Standardization*.

*fib* - International Federation for Structural Concrete (2010). *Model Code: final draft. Vol. 1 for Concrete Structures*.

Foster, S. J., Agarwal, A., & Amin, A. (2018). “Design of steel fibre reinforced concrete beams for shear using inverse analysis for determination of residual tensile strength.” *Structural Concrete*, Vol. 19, No. 1: 129–140.

Hugo, S., Bantia, N. (1997). “Predicting the Flexural Post-cracking Performance of Steel Fibre Reinforced Concrete from the Pullout of Single Fibres.” *ACI Materials Journal*, Vol. 94, No. 1.

Kooiman, A. G., Veen, V. D., Walgreen, J. C. (2000). “Modelling the post-cracking behaviour of steel fibre reinforced concrete for structural design purposes”. *HERON*, Vol. 45, No. 4.

Kooiman, A. G., (2000) “Modelling Steel Fibre Reinforced Concrete for Structural Design.” *PhD Thesis*, Technische Universiteit Delft.

Kurihara, Norihiko, Kunieda, M., Kamada, T., Uchida, Y., & Rokugo, K. (2000). “Tension Softening Diagrams and Evaluation of Properties of Steel Fibre Reinforced Concrete.” *Engineering Fracture Mechanics*, Vol. 11.

Lee, S.C., Cho, J. Y., Vecchio, F. J. (2013). “Simplified Diverse Embedment Model for Steel Fibre- Reinforced Concrete Elements in Tension.” *ACI Materials Journal*, Vol. 110, No. 4.

Li, V. C., Stang, H., Krenchel, H. (1993). “Micromechanics of Crack Bridging in Fibre Reinforced Concrete.” *Materials and Structures*, Vol. 26, 486 - 494.

Planas, J., Guinea, G. V., & Elices, M. (1999). “Size effect and inverse analysis in concrete fracture.” In Z. P. Bažant & Y. D. S. Rajapakse (Eds.), *Fracture Scaling* (pp. 367–378).

RILEM TC 162-TDF (2002). “Test and Design Methods for Steel Fibre Reinforced Concrete: Design of Steel Fibre Reinforced Concrete Using  $\sigma - w$  Method: Principles and Applications.” *Materials and Structures*, 35, 262-278.

Soetens, T., Van Gysel, A., Matthys, S., & Taerwe, L. (2013). “A semi-analytical model to predict the pull-out behaviour of inclined hooked-end steel fibres.” *Construction and Building Materials*, Vol. 43: 253–265.

Soetens, T., & Matthys, S. (2014). “Different methods to model the post-cracking behaviour of hooked-end steel fibre reinforced concrete.” *Construction and Building Materials*, Vol. 73: 458–471.

Vandawalle, L & Dupont, D. (2002). “Bending Test and Interpretation.” *RILEM TC 162-TDF: Test and Design Methods for Steel Fibre Reinforced Concrete*. Pro. 31.

Yoo, D.-Y., Yoon, Y.-S., & Banthia, N. (2015a). "Predicting the post-cracking behaviour of normal- and high-strength steel-fibre-reinforced concrete beams." *Construction and Building Materials*, Vol. 93: 477–485.

Zhang, J., & Stang, H. (1998). "Applications of Stress Crack Width Relationship in Predicting the Flexural Behaviour of Fibre-Reinforced Concrete." *Cement and Concrete Research*, Vol. 28, No. 3: 439–452.

## **6.0. SUMMARY AND CONCLUSION**

The research program and its findings are summarized in this chapter. Both experimental and analytical research is included, with relevant conclusions drawn from the entire research program.

### **6.1. Discussion**

FRC is a promising material for structural use due to its numerous advantages. The current research was undertaken to contribute towards the knowledge in the area of fibre reinforced concrete through studies and experimental analysis on the various types of fibres and their responses to load in terms of capacity, crack formation and propagation. It was the author's opinion to investigate the behaviour of fibre reinforcement when used in low-density concrete because of the advantages of using low-density concrete in construction. The research program consists mainly of experimental work using four point bending tests. The work is divided into four main parts:

The first part (Chapter 2) provided an extensive review of the literature and state of the art for FRC. The review included various fibre types, their behaviour when subjected to shear, compression, tension forces, experimental methods to determine the tensile behaviour, fibre pull-out behaviour, modelling techniques. It was observed from the literature review that a study on the crack propagation and behaviour was not so elaborate especially in regards to low-density concrete, also it was noticed that a majority of the authors still relied

on traditional methods of strain and deflection measurements, use of clip gauge to measure crack mouth opening deflection thus prompting the use of DIC to study crack propagation and formation and to carry out these measurements.

The second part (chapter 3) aimed at understanding the behaviour of FRC with steel and polypropylene fibres in four-point bending in terms of crack propagation, propagation and neutral axis movement using DIC. From the experimental work, deflection was measured with DIC and also with traditional LVDT to make a case for the use of DIC as an alternate means of measurement.

The third part (chapter 4) went further to explore steel and polypropylene fibre at various aspect ratios of 0.5%, 1.0% and 1.5%. It was centered on sectional analysis of a cracked section. Applied moment and curvature plots, load- deflection plots, force location and magnitudes of the cracked section were examined.

In chapter 5, an existing model was used to model the results from the experimental works considering both normal weight fibre reinforced concrete and low-density fibre reinforced concrete and conclusions were drawn.

## **6.2. Conclusions**

The following conclusions can be drawn from the experimental and analytical work carried out in this research program:

- Steel fibres at volume fraction as low as 0.5% are effective in arresting crack propagation
- Steel fibres in general are more effective in arresting crack than polypropylene fibres.
- Steel fibres show hardening behaviour when used in low-density concrete.
- Compressive strength is slightly improved with the addition of fibres.
- For both steel and synthetic fibres, increase in fibre content results in a corresponding increase in compressive strength and corresponding strain at peak load.
- Flexural strength and ductility are also improved with addition of both fibre types.
- Digital image correlation is a better and more convenient way of measuring deflection, strains and fracture of specimens.
- The location of the compression force in the flexural prisms was found to be at 64% of the neutral axis measurement above the neutral axis.
- For the mix design studied, 1.0% fibre content was found to be the optimum dose of fibre in low-density concrete
- The neutral axis movement was affected by fibre type with steel fibre showing a gradual decrease while polypropylene fibre showing a more rapid increase. This increase was also proportional to the fibre content.

- The magnitude of the compression force in the prisms was higher for the steel fibre specimens compared to the synthetic fibre specimens.
- Results from the inverse analysis modelling showed a multi-linear stress-crack width relationship for low-density concrete and a bilinear relationship for normal weight concrete.
- From the modelling, deflection hardening was differentiated from tension hardening.
- An increase in tensile strength was observed for increase in fibre content.
- It was observed that low-density concrete had lower tensile strength when compared with normal density concrete.

### **6.3. Recommendations for Future Research**

The following recommendations are made for future research:

- Further studies using DIC should be carried out on uniaxial tension test of low-density FRC in order to obtain a relationship between the flexural test results and further modify existing design models.
- Future studies on low-density and normal density concrete should also investigate on the use of hybrid fibre reinforced concrete specifically the combination of different types of steel fibre and other fibre types.
- Experimental and analytical research on other types of fibres should also be investigated.

- Investigations on the behaviour of the various fibres types under dynamic loads.
- It is recommended that finite element analysis in combination with DIC be used to establish a suitable model or develop the existing modelling methods.
- Other experimental methods such as plate test and wedge splitting test should be further studied.
- DIC should be employed in the study of pull-out behaviour of fibres.

## 7.0. REFERENCES

American Concrete Institute. Committee 213. (2003). “Standard practice for selecting proportions for structural lightweight concrete.” ACI 213R, Farmington Hills, MI.

American Concrete Institute. Committee 544. (2010). “State of the art report on fibre reinforced concrete.” ACI 544.1R, Farmington Hills, MI.

ASTM C332 (2009). “Standard specification for lightweight aggregates for insulating concrete.” *ASTM International*. West Conshohocken, PA, United States.

ASTM C78/78M. (2010). Standard test method for flexural strength of concrete (using simple beam with third point loading) *ASTM International*, West Conshohocken, PA, United States.

ASTM Standards C1609/C1609M. (2010). “Standard test method for flexural performance of fibre-reinforced concrete.” *ASTM International*, West Conshohocken, PA, United States.

ASTM C1550. (2003). “Standard test method for flexural toughness of fibre reinforced concrete (using centrally-loaded round panel).” *ASTM International*. West Conshohocken, PA, United States.

ASTM C330 (2014). “Standard specification for lightweight aggregates for structural concrete.” *ASTM International*. West Conshohocken, PA, United States.

ASTM C1018. (1997). “Standard test method for flexural toughness and first-crack strength of fibre- reinforced concrete (using beam with third-point loading).” *ASTM International*. West Conshohocken, PA, United States.

Allos, A. E. (1989). "Shear transfer in fibre reinforced concrete." In *Fibre Reinforced Cements and Concretes – Recent Developments*, eds. R.N. Swamy and B. Barr, Elsevier Science Publishers, 146-156.

Alwan, J. M., Naaman, A. E., Guerrero, P. (1999). "Effect of mechanical clamping on the pull-out response of hooked steel fibres embedded in cementitious matrices." *Concrete Science and Engineering*, Vol. 1:15-25.

Asik, M. (2006). "Structural lightweight concrete with natural perlite aggregate and perlite powder." *Masters thesis*. Middle East Technical University, Ankara.

Aitcin, P. C. & Nilsen, A. U. (1992). "Properties of high-strength concrete containing light, normal, and heavyweight aggregate." *Cement Concrete and Aggregates*, Vol. 14, No. 1.

Armelin, H. S., Banthia, N. (1997). "Predicting the flexural post cracking performance of steel fibre reinforced concrete from the pullout of single fibres." *ACI Materials Journal*, Vol. 94, No. 1:18-31.

Amin, A., & Foster, S. J. (2016). "Predicting the flexural response of steel fibre reinforced concrete prisms using a sectional model." *Cement and Concrete Composites*, Vol. 67: 1–11.

Amin, A., Foster, S. J., & Muttoni, A. (2015). "Derivation of the  $\sigma$ -  $w$  relationship for SFRC from prism bending tests." *Structural Concrete*, Vol. 16, No. 1: 93–105.

Al-Khaiat, H., & Haque, N. (1998). "Effect of initial curing on early strength and physical properties of a lightweight concrete." *Cement and Concrete Research*, Vol. 28, No. 6: 859-866.

Al-Khaiat, H., & Haque, N. (1999). "Strength and durability of lightweight and normal weight concrete." *Journal of Materials in Civil Engineering*, Vol. 11: 231-235.

Bazant, Z. P., Oh, B. H. (1983). "Crack band theory for fracture of concrete." *Materials and Structures*, Vol. 16: 155-177.

Barros, J. A. O., Figueiras, J. A. (1999). "Flexural Behaviour of SFRC: Testing and Modeling." *Journal of Materials in Civil Engineering*, Vol. 11, No. 4: 331-339.

Banholzer, B., Brameshuber, W., Jung, W. (2005). "Analytical simulation of pull-out test – the direct problem." *Cement and Concrete Composites*, Vol. 27:93-101.

Barnes, A. J. (2007). "Uniaxial Compression and Flexural Behaviour of High Performance Cementitious Composites (HPFRCC)" *Master thesis*". University of Wisconsin.

Balaguru, P., & Najm, H. (2004). "High Performance Fibre Reinforced Concrete Mixture Proportions with High Fibre Volume Fractions." *ACI Materials Journal*, Vol. 101: 281-286.

Balaguru, P., & Khajuria, A. (1996). "Properties of Polymeric Fibre Reinforced Concrete." *Transportation Research Record*, 27-35.

Balaguru, P., and Ramakrishnan, V. (1986) "Freeze-Thaw Durability of Fibre Reinforced Concrete." *ACI Journal, Proceedings*, Vol. 83, No. 3: 374-382.

Bolzon, G., Fedele, R., and Maier, G. (2002). "Parameter identification of a cohesive crack model by Kalman filter." *Computational Methods Applied Mechanics Engineering*. Vol. 191: 2847-2871.

Brühwiler, E. and Wittmann, F. H. (1990). "The wedge splitting test, a new method of performing stable fracture mechanics test." *Engineer Fracture Mechanics*, Vol. 35, No. 1/2/3: 117-125.

Barragán, B.E. (2002). "Failure and toughness of steel fibre reinforced concrete under tension and shear." *Ph.D. Thesis*, Universitat Politècnica de Catalunya, Barcelona, Spain.

Banthia, N., Trottier, J. (1994). "Concrete reinforced with deformed steel fibres, part i: bond-slip mechanisms." *ACI Materials Journal*, Vol. 91, No. 5: 435-446.

BS EN14845-1 (2007). "Test methods for fibres in concrete." *British Standards Institution*, London, United Kingdom.

BS EN 14488-5. (2006). "Testing sprayed concrete. Determination of energy absorption capacity of fibre reinforced slab specimens." *British Standards Institution*, London, United Kingdom.

Barnes, A. J. (2007). "Uniaxial compression and flexural behaviour of high performance cementitious composites (HPFRCC)." *Master thesis*. University of Wisconsin.

Cunha, V. M. C. F., Barros, J. A. O, Sena-Cruz, J. M. (2007). "Pullout behaviour of hooked-end steel fibres in self-compacting concrete." Report 07-DEC/E06, University of Minho.

Cailleux, E., Cutard, T., Bernhart. G. (2005). "Pullout of steel fibres from a refractory castable: experiment and modeling." *Mechanics of Materials*, Vol. 37:427-445.

De Oliveira, F. L. (2010). "Design-oriented constitutive model for steel fibre reinforced concrete." *PhD thesis*, Universitat Politècnica de Catalunya.

Dupont, D. (2003). "Modelling and experimental validation of the constitutive law ( $\sigma$ - $\epsilon$ ) and cracking behaviour of steel fibre reinforced concrete." *PhD Thesis*, Catholic University of Leuven.

DBV (2001). "Guide to good practice: steel fibre concrete." *German Society for Concrete and Construction Technology (Deutsche Beton-Und Bautechnik Verein)*, Berlin, Germany.

Eser, H. (2014). "High performance structural lightweight concrete utilizing natural perlite aggregate and perlite powder." *Masters thesis*. Middle East Technical University, Ankara.

EFNARC (1996). "European Specification for Sprayed Concrete." *European Federation of Producers and Applicators of Specialist Products for Structures*, Surrey, United Kingdom.

Ezeldin, A., Balaguru, P., & Perumalsamy, N. (1992). "Normal and High-Strength Fibre Reinforced Concrete under Compression." *ASCE Journal of Materials in Civil Engineering*, Vol. 4, No. 4: 415-429.

*fib* Bulletin 8 (2000). "*Lightweight Aggregate Concrete, Recommended extension to Model Code 90.*" Lausanne, Switzerland.

Fantilli, A. P., Vallini, P. (2007). "A cohesive interface model for the pullout of inclined steel fibres in cementitious matrices." *Journal of Advanced Concrete Technology*, 5(2):247-258.

Fanella, D. A., & Naaman, A. E. (1985). "Stress-Strain Properties of Fibre Reinforced Mortar in compression." *Journal of the American Concrete Institute*, 82(4), 475-483.

*fib* - International Federation for Structural Concrete (2010). *Model Code: final draft. Vol. 1 for Concrete Structures.*

Fischer, G. and V. Li (2006). "Effect of fibre reinforcement on the response of structural members." *Engineering Fracture Mechanics* 74: pp. 258-272.

Guerrero, P., Naaman, A. E. (2000). "Effect of mortar fineness and adhesive agents on pullout response of steel fibres." *ACI Materials Journal*, 97(1):12-20.

Gray, R. J., and Johnston, C. D. (1978). "Measurement of fibre-matrix interfacial bond strength in steel fibre reinforced cementitious composites," *Proceedings, RILEM Symposium of Testing and Test Methods of Fibre Cement Composites*, Sheffield, Construction Press, Lancaster, pp. 317-328.

Hoff, G. C. (1992). "High strength lightweight aggregate concrete for Arctic applications." ACI SP 136, T. A. Holm and A. M. Vaysburd, ed., *American Concrete Institute*, Detroit, MI, 1-245, Parts 1-3.

Holm, T. A. & Bremner, T. W. (2000). "State-of-the-Art on High-Strength, High-durability Structural Low-density Concrete for Applications in severe Marine Environments." *US Army Corps of Engineers, Engineer Research and development Center*.

Hoff, G. C. (1986). "Use of Steel Fibre Reinforced Concrete in Bridge Decks and Pavements." *Steel Fibre Concrete*, Elsevier Applied Sciences Publishers, Ltd., 67-108.

Homrich, J. R., and Naaman, A. E. (1987). "Stress-Strain Properties of SIFCON in Compression," *Fibre Reinforced Concrete Properties and Applications*, SP-105, American Concrete Institute, Detroit, 283-304.

Hockenberry, T., & Lopez, M. M. (2012). "Performance of Fibre Reinforced Concrete Beams with and without Stirrups." *Journal of Civil Environmental and Architectural Engineering*, 4(1).

Hordjik, D. (1991). "Local approach to fatigue of concrete." *PhD Thesis*, Delft University of Technology.

Hillerborg, A., Mod er, M., Petersson, P. E. (1976). "Analysis of crack formation and crack growth in concrete by means of fracture mechanics and finite elements." *Cement and concrete research*. 6:773-782.

Hillerborg, A. (1980). "Analysis of fracture by means of the fictitious crack model, particularly for fibre reinforced concrete." *International journal of cement composites*, 2(4), 177-184.

Jansson, A. (2011). "Effects of Steel Fibres on Cracking in Reinforced Concrete." *PhD thesis*, Chalmers University of Technology, Sweden.

Johnston, C. D. & Gray, R. J. (1986). "Flexural Toughness and First-Crack Strength of Fibre Reinforced Concrete Using ASTM C 1018." *Proceedings*, Symposium on Developments in Fibre Reinforced Cement and Concrete, RILEM Committee 49-TFR, Paper 5.1.

JCI-SF4. (1984). "Method of tests for flexural strength and flexural toughness of fibre reinforced concrete." *Japan Concrete Institute*, Tokyo, Japan.

Jansson, A., Löfgren, I. and Gylltoft, K. (2008a). "Applying a fracture mechanics approach on FRC beams, material testing and structural analysis." Submitted to: *Journal of Advanced Concrete Technology*.

Jansson A., Löfgren I. and Gylltoft K. (2008b). "Design methods for fibre-reinforced concrete: a state-of-the-art review." Submitted to. *Nordic Concrete Research*.

Jansson, A. (2008). "Fibres in reinforced concrete structures - analysis, experiments and design." Chalmers University of Technology, Sweden.

Kitsutaka, Y. (1997). "Fracture parameters by polylinear tension-softening analysis." *Journal of Engineering Mechanics*, 123(5), 444-450.

Kooiman, A. G. (2000). "Modelling Steel Fibre Reinforced Concrete for Structural Design." *PhD Thesis*, Delft University of Technology.

Kooiman, A. G., Van Der Veen & Walraven, J. C. (2000). "Modelling the post-cracking behaviour of steel fibre reinforced concrete for structural design purposes". *HERON*, 45(4), ISSN 0046-7316, 275-307.

Klieger, P. & Lamond, J. F. (1994). "Significance of tests and properties of concrete and concrete-making materials." ASTM Philadelphia. 04-169030-07.

Kim, J. Y., Choi, W. Y., Lachemi, M. (2010). "Characteristics of self consolidating concrete using two types of lightweight coarse aggregates." *Construction and Building Materials* 24, 11-16.

Li, V., Mihashi, H., Wu, H., Alwan, J., Brincker, R., Horii, H., Stang, H. (1995). "Micromechanical Models of Mechanical Response of HPFRCC." In RILEM High Performance Fibre Reinforced Cement Composites 2.

Li, V. C., D. K. Mishra and H. C. Wu (1995). "Matrix design for pseudo strain-hardening fibre reinforced cementitious composites." *Materials and Structures*, Vol. 28, No. 183: pp. 586-595.

Li, V., & Mishra, D. (1992). "Micromechanics of Fibre Effect on the Uniaxial Compressive Strength of Cementitious Composites." *RILEM 4th Inter.*

Linsbauer, H. N. and Tschegg, E. K. (1986). "Fracture energy determination of concrete with cube shaped specimens." *Zement und Beton*, 31, 38-40.

Li, V. C., Stang, H., & Krenchel, H. (1993). "Micromechanics of crack bridging in fibre reinforced concrete." *Materials and Structures*, 26, 486-494.

Li, V. C., Wang, I., Backer, S. (1990). "Effect of inclining angle, bundling and surface treatment on synthetic fibre pullout from a cement matrix." *Composites*, 21(2):132-140.

Lim, D. H., & Nawy, E. G. (2005). "Behaviour of plain and steel fibre reinforced high-strength concrete under uniaxial and biaxial compression." *Magazine of Concrete research*, 57(10), 603-610.

Lambrechts, A. N. (2007). "Performance Classes for Steel Fibre Reinforced Concrete: Be Critical." Bekaert, Belgium.

Lok, T. S. and Pei, J.S. (1998). "Flexural Behaviour of Steel Fibre Reinforced Concrete," *Journal of Materials in Civil Engineering*, 10(2), 86-97.

Lok, T. S. and Xiao, J. R. (1999). "Flexural Strength Assessment of Steel Fibre Reinforced Concrete." *Journal of Materials in Civil Engineering*, 11(3), 188-196.

Löfgren, I. (2005). "Fibre-reinforced concrete for industrial construction- a fracture mechanics approach to material testing and structural analysis." *PhD thesis*, Chalmers University of Technology, Sweden.

Mohammed, J. H. & Hamad, A. J. (2014). "A classification of lightweight concrete: materials, properties and application review." *International Journal of Advanced Engineering Applications*, 7(1): 52-57.

Malik, A. (2016). "An Experimental Study on Properties of No-Fines Concrete." *Imperial Journal of Interdisciplinary Research*, 2(10), 2454-1362.

Mehta, P.K. and Monteiro, P.J.M. (2006) "Concrete: Microstructure, Properties, and Materials." 3rd Edition. McGraw-Hill, New York.

Mindess, S., Young, J. F., and Darwin, D. (2003) *Concrete*, 2nd ed. Prentice Hall, Upper Saddle River New Jersey.

Morton, J., Groves, G. W. (1974). "The cracking of composites consisting of discontinuous ductile fibres in brittle matrix – effect of fibre orientation." *Journal of Materials Science*, 9:1436-1445.

Muralitharan, R. S. & Ramasamy, V. (2017). "Development of lightweight concrete for structural applications." *Journal of Structural Engineering*, 44(4), 1-5.

Neville, A.M. and Brooks, J.J. (2010). "Concrete Technology", second edition, Prentice Hall, Pearson Education.

Neville, A. M. and Brooks, J. J. (1987). "Concrete Technology." *Longman Group UK Limited*, Essex, UK, 74-75.

Neville, A. M. (2003). *Properties of Concrete* (4th ed.). Harlow, England: Prentice Hall.

Narayanan, R., and Darwish, I. Y. S. (1987). "Use of Steel Fibres as Shear Reinforcement," *ACI Structural Journal*, 84(3), 216-227.

Naaman, A., & Chandrangsou, K. (2003). "Comparison of Tensile and Bending Response of Three High Performance Fibre Reinforced Composites." *High Performance Fibre Reinforced Cement Composites*. Ann Arbor, Michigan: HPFRCC4 Workshop.

Naaman A. E. (2003). "Engineered steel fibres with optimal properties for reinforcement of cement composites." *Journal of Advanced Concrete Technology*, 1(3). 241-252.

Naaman, A. E., Najm, H. (1991). "Bond-slip mechanisms of steel fibres in concrete." *ACI Materials Journal*, 88(2):135-145.

Naaman, A. E., Nammur, G., Alwan, J., Najm, H. (1991). "Fibre pullout and bond slip: Analytical study." *Journal of Structural Engineering*, 117(9): 2769-2790.

Naaman, A. E. and Shah, S. P. (1976). "Pull-Out Mechanism in Steel Fibre-Reinforced Concrete." *Journal of the Structural Division*, ASCE, 102(ST8), 1537-1548.

Naaman, A. E. (2003). "Engineered steel fibres with optimal properties for reinforcement of cement composites." *Journal of advanced concrete technology*, 1(3), 241-252.

Nanakorn, P. and Horii, H. (1996). "A fracture-Mechanics-Based Design Method for SFRC Tunnel Linings." *Tunneling and Underground Space Technology*, 11(1), 39-43.

Nanakorn P. and Horii H. (1996b) “Back analysis of tension-softening relationship of concrete.” *Journal of Materials, Concrete Structures, Pavements*, 32(544), 265-275.

Oikonomou-Mpegetis, S. (2013). “Behaviour and design of steel fibre reinforced concrete slabs.” *PhD thesis*, Imperial College London.

Østergaard, L. (2003). “Early-age fracture mechanics and cracking of concrete – experiments and modelling.” *Ph.D. thesis*, Department of Civil Engineering, Technical University of Denmark.

Østergaard, L., Olesen, J. F., Stang, H. and Lange, D. (2003). “A method for fast and simple interpretation and inverse analysis of the wedge splitting test.”

Patil, P. S., Sonar, I. P., Shinde, S. (2017). “No Fine Concrete.” *International Journal of Concrete technology*, 3(2): 1-13.

Ramakrishnan, V., Wu, G. Y., and Hosalli, G. (1989). “Flexural Fatigue Strength, Endurance Limit, and Impact Strength of Fibre Reinforced Concrete,” *Transportation Research Record, National Research Council, Washington D. C.*, 1226, 17-24.

Racines, P. G. and Pama, R. P. (1978). “A study of Bagasse fibre-cement composite as low-cost construction materials.” *Proc. Int. conf. Materials for Developing Countries*, Bangkok, 191-206.

RILEM TC 162-TDF. (2002). “Test and design methods for steel fibre reinforced concrete – Design of steel fibre reinforced concrete using the  $\sigma$ -w method: principles and applications.” *Materials and Structures*, 35:262-278.

Roelfstra, P. E., Wittmann, F.H. (1986). “Numerical method to link strain softening with failure of concrete, Fracture Toughness and Fracture Energy of Concrete.” Elsevier Science Publishers B.V., Amsterdam.

Robins, P., Austin, S., Jones, P. (2002). "Pull-out behaviour of hooked steel fibres." *Materials and Structures*, 35:434-442.

Sayadi, A. A., Tapia, J. V., Neitzert, T. R. and Clifton, G. C. (2016). "Effects of Expanded Polystyrene (EPS) Particles on Fire Resistance, Thermal Conductivity and Compressive Strength of Foamed Concrete," *Construction and Building Materials* 112: 716–24.

Serna, P., Arango, S., Ribeiro, T., Núñez, A. M., Garcia-Taengua, E. (2009). "Structural cast-in-place SFRC: technology, control criteria and recent applications in Spain." *Materials and Structures*, DOI: 10.1617/s11527-009-9540-9.

Sousa, J. L. A. O., Gettu, R. (2006). "Determining the tensile stress-crack opening curve of concrete by inverse analysis." *Journal of Materials in Civil Engineering*, Vol. 132, No. 2: 141-148.

Swamy, R. N., and Bahia, H. M. (1985). "The effectiveness of steel fibres as shear reinforcement," *Concrete International: Design & Construction*, V. 7, No. 3, pp. 35-40.

Shannag, M., Brincker, R., Hansen, W. (1997). "Pullout behaviour of steel fibres from cement-based composites." *Cement and Concrete Research*, 27(6):925-936.

Shah, S. P., Ouyang, C. (1991). "Mechanical behaviour of fibre-reinforced cement-based composites." *Journal of the American Ceramic Society*, 74:2727-2738.

Sujivorakul, C., Waas, A. M., Naaman, A. E. (2000). "Pullout response of a smooth fibre with an end anchorage." *Journal of Engineering Mechanics*, 126(9):986-993.

Tschegg, E. K., Linsbauer, H. N. (1986). "Testing procedure for determination of fracture mechanics parameters." Patentschrift no. A-233/86, Österreichisches Patentamt.

Trub, M (2011). "Numerical modeling of high performance fibre reinforced cementitious composites." *Institute of Structural Engineering*, Swiss Federal Institute of Technology.

UNI U73041440. (2004). "Design, production and control of steel fibre reinforced structural elements." Milan, Italy.

Van Gysel, A. (2000). "Study of the pullout behaviour of steel fibres embedded in one cement-bound matrix with application to steel fibre concrete subjected to bending." *PhD Thesis*, Gent University.

Van Rooyen, A. S. (2013). "Structural lightweight aerated concrete." *Masters thesis*, Stellenbosch University, South Africa.

Williamson, Gilbert R. (1974) "The Effect of Steel Fibres on the Compressive Strength of Concrete," *Fibre Reinforced Concrete*, SP-44, American Concrete Institute, Detroit, pp. 195-207.

Yurtseven, A. E. (2004). "Determination of mechanical properties of hybrid fibre reinforced concrete." *Master thesis*. Middle East Technical University.

Yang, I. H., Joh, C., & Kim, B. S. (2011). "Shear behaviour of ultra-high performance fibre-reinforced concrete beams without stirrups." *ICE-Magazine of Concrete Research*, Vol. 11, 979–993.

Zareh, M. (1971). "Comparative study of lightweight and normal weight concrete in flexure." *Masters thesis*, Portland State University.

## **Curriculum Vitae**

Candidate's full name: John Chimaobi Ibeawuchi

Universities attended: Bachelor of Engineering in Civil Engineering: Federal University Of Technology Owerri, Nigeria. (2008-2014)

Publications: "Evaluation of Flexural Behaviour of Low-Density Fibre Reinforced Concrete Using Digital Image Correlation. CSCE 2018."

Conference Presentations: "Evaluation of Flexural Behaviour of Low-Density Fibre Reinforced Concrete Using Digital Image Correlation. CSCE 2018."